R. & M. No. 2294
(8831 & 9639)
A.R.C. Technical Report

MINISTRY OF SUPPLY

AERONAUTICAL RESEARCH COUNCIL
REPORTS AND MEMORANDA

A Theoretical Investigation of the Response of a High-speed Aeroplane to the Application of Ailerons and Rudders

By

K. MITCHELL, Ph.D., A. W. THORPE, B.A. and E. M. FRAYN, B.Sc.

LONDON: HIS MAJESTY'S STATIONERY OFFICE
1952
PRICE £1 5s 0d NET

A Theoretical Investigation of the Response of a High-speed Aeroplane to the Application of Ailerons and Rudder

By

K. MITCHELL, Ph.D., A. W. THORPE, B.A. and E. M. FRAYN, B.Sc.

COMMUNICATED BY THE PRINCIPAL DIRECTOR OF SCIENTIFIC RESEARCH (AIR,)
MINISTRY OF SUPPLY

Reports and Memoranda No. 2294

May, 1945*

Summary.—The response of a fast moving aeroplane to a lateral gust, and to applied rolling and yawing moments, is examined by means of the differential analyser, taking a range of values of the principal lateral stability parameters, and including sufficient ranges of the other stability and inertia parameters to make the conclusions of general validity for high-speed flight.

The motion following a sharp-edged side-gust is shown to be of a markedly oscillatory character, with an unpleasantly short period, particularly in small aeroplanes. The shortness of the period is probably the worst feature. A general survey is made of the dependence of the motion upon the various parameters, the differential analyser results being supplemented by the use of approximate formulae, which were developed with a view to this application. Particular attention is paid to the amplitudes of the motion in roll, yaw, and sideslip, and it is seen that it may be difficult to make the motion less unpleasant. The period may be lengthened by reducing n_v, but the improvement that is possible in this way is limited. Damping can be improved by reducing dihedral, or by increasing body side area : the addition of a forward fin, ahead of the centre of gravity, would therefore be doubly helpful, lengthening the period and improving the damping.

In studying response to applied moments attention is chiefly concentrated upon response to ailerons, and the theoretical results are compared with a theoretical standard motion produced by a constant rolling moment together with a yawing moment varied so as to suppress sideslip. Response at high speeds is shown to be insensitive to changes in l_v and n_v within their normal ranges, and good response to pure rolling moment is assured for all lateral stability characteristics other than those associated with the combination of small fin with large dihedral : this combination is worst at high values of the lateral relative density. The effect of adverse yawing moment from the ailerons is detrimental, and becomes worse as the dihedral is increased or fin area decreased.

CONTENTS

* R.A.E. Report Aero. 2040 received 18th July, 1945, and R.A.E. ~~Technical Note~~ Report Aero. 1952 received 20th May, 1946.

CONTENTS—*contd.*

Part II. Response to a Sharp Edged Side-gust

Part III. Response to Rolling and Yawing Moments

CONTENTS—*contd.*

PART I

Preliminary

1. *Introduction.*—The present report describes the results of a small part of the work on lateral response carried out on the differential analyser at Manchester University from December, 1943, to February, 1944. Sufficient work was done in the period to get a good general picture of the response of an aeroplane to applied rolling and yawing moments, or to a side-gust, over a wide range of parameters. The part of this programme dealing with lateral response of aeroplanes moving at high speeds has now been thoroughly analysed, and the results are presented herein. Further work on response at slow speeds, in ultra-high-lift conditions, and on the lateral response of tailless aeroplanes, was also done, and will be discussed in later reports.

The report has been split into two sections, Parts II and III dealing with response to side-gusts, and to applied moments, being preceded by Part I containing the analytical preliminaries, while the final discussion and conclusions are contained in Part IV. Some matters of detail are contained in Appendices I and II, while a list of symbols is given in Appendix III. In this form the report replaces two original R.A.E. reports, treating the response to side-gust and response to applied moments separately, and consisting broadly of the present Parts II and III with separate introductions and conclusions.

A word should be added about the unconventional numbering of the figures in this report. The differential analyser is a powerful and rapid tool in response investigations, and the preparation of a report on work carried out with its aid brings one up against the difficulty of selecting a relatively small number of report figures from the vast mass of results turned out by the machine. The method employed on the machine is to vary the numerous parameters over their appropriate ranges and to determine the changes in the resulting solutions. This method shows us the effect of varying one parameter for different sets of values of the others: if this variation has the same general effect in all such sets, the reproduction of all sets in a report is hardly justified. Nor, on the other hand, should reference to the missing evidence be suppressed. It was felt that the problem could best be solved by preparing a full set of figures covering all the work done by the machine, numbering this set seriatim, and referring when necessary to the figures of this set by the serial number prefixed by the letter S, to avoid confusion with the figures published in this report, which have their own serial numbering. Figures referred to in the text and enclosed in square brackets, *e.g.* Fig. [S.44], are not included in the selection given herewith.

The authors wish to express their warmest thanks to Professor Hartree and his staff at Manchester for instructing them in the use of the differential analyser, and to Miss M. M. Dent for assistance in the running of the machine: also to Messrs. J. A. H. Shepperd and V. D. Naylor, and to Misses M. Lofts and F. M. Ward, for part of the analytical work involved in the preparation of this report.

2. *Equations of Motion and Scope of the Calculations.*—2.1. *Equations of Motion.*—The lateral equations of motion were used in the standard form (Mitchell[1], 1943) valid for small disturbances,

$$\left.\begin{aligned} \frac{d\hat{v}}{d\tau} + \bar{y}_v\hat{v} + \hat{r} - k\phi &= 0 \\ \mathscr{L}\hat{v} + \frac{d\hat{p}}{d\tau} + l_1\hat{p} - l_2\hat{r} &= \mathscr{C}_l \\ -\mathscr{N}\hat{v} + n_1\hat{p} + \frac{d\hat{r}}{d\tau} + n_2\hat{r} &= \mathscr{C}_n \\ -\hat{p} + \frac{d\phi}{d\tau} &= 0 \\ -\hat{r} + \frac{d\psi}{d\tau} &= 0 \\ \frac{d\hat{y}}{d\tau} - \hat{v} - \psi &= 0 \end{aligned}\right\}, \quad \ldots \quad (2.1.1)$$

where the notation used is as follows: $\hat{v}$, ϕ, ψ are the angles of sideslip, bank, and yaw, in radians, $\hat{p}$ and $\hat{r}$ the angular velocities in roll and yaw, in radians per airsec. The airsec is

$$\hat{t} = \frac{W}{g\rho SU_e} \quad \ldots \quad (2.1.2)$$

true secs., where W is the weight of the aeroplane (lb.), g the acceleration due to gravity (ft./sec.^{2}), ρ the air density (slugs/ft.^{3}), S the wing area of the aeroplane (ft.^{2}), and U_e its forward velocity (ft./sec.): τ denotes time in airsecs. The lateral distance of the airoplane from its steady flight path is $\hat{y}$, in units $U_e\hat{t}$ ft. The aerodynamic derivatives are

$$\left.\begin{aligned} \bar{y}_v &= -y_v\,, \quad \mathscr{L} = -\mu_2 l_v/i_A\,, \quad \mathscr{N} = \mu_2 n_v/i_C \\ l_1 &= -l_p/i_A\,, \quad l_2 = l_r/i_A\,, \quad n_1 = -n_p/i_C\,, \quad n_2 = -n_r/i_C \end{aligned}\right\}, \quad \ldots \quad (2.1.3)$$

the quantities y_v, μ_2, l_v, n_v, l_p, l_r, n_p, n_r, i_A, i_C and $k = \frac{1}{2}C_L$ having the meanings given by Bryant and Gates[2] (1937). To allow for the variation of n_r and n_v, we write

$$\left.\begin{aligned} n_v &= n_{v0} + n_{vf} \\ n_r &= -ln_{vf} \end{aligned}\right\}, \quad \ldots \quad (2.1.4)$$

where n_{v0}, n_{vf} are body and fin contributions respectively, and l is the fin and rudder arm, in units of the semi-span $\frac{1}{2}b$. Further

$$\mathscr{C}_l = \mu_2 C_l/i_A\,, \quad \mathscr{C}_n = \mu_2 C_n/i_C\,, \quad \ldots \quad (2.1.5)$$

where C_l, C_n are the ordinary rolling and yawing moment coefficients.

The equations, in the above form, are valid for an aeroplane in level flight at high speeds, when the effect of the product of inertia terms in the moment equations[2] is almost certainly negligible.

2.2. *Scope of the Calculations.*—The primary aim of the investigation, and the aspect from which it is mainly approached in this paper, was to make a general survey of the response of a high speed aeroplane to a side-gust or to the application of ailerons and rudder, as a function not only of the main stability parameters n_{vf}, l_v, but also of the lateral relative density μ_2, the inertia coefficients i_A, i_C, and the rotary derivatives, none of which are easily variable once the broad features of a design have been laid down. The procedure that appeared most pertinent was to make a survey, in some detail, of the dependence of response upon l_v and n_v for fixed values

of the remaining parameters, and then to vary the latter, for a small number of combinations of l_v and n_v, so as to establish the general manner of variation with the inertia coefficients and rotary derivatives. The programme carried out therefore splits naturally into four stages, which we have called basic, variation of inertias, variation of μ_2, and variation of rotary derivatives. Full details of these stages are given below.

It should be noted that the procedure was not quite as consistent as the above statement suggests. Broadly speaking the same basic values of the various parameters are used throughout. The exception to this is the parameter μ_2, which had the value 20 throughout the basic and variation of inertia stages, but for which the value 5 was used in examining the variation of rotary derivatives. The reason for this procedure was that the first programme of calculations carried out at Manchester during this visit was intended to cover conventional aeroplane in high-speed flight, and variation of rotary derivatives was not originally intended. The programme continued, however, with an investigation of a proposed large transport aeroplane, the Bristol 167, and, as time permitted, the effects of the rotary derivatives were investigated by changing them one by one from their basic values to the values calculated for this aeroplane. The calculations were naturally made for the value $\mu_2 = 5$ appropriate to the Bristol 167, and since $\mu_2 = 5$ was also examined in the variation of μ_2 stage, a direct discussion of the effects of changes in the rotary derivatives is still possible.*

It is to be noted also that the fixed value $C_L = 0{\cdot}2$ was used throughout the conventional high-speed and Bristol 167 programmes. The primary reason for this is that so many parameters vary, and the character of the results changes so much, as C_L varies, that an alteration in C_L necessarily involves a very considerable change in the set-up on the differential analyser, whereas a change in any other parameter involves changing only one or two gear trains, and the time taken can be cut to an almost negligible proportion of the total running time if the changes are well thought out in advance. Further, some results for $C_L = 1{\cdot}0$ were already available†, before the present programme was started.

2.3. *Basic Stage.*—The following values were taken for the fixed parameters

$$\left.\begin{array}{lll} C_L = 0{\cdot}2\,, & k = 0{\cdot}1\,, & \mu_2 = 20 \\ \bar{y}_v = 0{\cdot}2\,, & l_p = -\,0{\cdot}42 & \\ l_r = 0{\cdot}06\,, & n_p = -\,0{\cdot}03 & \\ l = 1\,, & n_{v0} = -\,0{\cdot}024 & \\ i_A = 0{\cdot}12\,, & i_C = 0{\cdot}18 & \end{array}\right\}, \quad .. \quad .. \quad .. \quad (2.3.1)$$

while n_{vf} and l_v were taken as variable parameters, given all combinations of the following values:—

$$\left.\begin{array}{llll} n_{vf} = 0\,, & 0{\cdot}024\,, & 0{\cdot}072\,, & 0{\cdot}120 \\ l_v = 0{\cdot}06\,, & 0\,, & -0{\cdot}06\,, & -0{\cdot}12 \end{array}\right\}. \quad .. \quad .. \quad .. \quad (2.3.2)$$

By inadvertence, some calculations were made with $n_v = 0{\cdot}06$, and some with $l_v = 0{\cdot}12$, and in addition, the relatively small change in response from $n_{vf} = 0{\cdot}072$ to $n_{vf} = 0{\cdot}120$ suggested the advisability of using $n_{vf} = 0{\cdot}048$ and $n_{vf} = 0{\cdot}120$ in the remaining stages of the calculation, so the cases

$$n_{vf} = 0{\cdot}048\,, \qquad l_v = 0\,, \qquad -0{\cdot}12\,, \qquad .. \quad .. \quad .. \quad .. \quad (2.3.3)$$

were added.

These values were chosen to cover the reasonably attainable ranges in l_v and n_{vf} consistent with stability, and in addition to include cases showing marked instability (*see* section 4).

---

* The effects of changes in rotary derivatives are probably most important at low values of μ_2.

† Gandy[3] (1943), Mitchell and Thorpe[5] (1943), and Fehlner[7] (1942).

2.4. *Variation of Inertias.*—The fixed parameters were given their basic values, except for i_A and i_C, which were given the three other combinations of values

$$\left.\begin{aligned} i_A &= 0{\cdot}06 \text{ with } i_C = 0{\cdot}12 \\ i_A &= 0{\cdot}06 \text{ with } i_C = 0{\cdot}18 \\ i_A &= 0{\cdot}12 \text{ with } i_C = 0{\cdot}12 \end{aligned}\right\} \quad \ldots \quad (2.4.1)$$

The parameters n_{vf} and l_v were given all combinations of the values

$$\left.\begin{aligned} n_{vf} &= 0{\cdot}048\,, \quad 0{\cdot}120 \\ l_v &= 0\,, \quad -0{\cdot}12 \end{aligned}\right\} \quad \ldots \quad (2.4.2)$$

The results of these calculations show, for the four l_v, n_{vf} combinations taken, the effects of

(*a*) change of i_A at a fixed i_C,

(*b*) change of i_C at a fixed i_A,

(*c*) simultaneous change of i_A and i_C so as to keep $i_A - i_C$ constant.

2.5. *Variation of* μ_2.—The fixed parameters were given their basic values, except for μ_2, which was given the four other values

$$\mu_2 = 5,\ 10,\ 40,\ 80. \quad \ldots \quad (2.5.1)$$

Four l_v, n_{vf} combinations, as (2.4.2), were taken.

2.6. *Variation of Rotary Derivatives.*—The following parameters were taken as fixed, with the values given

$$\left.\begin{aligned} C_L &= 0{\cdot}2\,, \quad k = 0{\cdot}1\,, \quad \mu_2 = 5 \\ i_A &= 0{\cdot}12\,, \quad i_C = 0{\cdot}18 \end{aligned}\right\} \quad \ldots \quad (2.6.1)$$

The remaining parameters, other than n_{vf}, l_v, were changed one by one, in the order given (the changes being cumulative) :—

$$\left.\begin{aligned} n_p &\text{ from } -0{\cdot}03 \text{ to } -0{\cdot}015 \\ l_r &\text{ from } \ 0{\cdot}06 \text{ to } \ 0{\cdot}052 \\ l_p &\text{ from } -0{\cdot}42 \text{ to } -0{\cdot}54 \\ \bar{y}_v &\text{ from } \ 0{\cdot}2 \text{ to } \ 0{\cdot}233 \\ l &\text{ from } \ 1 \text{ to } \ 0{\cdot}652 \\ n_{v0} &\text{ from } -0{\cdot}024 \text{ to } -0{\cdot}033 \end{aligned}\right\} \quad \ldots \quad (2.6.2)$$

Calculations were made, after each change, for each of the four n_{vf}, l_v combinations (2.4.2).

2.7. *Initial Conditions, etc.*—Three calculations were made for every combination of derivatives considered, as follows :—

(i) Response to side-gust:

$$\left.\begin{aligned} &\hat{p} = \hat{r} = \phi = \psi = \hat{y} = 0\,,\ \hat{v} = 1\text{: initially} \\ &\mathscr{C}_l = \mathscr{C}_n = 0\text{: throughout} \end{aligned}\right\}, \quad \ldots \quad (2.7.1)$$

(ii) Response to rolling moment:

$$\left.\begin{aligned} \hat{p} = \hat{v} = \hat{r} = \phi = \psi = \hat{y} = 0 &: \text{ initially} \\ \mathscr{C}_l = 1,\ \mathscr{C}_n = 0 &: \text{ throughout} \end{aligned}\right\}, \quad .. \quad .. \quad .. \quad .. \quad (2.7.2)$$

(iii) Response to yawing moment:

$$\left.\begin{aligned} \hat{p} = \hat{v} = \hat{r} = \phi = \psi = \hat{y} = 0 &: \text{ initially} \\ \mathscr{C}_l = 0\ ,\ \mathscr{C}_n = 1 &: \text{ throughout} \end{aligned}\right\} \ldots \quad .. \quad .. \quad .. \quad (2.7.3)$$

The full scheme of cases solved is given in Tables 1 and 2, where each case is identified by the serial number of the " run " on the differential analyser.* The side-gust case (Table 1) accounted for 82 runs, and the rolling and yawing moment cases (Table 2) for a further 159 runs, giving a total of 241. Of these 86 were devoted to the basic programme, the exploration of the variation with n_{vf}' and l_v' being carried well into unstable regions. A further 40 and 51 runs were made in the variation of inertia and variation of μ_2 stages. The remaining 64 runs were devoted to the changes of rotary derivatives, and were carried out in skeleton form, the machine being stopped to take readings at intervals of $\frac{1}{2}$ or 1 airsec, instead of $\frac{1}{4}$ airsec, which was taken as standard throughout the remainder of the programme.

3. *Application of the Results to Particular Cases.*—The differential analyser results were obtained for one value of C_L, and for five values of μ_2. Now we have

$$\mu_2 = \frac{2W}{g\rho S b}, \qquad C_L = \frac{W}{\frac{1}{2}\rho S U_e^2}, \quad .. \quad .. \quad .. \quad .. \quad .. \quad (3.1)$$

whence

$$\left.\begin{aligned} U_e &= b^{1/2}\,(g\mu_2/C_L)^{1/2} \\ W/(S\sigma) &= \tfrac{1}{2}b\mu_2 g\rho_0 \end{aligned}\right\}, \quad .. \quad .. \quad .. \quad .. \quad .. \quad .. \quad .. \quad (3.2)$$

and from (2.1.2)

$$\hat{t} = \tfrac{1}{2}b^{1/2}\,(\mu_2 C_L/g)^{1/2} = \tfrac{1}{2}U_e C_L/g\ , \quad .. \quad .. \quad .. \quad .. \quad .. \quad .. \quad (3.3)$$

where ρ_0 is the air density (slugs/ft.^{3}) at sea level, and $\sigma = \rho/\rho_0$ is the ratio of the atmospheric density to that at sea level. Given the span of an aeroplane, these formulae enable us to calculate the particular velocity and effective wing loading $W/(S\sigma)$ to which the results apply, and the corresponding aerodynamic unit of time Numerically, for $\mu_2 = 20$,

$$\left.\begin{aligned} U_e &= 56{\cdot}745 b^{1/2} \text{ ft./sec. } (= 38{\cdot}69 b^{1/2} \text{ m.p.h.}) \\ W/(S\sigma) &= 0{\cdot}7657 b \text{ lb./ft.}^2 \\ \hat{t} &= 0{\cdot}1762 b^{1/2} = 0{\cdot}3106\ (U_e/100) \text{ secs.} \end{aligned}\right\} \quad .. \quad .. \quad .. \quad (3.4)$$

These relationships have been plotted in Figs. 1 and 2, which give $\hat{t}$ and U_e, and $W/(S\sigma)$ for $C_L = 0{\cdot}2$, $\mu_2 = 5$, 10, 20, 40, 80, as functions of b. Fig. 2 also contains a series of curves from which W/S can be deduced, for a series of operational heights. These curves give a clear general picture of the ranges of size, wing loading and speed to which the results apply. A more definite idea of the meaning of the results can be obtained by considering typical aeroplanes. As representative of $\mu_2 = 20$ we may take an aeroplane of span 42·25 ft. and wing loading 32·35 lb./ft.^{2}. This flies at sea-level at $C_L = 0{\cdot}2$ at 251·5 m.p.h., the airsec being 1·1455 true secs. The whole set of curves for varying μ_2 can similarly be regarded as applying to five aeroplanes of spans 169, 84·5, 42·25, 21·125 and 10·56 ft., all flying at the typical speed and loading above, $\hat{t}$ being 1·1455 throughout. From this point of view the curves for different values of μ_2 are directly

* The term " run ", in differential analyser jargon, describes the process of obtaining a single complete solution of a system of differential equations, with given initial conditions.

comparable without change of scale, and we have provided the curves of response to side-gust reproduced in this report with alternative scales, in natural units, to suit this range of typical aeroplanes (for which $\mu_2 b = 845$). The quantities $\hat{v}/\hat{v}_0$, $\phi/\hat{v}_0$, $\psi/\hat{v}_0$ of course, are dimensionless, while $\hat{p}/\hat{v}_0$ and $\hat{r}/\hat{v}_0$ are measured in radians per airsec per radian initial sideslip, so the dimensionless curves can be compared directly for any cases in which the lengths of the airsec are the same.

Alternatively, the curves for different values of μ_2 may be thought of as referring to one and the same aeroplane flying under various conditions, the effective loading $W/(\sigma S)$ and speed being varied together so as to keep C_L constant. Change of μ_2 from this point of view is change of height at constant indicated airspeed: the airsec varies, so that the time-scales of the curves need adjustment before they can be compared. Thus the curves for $\mu_2 = 20$, 40, 80 may be supposed to refer to the typical aeroplane of 42·25 ft. span at sea level, 20,000 and 40,000 ft. respectively, the airsec having the respective values 1·1455, 1·620 and 2·291 true secs. Some examples of such curves, brought to the same natural time scale, are given in Figs. 3, 4 and 5.

We have not considered it advisable to provide the curves of response to rolling and yawing moment with alternative scales in natural units. The original curves obtained give $\hat{p}$, $\hat{v}$, $\hat{r}$, ϕ, ψ, $\hat{y}$ for $\mathscr{C}_l = 1$, or $\mathscr{C}_n = 1$, and would naturally be labelled $\hat{p}/\mathscr{C}_l$, $\hat{v}/\mathscr{C}_l$, etc. Now we have

$$\left.\begin{aligned} &\frac{\hat{p}}{\mathscr{C}_l} = \frac{i_A}{C_l}\frac{pb}{2U_e}, \quad \frac{\hat{r}}{\mathscr{C}_l} = \frac{i_A}{C_l}\frac{rb}{2U_e}, \\ &\frac{\hat{v}}{\mathscr{C}_l} = \frac{1}{\mu_2}\frac{i_A}{C_l}\hat{v}, \quad \frac{\phi}{\mathscr{C}_l} = \frac{1}{\mu_2}\frac{i_A}{C_l}\phi, \frac{\psi}{\mathscr{C}_l} = \frac{1}{\mu_2}\frac{i_A}{C_l}\psi \\ &\frac{\hat{y}}{\mathscr{C}_l} = \frac{1}{\mu_2^2}\frac{i_A}{C_l}\frac{2y}{b}, \end{aligned}\right\} \ldots \quad (3.5)$$

where p and r are rates of roll and yaw in radians per (true) second, and y is sideways displacement in feet. The alternative forms given here are more convenient for some purposes, and we have therefore added them to the bulk of our curves. The labels $\hat{p}/\mathscr{C}_l$, etc. are also given, being standard in the full set of curves. Now when i_A is changed, the resulting response curves are effectively plotted on a different scale, for the same initial C_l. We have therefore multiplied all components by $0{\cdot}12/i_A$, and the curves showing the effects of variation of inertias have been labelled accordingly, $\frac{0{\cdot}12}{i_A}\frac{\hat{p}}{\mathscr{C}_l}$, etc., or $\frac{0{\cdot}12}{C_l}\frac{pb}{2U_e}$, $\frac{0{\cdot}12}{C_l}\frac{rb}{2U_e}$, $\frac{1}{\mu_2}\frac{0{\cdot}12}{C_l}\hat{v}$, $\frac{1}{\mu_2}\frac{0{\cdot}12}{C_l}\phi$, $\frac{1}{\mu_2}\frac{0{\cdot}12}{C_l}\psi$, $\frac{1}{\mu_2^2}\frac{0{\cdot}12}{C_l}\frac{2y}{b}$. The dual labelling removes, we think, all need for the addition of natural units.

As regards the time, addition of a natural time scale would perhaps be helpful. For the typical aeroplane, however, the dimensionless and natural time scales are very similar, and we have preferred the alternative of labelling the time scale as

$$\tau = (322/U)t, \quad (U_e \text{ in ft./sec.}). \quad \ldots \quad (3.6)$$

The yawing moment curves have been similarly treated, being brought where necessary to a standard value of 0·18 for i_C, and labelled dually as $\frac{\hat{p}}{\mathscr{C}_n}$, etc., or $\frac{i_C}{C_n}\frac{pb}{2U_e}$, $\frac{i_C}{C_n}\frac{rb}{2U}$, $\frac{1}{\mu_2}\frac{i_C}{C_n}\hat{v}$, $\frac{1}{\mu_2}\frac{i_C}{C_n}\phi$, $\frac{1}{\mu_2}\frac{i_C}{C_n}\psi$, $\frac{1}{\mu_2^2}\frac{i_C}{C_n}\frac{2y}{b}$ for most of the curves given, or $\frac{0{\cdot}18}{i_C}\frac{\hat{p}}{\mathscr{C}_n}$ etc., or $\frac{0{\cdot}18}{C_n}\frac{pb}{2U_e}$, $\frac{0{\cdot}18}{C_n}\frac{rb}{2U_e}$, $\frac{1}{\mu_2}\frac{0{\cdot}18}{C_n}\hat{v}$, $\frac{1}{\mu_2}\frac{0{\cdot}18}{C_n}\phi$, $\frac{1}{\mu_2}\frac{0{\cdot}18}{C_n}\psi$, and $\frac{1}{\mu_2^2}\frac{0{\cdot}18}{C_n}\frac{2y}{b}$, in the curves showing variation of inertias.

4. *Stability of the Cases Examined.*—In any investigation of response, one point of interest will always be the examination of the correlation, if any, between stability roots and response characteristics. It it therefore of interest to study the stability roots for the various cases considered, before passing on to a discussion of the response results. Stability roots for all the cases examined are shown in Table 3, classified under headings indicating the appropriate stages of the programme to which they belong. The figures entered in the columns headed " exact " are obtained by solution of the stability equations, those in the columns headed " approximate " from the formulae of section 7.1. Besides the roots, the numbers of swings to halve amplitude are given, for the lateral oscillation.

The basic programme, with its inadvertent extensions, covered a very wide range of n_v and l_v, going well outside the normal range of positive n_v and negative l_v, where the stability equation has two real and two complex roots, into regions with very different characteristics. To illustrate the variation in the nature of the roots Fig. 6 was prepared, showing the spiral and oscillatory stability boundaries for the basic conditions, together with the curve of equal roots which separates regions with four real roots from those with the normal root distribution. This curve has two branches, parts of both appearing in Fig. 6. while near the origin of the (n_v, l_v) diagram it possesses a loop, shown on an enlarged scale in the inset Fig. 6A. Within this loop the stability equation has two pairs of complex roots; otherwise the character of the roots is as indicated in Fig. 6.

As Fig. 6 indicates, and the numerical values of the roots confirm, instability of the lateral oscillation is encountered only in the region of small n_v and large dihedral $(-l_v)$, and then only when μ_2 is large. The damping is, however, generally inadequate, as is more clearly seen from the numbers of swings to halve amplitude, which for the basic cases range from 0·81 upwards, for the usual negative values of l_v, though better damping could be obtained by using positive values of l_v. The general way in which the number of swings to halve amplitude varies is shown by the curves along which this quantity is constant, which are shown for the basic case in Fig. 7, together with lines of constant frequency and constant oscillation damping. Variations of the inertia parameters slightly affect the picture, but the main variable is the quantity μ_2, high values of this leading to particularly distressing oscillations.

It will be noted from an examination of Table 3 and Fig. 6, that regions where there is no oscillation, broadly speaking those where n_v is negative, are all unstable, with at least one divergence, which is very sensitive to n_v and reaches a dangerous value for only slightly negative n_v. Stability considerations, therefore, suggest that such regions are to be avoided.

In regions with positive n_v spiral instability occurs if the value of l_v is too small, but it is never serious, even for the large positive values of l_v included in the scheme by inadvertance. In the very worst case included the time to double amplitude is likely to exceed 5 (true) seconds, which should give the pilot ample time to control the motion. From the pure stability point of view, therefore, event he largest positive values of l_v examined would seem to be admissible at the value of C_L considered.

To give an idea of the meaning of the stability roots in natural units, the periods and times to half amplitude of spiral motion and lateral oscillation have been evaluated for the typical aeroplane of section 3. The results are given in Table 4.

PART II

Response to a Sharp-edged Side-gust

5. *Introduction.*—The lateral response of a high-speed aeroplane to a sharp-edged side-gust has been selected as the first topic of discussion, not on account of its theoretical importance, but because of the troubles recently experienced by certain small aeroplanes in this connection. The importance of this problem, too, has led to the development of an approximate treatment of response to a side-gust, which has been used below to extend and generalise the differential analyser results.

Complaints have been made of the behaviour of small ultra-high-speed aeroplanes in bumpy air conditions: the trouble is described as a rapid oscillation in sideslip and yaw, with a period of order $1\frac{1}{2}$ to 2 secs., and with a poor damping, of the order one to two complete swings to halve amplitude. This oscillation occurs in many high-speed aeroplanes, and apparently becomes a serious difficulty when its period is too short to permit of effective corrective action being taken by the pilot. The train of oscillations arising from one bump is then still perceptible when the next bump strikes the aeroplane, and the oscillation therefore acquires a permanent character, most unpleasant for the pilot, and prejudicial to accurate gunfire. This situation arises most noticeably with small aeroplanes, and we have paid particular attention to this application of the work.

6. *The Response Curves.*— 6.1. *Basic.*—We have discussed above the main conclusions to be drawn from an examination of the stability roots and their variation with the main parameters. These conclusions are necessarily vague; the knowledge that a certain mode of motion exists is incomplete without the knowledge of the extent to which it is excited. In the case before us, we know that initially $\hat{v} = \hat{v}_0$, $\hat{p} = \hat{r} = \phi = \psi = \hat{y} = 0$: if a stable case is considered, we know that this will subside to the steady motion condition, but we do not know, nor can we infer without a complete solution, to what extent the initial amplitudes are shared between the spiral and rolling subsidences, and the lateral oscillation. We can, it is true, get an idea of the extent to which other components are involved, from the fact that initially

$$\left.\begin{aligned} \frac{d\hat{p}}{d\tau} &= -\mathscr{L}\hat{v} \\ \frac{d\hat{r}}{d\tau} &= \mathscr{N}\hat{v} \end{aligned}\right\}, \qquad \text{(6.1.1)}$$

so that l_v and n_v control the magnitude and direction of the initial swings in $\hat{p}$ and $\hat{r}$ respectively, and may reasonably be expected to affect the general extent to which roll and yaw are involved in the subsequent motion.

The response curves, however, give a much clearer picture of the behaviour. Taking the basic set as a whole, Figs. [S.1–S.48], the oscillatory character of the motion is so marked that it is impossible to tell whether there is any excitation of the other modes: the only exceptions to this are those directionally neutral or unstable cases where the oscillation has been replaced by two real roots, and the violent instability in these cases should be noted. Figs. 9, 10, 13 and 16 (S.2, S.8, S.14 and S.20) have been chosen to illustrate this: these figures show the response in $\hat{v}$ against time, each figure showing the results for several values of n_v at a fixed value of l_v: in addition, Fig. 20 (S.38) shows a cross-plot of the same quantity against τ for $n_v = 0{\cdot}048$, for various values of l_v. Curves of $\hat{v}$ are the most natural to study from the point of view of the damping of the motion: they show the effect of dihedral very clearly, the effect of making l_v more positive being to increase the damping (very materially in Fig. 20 but not to such a marked extent with greater n_v as in Fig. 22 = S.44 and at the same time slightly to increase the period. The way in which n_v controls the period is also clearly seen, particularly in Figs. 13 and 16: the improvement in damping as n_v increases is also clear, and the curves of $\hat{v}$, superficially regarded, would suggest that the best conditions would be obtained with large n_v and small or positive l_v.

This conclusion cannot be maintained when we look a little more deeply into the meaning of the $\hat{v}$ curves, or examine the associated curves of other components. This investigation is essentially concerned with response to gusts: in reasonably calm conditions the steady motion may be disturbed by an occasional side-gust, the response to which should be damped out before the arrival of the next, and should in any case be small. Damping as such is important in this connection, but is not of such immediate importance when we consider behaviour in gusty weather, where the aircraft will be disturbed by a second gust before the motion due to the first has damped out. In such a case it is the magnitude of the overall response which matters, and the investigation of this demands the study of other components, which shows the effect of n_v in quite a different light. The components $\hat{r}$ and ψ are probably the most important quantities in this connection, and are shown in Figs. 17 (S.21) and 19 (S.23) respectively. The result shown in Fig. 19 is quite typical. The initial kick in ψ is almost independent of n_v (and almost independent of l_v as in Fig. 25 = S.47, and in virtue of the rapid decrease of period with increasing n_v, this implies an initial kick in $\hat{r}$ which increases strongly as n_v increases. This is well seen in Fig. 17, which also shows that the improved damping with larger n_v has taken control before the end of 5 airsecs: in Fig. 11 (S.9) on the other hand, where reduced dihedral has already given an improved damping, the amplitude in $\hat{r}$ at the end of 5 airsecs. is seen to be tolerably independent of n_v. Clearly a typical gust structure must be assumed before we can get any definite answer: it must be remarked, however, that our curves represent the motion of an aeroplane after passing into a region where there is a constant side velocity, which is thereafter maintained. A true gust could probably be represented by such a side-gust lasting for a short time only, almost certainly very much less than 5 airsecs. even for the smallest likely values of $\hat{t}$. Records of the motion due to such a gust could be obtained from our curves by superposition: the results would, however, depend very markedly upon the assumed time of continuation of the sideways velocity, and it is probably sufficient for our purpose to say that the important point is the magnitude of the response to the constant side-gust for the first 1 to 2 secs. This makes smallness of response more important than damping, where these requirements are in conflict, and a small value of n_v is therefore indicated, as shown also by the full set of $\hat{r}$ and ψ curves, Figs. 11, 17, 23 (S.45) [and S.3, S.15, S.27, S.33, S.39] for $\hat{r}$, Figs. 19, 25 [and S.5, S.11, S.17, S.29, S.41] for ψ.

The argument in favour of a small value of n_v is further strengthened by the following considerations. If the pilot sits at the centre of gravity of the aircraft, his motion is the same as that of the C.G., and his seat must therefore exert upon him a side-force corresponding to the aerodynamic force on the aircraft, measured by the accelerative effect ng, where

$$n = -\frac{Y_v U_e \hat{v}}{W}$$

$$= \frac{\rho U_e}{w} \bar{y}_v \frac{\hat{v}}{\hat{v}_0} V_g, \quad \ldots \quad \ldots \quad \ldots \quad \ldots \quad \ldots \quad \ldots \quad (6.1.2)$$

where $V_g = U_e \hat{v}_0$ is the gust velocity, $w = W/S$. The force acting upon the pilot at the C.G. is therefore proportional to the ordinate of a $\hat{v}/\hat{v}_0$ curve, and depends initially upon the derivative $\bar{y}_v$ alone: its subsequent variations depend upon all the derivatives, but its general magnitude is largely independent thereof.

Now a pilot, subjected to a constant accelerating force, will compensate for it by constant muscular tensions of which he will be relatively unconscious: change of acceleration will involve change of muscular tension, and it appears likely that the more rapidly a periodic acceleration changes from a maximum in one direction to a maximum in the other, the more conscious will be the resulting adjustments in muscular tension. Thus " jerk ", or rate of change of acceleration,* may be the criterion of the unpleasantness of a particular motion, and on this ground a slow oscillation is to be preferred to a more rapid one. These is also the point that the pilot's reaction time may be too great to permit of his making the necessary control movements to damp out

* The term " jerk " is used with this strict meaning by automobile spring designers and is worthy of retention here.

artificially an oscillation having less than a certain critical period. These arguments would indicate that when the period of oscillation is very short, a poorly damped but slow motion may be preferable to a well damped but quick one. At what period in seconds this consideration begins to dominate is a question for physiology rather than stability, but the available evidence appears to indicate that a period of the order encountered here, possibly $1\frac{1}{2}$ to 2 secs. is somewhere near or beyond the limit of controllability for most pilots.

A new point arises when we consider the force acting upon a pilot seated away from the C.G. The accelerative effect is then $n'g$, where

$$n' = \frac{\rho U_e}{w} V_g \left\{ \bar{y}_v \left(\frac{\hat{v}}{\hat{v}_0}\right) - \frac{1}{\mu_2} \frac{2l}{b} \frac{d}{d\tau} \left(\frac{\hat{r}}{\hat{v}_0}\right) \right\}$$

$$= \frac{\rho U_e}{w} V_g \left\{ \bar{y}_v \left(\frac{\hat{v}}{\hat{v}_0}\right) - \frac{2l}{b\mu_2} \mathscr{N} \left(\frac{\hat{v}}{\hat{v}_0}\right) + \frac{2l}{\mu_2 b} n_1 \left(\frac{\hat{p}}{\hat{v}_0}\right) + \frac{2l}{\mu_2 b} n_2 \left(\frac{\hat{r}}{\hat{v}_0}\right) \right\} , \qquad .. \quad (6.1.3)$$

where l is the distance (ft.) of the pilot's seat ahead of the C.G., and where $d(\hat{r}/\hat{v}_0)/d\tau$ has been expressed in terms of calculated quantities by means of the equations of motion. This expression has been evaluated from the differential analyser results for the basic conditions, $n_{vf} = 0{\cdot}120$, $l_v = -0{\cdot}12$, for $2l/b = 0, \pm\frac{1}{2}$. The results are shown in Fig. 8, together with the appropriate ψ curve. It will be seen that a rear position of the pilot's seat increases the magnitude of the accelerating force felt by the pilot, without changing appreciably its phase relationship with the angle of yaw, and is not likely to affect the pilot's reactions materially. On the other hand, a forward position of the pilot's seat reduces the accelerating force, and may reverse its phase relationship to the yaw. Thus the sensitivity of the pilot's muscular system as a yawmeter will be much reduced, and the whole system of conditioned reflexes on which the pilot relies to control a rapid oscillatory motion may be upset, if the seat position is too far forward. This point may explain the complaints which have been made about certain small aeroplanes, in which the pilot's position is well forward of the C.G., on the score of troublesome lateral oscillations, and it is intended to discuss the matter further in a separate report when the necessary calculations have been completed.

The choice of l_v is not such a thorny problem: response in $\hat{p}$ and ϕ is shown in Figs. 21 and 24 (S.43 and S.46), for large fin at various values of l_v, and ϕ is also shown in Fig. 14 (S.16) for $l_v = -0{\cdot}06$ for various fins. The magnitude of the initial kick in $\hat{p}$, and the general magnitude of this quantity, depend strongly upon l_v, and the motion in bank is very small when l_v is zero. Thus damping and magnitude of response alike suggest that l_v should be small: if we go on to make l_v positive the damping of the oscillation becomes better, but more rolling motion is excited. Further, the spiral instability does become evident, as is seen particularly in Fig. 24, where the aeroplane does not return to an even keel at any stage of the motion: the degree of instability shown is not, however, very marked. The fin size also has a marked effect on the development of angle of bank, mainly by controlling the period, so that with larger n_v and quicker period reversal of the rate of roll takes place sooner, and the angle of bank attained is smaller. The effect is very marked, as seen in Fig. 14, but is of no importance when $l_v = 0$, Fig. 12 (S.10).

6.2. *Variation of Inertias.*– The effects of variations in the inertia coefficients i_A, i_C are very small, as shown in the full set in Figs. [S.49 to S.72]. Change in i_C has the more noticeable effect, reduction in i_C diminishing the period of the motion and giving a slight increase in damping, as in Fig. 26 (S.62,) while the initial kicks in $\hat{r}$ are increased. Change in i_A has an almost negligible effect on $\hat{v}$, $\hat{r}$ and ψ, for small i_C, but is slightly more noticeable when i_C is large. The rate of roll and angle of bank are very small for $l_v = 0$: with large dihedral ($l_v = -0{\cdot}12$) they are more important, and effects due to inertia are noticeable, the motion being noticeably flattened on reducing i_C: increasing i_A has a small tendency in the same direction.

In general the effects due to changes in these parameters are less than an examination of the stability roots would suggest: the only important effect is the dependence of period upon i_C.

6.3. *Variation of* μ_2.—The curves showing the dependence of the motion upon the parameter μ_2, Figs. [S.73 to S.96,] must be studied with circumspection, since μ_2 cannot be changed on a particular aeroplane at a given C_L without changing the unit of aerodynamic time and the true speed. We may, however, picture a series of five aeroplanes of different spans such that $b\mu_2$ is the same for all: these then have the same wing loading and same unit of aerodynamic time, and fly at the same speed. The dimensionless time scales are then immediately applicable, and the results for varying μ_2 are most easily regarded in this way, as showing primarily the effect of diminishing span, as μ_2 increases.

The evil effects of decrease in span under these conditions are shown very clearly in Fig. 27 (S.74,) which shows the response in $\hat{v}$ for the case $l_v = 0$, $n_v = 0{\cdot}024$, also in Fig. 31 (S.86) for $l_v = 0$, $n_v = 0{\cdot}096$. In both these figures the damping is seen to be tolerably independent of μ_2, while the period decreases markedly as μ_2 increases, and span decreases. The effect is even worse in Fig. 30 (S.80,) for $l_v = -0{\cdot}12$, $n_v = 0{\cdot}024$, where the destabilising effect of dihedral is increased with increased μ_2, and the high values of μ_2 show divergent oscillations of very quick period: $l_v = -0{\cdot}12$, $n_v = 0{\cdot}096$ (Fig. 32 = S.92) is half-way to this stage, the oscillations still being damped at $\mu_2 = 80$, but with much diminished damping. Increase of μ_2 also makes ψ, and more so $\hat{r}$, oscillate more rapidly between wider limits, as in Figs. 28 (S.75) and 29 (S.77), for $l_v = 0$, $n_v = 0{\cdot}024$. It will be seen also, on comparing Figs. 29 and 33 (S.95), which show roughly equal initial kicks in ψ for all μ_2 and both n_v covered, that the initial kick in $\hat{r}$ is roughly proportional to $\mu_2 n_v$, or, as (6.1.1) would indicate, to the parameter $\mathcal{N}$. Thus the greater μ_2 is, the greater is the amount of response in rate of yaw to a given initial gust, and the more rapid the motion. The considerations which, in the basic case $\mu_2 = 20$, led us to prefer a reduction in n_v for its effect in lengthening the period to an increase in this parameter with the resulting increase in damping, therefore apply with even more force here, so that with decreasing size of aeroplane the problem becomes more and more difficult of solution.

With $l_v = 0$, there is little response in rate of roll or bank; with dihedral, however, these quantities are excited to an extent increasing with increase of n_v.

Alternatively, as suggested in section 3, the variation of μ_2 can be regarded as due to a change of height for the same aircraft flying at the same C_L and therefore at the same I.A.S. The marked effect upon period is in this case spurious, since it is counterbalanced by an equivalent change in the unit of aerodynamic time: a similar effect takes place with rate of yaw, which is found to be tolerably independent of height. These effects are illustrated in Figs. 3, 4, 5, corresponding to Figs. 27, 30 and 28 respectively, and giving their results in natural units. The effect of change of height is therefore seen to be a loss of damping, with little change in period, or amplitude in rate of yaw: increase in height is seen to cause instability in Fig. 4.

6.4. *Variation of Rotary Derivatives.*—The set of curves showing the effect of variations in the rotary derivatives [Figs. 97 to 120], all calculated for $\mu_2 = 5$, when the problem presented by the lateral oscillation is not so serious, indicate that these variations produce only minor changes in the response curves, and produce no drastic effects which could not have been foreseen from an examination of the stability roots. It has not been thought advisable, therefore, to give any of the curves illustrating these changes, particularly since their reproduction in report form would not be very satisfactory.

7. *Approximate Treatment.*—7.1. *Approximate formulae for the roots.*—Examination of the response curves as above brings out well certain general features of the motion, but the limitation to $C_L = 0{\cdot}2$ is restrictive, and prevents us from following the change in character of the motion with changes from this condition. Attention has therefore been turned to the development of an approximate treatment, leading to general formulae for the periods and dampings and amplitudes of the various components under quite general conditions. With this end in view, use has been made of certain approximate expressions for the roots of the lateral stability equation, developed by one of the authors (K.M.) in connection with unpublished glider stability calculations.* These expressions are as follows :—

* A brief derivation of these approximations has been added (Appendix I) in preparing this report for publication in the R. & M. series.

The damping r_s of the spiral motion is given, for level flight, by*

$$r_s = \frac{n_r \bar{l}_v - l_r n_v}{\bar{l}_p n_v + (\bar{n}_p + \frac{1}{2} i_C C_L) \bar{l}_v} \frac{C_L}{2}, \quad .. \quad .. \quad .. \quad .. \quad .. \quad .. \quad (7.1.1)$$

where

$$\bar{n}_r = - n_r \text{ etc.}$$

The damping r_r of the rolling subsidence is given roughly by

$$r_r = l_1 - \frac{l_2 n_1}{l_1} + \frac{(n_1 + \frac{1}{2} C_L) \mathscr{L}}{(l_1 - l_2 n_1/l_1)^2 + 2 (n_1 + \frac{1}{2} C_L) \mathscr{L}/(l_1 - l_2 n_1/l_1)} \cdot \ldots \quad .. \quad (7.1.2)$$

The damping r_l of the lateral oscillation is given roughly by†

$$r_l = - \tfrac{1}{2} r_s + \tfrac{1}{2} n_2 + \tfrac{1}{2} \bar{y}_v + \frac{\frac{l_2 n_1}{r_r}\left(1 - \frac{\bar{y}_v}{r_r}\right) - \frac{l_2 C_L}{2 r_r^3} \mathscr{N} - \frac{\mathscr{L}}{r_r^2}\left\{n_1 + \frac{1}{2} C_L \left(1 - \frac{n_2}{r_r}\right)\right\}}{2\left\{\left(1 - \frac{\bar{y}_v}{r_r}\right)\left(1 - \frac{n_2}{r_r}\right) + \frac{\mathscr{N}}{r_r^2}\right\}} \cdot \ldots \quad .. \quad (7.1.3)$$

The frequency of the lateral oscillation is given roughly by

$$f_l^2 = \frac{l_1 \mathscr{N} + (n_1 + \frac{1}{2} C_L) \mathscr{L}}{r_r}. \quad .. \quad .. \quad .. \quad .. \quad .. \quad .. \quad (7.1.4)$$

With this notation, the four roots are

$$\lambda_1 = - r_s, \qquad \lambda_2 = - r_r, \qquad \lambda_{3,4} = - r_l \pm i f_l. \quad .. \quad .. \quad .. \quad (7.1.5)$$

These have been calculated from the above formulae for all the cases solved, and the results are given in Table 3, with the corresponding exact roots. Comparison of the various results shows that the formulae are within a few per cent. for all cases with a reasonable amount of directional stability, the worst result being obtained when $\mathscr{L}$ and $\mathscr{N}$ are both large. The spiral stability formula certainly fails when $D^2 - CE$ is small, where C, D, E, are coefficients in the stability equation,

$$\lambda^4 + B\lambda^3 + C\lambda^2 + D\lambda + E = 0, \quad .. \quad .. \quad .. \quad .. \quad .. \quad (7.1.6)$$

but no such cases have been considered in our programme.

Further, (7.1.3) and (7.1.4) do give a reasonable indication of the way in which the damping and frequency of the lateral oscillation vary with the rotary derivatives as well as with the major stability parameters.

7.2. *Approximate Formulae for the Period.*—These formulae have been tested also, in glider stability calculations, for $C_L = 0{\cdot}4$, and found to be equally reliable. They may therefore be used for more general values of C_L in the high-speed region, and the general formulae desired are thus obtained. The period of the lateral oscillation is thus

$$T = \frac{2\pi \hat{l}}{f_l} = \frac{\pi}{(\frac{1}{2} g \rho_0)^{1/2}} \frac{1}{U_c} \left(\frac{w i_C b}{\sigma n_v}\right)^{1/2} = 16{\cdot}06 \frac{1}{U_c} \left(\frac{w i_C b}{\sigma n_v}\right)^{1/2} \text{secs.} \quad .. \quad .. \quad .. \quad (7.2.1)$$

with reasonable accuracy, and is therefore inversely proportional to velocity, and proportional to the square root of the product of the wing loading by the span. It is obviously appropriate

* The same formula has recently been given by Gandy[3] (1943).

† A similar formula, which does not appear to be so accurate, has been given by Bryant and Hopwood[4].

to lay down some lower tolerable limit for the period: if we put this at 2 secs., we obtain the design criterion

$$\frac{wbi_C}{U_e^2\sigma} > 0{\cdot}0155\, n_v \ldots \qquad (7.2.2)$$

We may usefully form an idea of the order of the periods involved by considering a typical aeroplane, which we may take in round figures as having a span of 50 ft., effective wing loading $w/\sigma = 40$ lb./ft.^{2}, speed 400 ft./sec., with $i_C = 0{\cdot}10$, $n_v = 0{\cdot}05$. The period for this is $2{\cdot}54$ secs., and we thus have

$$T = 2{\cdot}54\,\frac{400}{U}\left(\frac{1}{40}\frac{w}{\sigma}\right)^{1/2}\left(\frac{i_C}{0{\cdot}1}\right)^{1/2}\left(\frac{b}{50}\right)^{1/2}\left(\frac{0{\cdot}05}{n_v}\right)^{1/2} \text{secs.} \ldots \qquad (7.2.3)$$

The fact that a period of this order is obtained in these conditions indicates that the motion is apt to be troublesome in general.

7.3. *Approximate Treatment of Damping.*—Calculation of the oscillatory damping by (7.1.3) indicates that the important contributions are those arising from the terms

$$\tfrac{1}{2}n_2 + \tfrac{1}{2}\bar{y}_v - \tfrac{1}{2}\frac{n_1 + \tfrac{1}{2}C_L\left(1 - \frac{n_2}{r_r}\right)}{\mathscr{N} + r_r^2\left(1 - \frac{\bar{y}_v}{r_r}\right)\left(1 - \frac{n_2}{r_r}\right)}\mathscr{L} \,. \qquad (7.3.1)$$

The effect of $\mathscr{L}$ is destabilising, so that small values of dihedral are indicated, and if these are already used, the only ways open to us by which the damping may be improved are the increase of n_2 and $\bar{y}_v$. Increase of fin area will increase n_2, but at the expense of a decrease of period: decrease of i_C will have the same joint effects, so that the only available method of making any substantial increase in damping is by an increase in the body side area, by a forward fin or otherwise, so as to increase both n_2 and $\bar{y}_v$ without producing an accompanying increase in n_v.

The entries in Table 3, Part IV, indicate that the effects on the damping of changes in the other derivatives are small; the only appreciable change there shown is the reduction in damping due to change of fin arm, and this is due to the smaller fin contribution to n_2. It should also be noted that it may well prove necessary, from other considerations, to have a fairly large dihedral*: the destabilising effect of this will be least when r_r is greatest, *i.e.* particularly for small values of i_A.

The effect of change in loading upon the character of the motion is best seen by evaluating the number of swings to half-amplitude, the dimensionless quantity

$$0{\cdot}110\,\frac{f_l}{r_l} = 0{\cdot}110\,\frac{\mathscr{N}^{1/2}}{\tfrac{1}{2}(n_2 + \bar{y}_v)}$$

very roughly, which is thus proportional to $(w/b\sigma)^{1/2}$. High wing loading and small span are therefore bad from this point of view. It is worthy of remark that this expression is independent of speed for a given aeroplane at constant loading. Pilots complaining of this oscillation have made little or no mention of the effect of speed, and this suggests that the number of swings for which the oscillation persists may be one of its most unpleasant features: possibly too one of the most valuable ways to regard the whole matter is that the pilot tends subconsciously to check the oscillation until, with increasing speed, the period becomes too short for him to do so, after which he notices mostly the number of swings to damp out.

* This depends largely upon the maximum admissible rate of spiral divergence at high values of C_L, when this feature becomes more disturbing. It is hoped to investigate this more fully in the near future.

7.4. *Approximate Treatment of Amplitudes.*—Application of operational methods to the complete solution of equations (2.1) shows that the motion following the prescribed initial conditions is given by

$$\left.\begin{aligned} \hat{v} &= \sum_{i=1}^{4} v_i\,\alpha_{iv}\exp(\lambda_i\tau) \\ \hat{p} &= \sum_{i=1}^{4} p_i\,\alpha_{iv}\exp(\lambda_i\tau) \\ \hat{r} &= \sum_{i=1}^{4} r_i\,\alpha_{iv}\exp(\lambda_i\tau) \\ \phi &= \sum_{i=1}^{4} \phi_i\,\alpha_{iv}\exp(\lambda_i\tau) \end{aligned}\right\}, \quad \ldots\ \ldots\ \ldots\ \ldots\ \ldots\ \ldots \quad (7.4.1)$$

where the λ_i are the roots of the stability equation, and where v_i, p_i, r_i, ϕ_i are the "modal amplitudes", and α_{iv} the "modal response coefficients to initial sideslip" defined by Mitchell[5] (1943). We have, when $\varepsilon_A = \varepsilon_C = \tan\gamma_e = 0$,

$$\left.\begin{aligned} v_i &= \lambda_i^2 + (l_1 + n_2)\,\lambda_i + l_1 n_2 + l_2 n_1 \\ p_i &= -\mathscr{L}\lambda_i - n_2\mathscr{L} + l_2\mathscr{N} \\ r_i &= \mathscr{N}\lambda_i + l_1\mathscr{N} + n_1\mathscr{L} \\ \phi_i &= p_i/\lambda_i \end{aligned}\right\}, \quad \ldots\ \ldots\ \ldots\ \ldots \quad (7.4.2)$$

and

$$\alpha_{iv} = \frac{\lambda_i}{\prod_{j\neq i}(\lambda_i - \lambda_j)}. \quad \ldots\ \ldots\ \ldots\ \ldots\ \ldots\ \ldots\ \ldots \quad (7.4.3)$$

We also have

$$\sum_{i=1}^{4} v_i\alpha_{iv} = 1. \quad \ldots\ \ldots\ \ldots\ \ldots\ \ldots\ \ldots\ \ldots\ \ldots \quad (7.4.4)$$

We may now proceed to approximate to these, confining our attention to cases with at least a certain positive degree of directional stability, and to values of μ_2 of the order of 20, where the lateral oscillation is likely to be troublesome. We may then proceed as follows:—

(i) λ_1 (spiral damping) may be neglected in comparison with λ_2 and λ_3, and λ_3 may be taken as if_l, to give α_{1v} roughly as $\alpha_{1v} = -r_s/(r_r f_l^2)$, a small number of order 0·001. It is easily seen also that v_1 is of order unity, so that the contribution to $\Sigma v_i\alpha_{iv}$ made by the spiral mode, $v_1\alpha_{1v}$, is negligible.

(ii) Arguing similarly, we find roughly $\alpha_{2v} = 1/(r_r^2 + f_l^2)$, of order 0·1 at most. Estimation of v_2 is not easy :—We must use the best available approximation, $-\lambda_2 = B - r_s - 2r_l$, to get

$$-\lambda_2 = l_1 - \frac{\dfrac{l_2 n_1}{l_1}\left(1 - \dfrac{\bar{y}_v}{r_r}\right) - \dfrac{l_2 C_L}{2r_r^3}\mathscr{N} - \dfrac{\mathscr{L}}{r_r^2}\left\{n_1 + \tfrac{1}{2}C_L\left(1 - \dfrac{n_2}{r_r}\right)\right\}}{\left(1 - \dfrac{\bar{y}_v}{r_r}\right)\left(1 - \dfrac{n_2}{r_r}\right) + \dfrac{\mathscr{N}}{r_r^2}}.$$

Hence

$$v_2 = (\lambda_2 + l_1)(\lambda_2 + n_2) + l_2 n_1$$

$$= l_2 n_1 \left| 1 + \frac{\frac{\lambda_2 + n_2}{l_1}\left(1 - \frac{\bar{y}_v}{r_r}\right)}{\left(1 - \frac{\bar{y}_v}{r_r}\right)\left(1 - \frac{n_2}{r_r}\right) + \frac{\mathscr{N}}{r_r^2}} \right|$$

$$- \frac{\frac{l_2 C_L}{2r_r^3}\mathscr{N} + \frac{\mathscr{L}}{r_r^2}\left\{ n_1 + \frac{1}{2}C_L\left(1 - \frac{n_2}{r_r}\right)\right\}}{\left(1 - \frac{\bar{y}_v}{r_r}\right)\left(1 - \frac{n_2}{r_r}\right) + \frac{\mathscr{N}}{r_r^2}} (\lambda_2 + n_2) .$$

The first term is likely to be much less than $0 \cdot 2$, the term in $\mathscr{N}$ is very small, while the $\mathscr{L}$ term can be estimated roughly as $-\frac{1}{4}\mu_2 l_v/l_p$, so may slightly exceed unity for large l_v and μ_2. The product $v_2\alpha_{2v}$ is therefore of maximum order $0 \cdot 1$ at most, and neglecting the contribution to $\hat{v}$ from the rolling subsidence will therefore be admissible with an error not more than 10 per cent.

(iii) Since both the real roots make contributions to $\hat{v}$ which we have seen to be negligible, we may take the motion given by

$$\left.\begin{aligned} \hat{v} &= \exp(-r_l\tau)\cos f_l\tau \\ \hat{p} &= |p_3/v_3| \exp(-r_l\tau)\sin f_l\tau \\ \hat{r} &= |r_3/v_3| \exp(-r_l\tau)\sin f_l\tau \\ \phi &= |\phi_3/v_3| \exp(-r_l\tau)\sin f_l\tau \end{aligned}\right\} \quad \ldots\ \ldots\ \ldots\ \ldots\ \ldots\ \ldots \quad (7.4.5)$$

as giving a reasonable first approximation to the oscillatory part of the motion in these components, with

$$\psi = \left|\frac{r_3}{v_3}\right| \frac{\exp(-r_l\tau)}{r_l^2 + f_l^2} \left\{ f_l(1 - \cos f_l\tau) - r_l \sin f_l\tau \right\} . \quad \ldots\ \ldots\ \ldots\ \ldots \quad (7.4.6)$$

These expressions are, of course, hopelessly in error in the matter of phase, but they do give reliable expressions for the amplitudes of the oscillatory parts of the motion in the various components. We may then proceed to express them in natural units, for a given gust velocity V_g, so that the initial amplitude of the oscillation in side-slip is V_g/U_e, inversely proportional to the speed of the aeroplane. We have, retaining only the major contributions,

$$\left.\begin{aligned} |v_3| &= |(-r_l + if_l)^2 + (l_1 + n_2)(-r_l + if_l) + l_1 n_2 + l_2 n_1| \\ &\simeq |-f_l^2 + il_1 f_l| = f_l(f_l^2 + l_1^2)^{1/2} \\ |p_3| &= |\mathscr{L}(r_l - n_2) + l_2\mathscr{N} - i\mathscr{L}f_l| \simeq \mathscr{L}f_l \\ |r_3| &= |\mathscr{N}(l_1 - r_l) + n_1\mathscr{L} + i\mathscr{N}f_l| \simeq \mathscr{N}(f_l^2 + l_1^2)^{1/2} \\ |\phi_3| &= |p_3/\lambda_3| \simeq \mathscr{L} \\ |\psi_3| &= |r_3/\lambda_3| \simeq \mathscr{N}(f_l^2 + l_1^2)^{1/2}/f_l \end{aligned}\right\} \quad \ldots\ \ldots\ \ldots \quad (7.4.7)$$

Thus the amplitudes of the oscillatory motion caused by a gust velocity V_g are:—

In sideslip $\quad V_g/U_e$,

In angle of yaw $\quad (V_g/U_e)(\mathscr{N}/f_l^2) \simeq V_g/U_e$,

In angle of bank $\quad \dfrac{V_g}{U_e} \dfrac{\mathscr{L}}{f_l(f_l^2 + l_1^2)^{1/2}}$,

In rate of yaw $$\frac{V_g}{U_e}\frac{1}{\hat{t}}\frac{\mathscr{N}}{f_l} = V_g\,(2g\rho_0)^{1/2}\left(\frac{\sigma}{wb}\frac{n_v}{i_C}\right)^{1/2},$$

In rate of roll $$\frac{V_g}{U_e}\frac{1}{\hat{t}}\frac{\mathscr{L}}{(f_l^2 + l_1^2)^{1/2}}.$$

The magnitudes of the oscillation in bank and roll depend upon the dimensionless frequency; when this is not too large the l_1^2 term will predominate, otherwise the f_l^2 term. We thus get amplitudes

In angle of bank: $$\frac{V_g}{U_e}\left(\frac{2}{g\rho_0}\right)^{1/2}\bar{l}_v\left(\frac{w}{\sigma b}\frac{i_C}{\bar{l}_p n_v}\right)^{1/2}$$ for small frequency,

$$\frac{V_g}{U_e}\frac{\bar{l}_v}{n_v}\frac{i_C}{i_A}$$ for large frequency,

In rate of roll: $$V_g\frac{2}{b}\frac{\bar{l}_v}{\bar{l}_p}$$ for small frequency,

$$V_g\,(2g\rho_0)^{1/2}\frac{\bar{l}_v}{i_A}\left(\frac{\sigma}{wb}\frac{i_C}{n_v}\right)^{1/2}$$ for large frequency.

The amplitude of the yawing acceleration should also be noted: this is

$$V_g\,2g\rho_0 U_e\left(\frac{\sigma}{wb}\frac{n_v}{i_C}\right).$$

It is not possible to use these formulae to give approximate response curves, because while we have been able to show that modes other than the oscillation make a negligible contribution to $\hat{v}$, there is no indication that they do not contribute to the other variables, particularly to ϕ and ψ. As a rough check, however, the first maxima in the $\hat{p}$ and $\hat{r}$ curves have been measured for the basic cases, and corrected for the effect of the damping acting from the start of the motion until the maximum is reached, to give amplitudes in rates of roll and yaw for comparison with those given by (7.4.5) and (7.4.7). The results, given in Table 5, indicate that the approximate formulae give excellent results for $\hat{r}$. The rate of roll, on the other hand, is not so well approximated: the numerical values are as much as 50 per cent. out, but the general trends of the variations with n_v and l_v are undoubtedly correct.

8. *Discussion.*—8.0. *General.*—The approximate formulae, together with the results obtained by the differential analyser, give a good general picture of the way in which the motion due to a side gust depends upon the aeroplane's size, weight, conditions of flight, and stability parameters.

It is clear that at low values of C_L this motion consists almost entirely of an oscillation of short period and that the number of swings to halve amplitude is unpleasantly large. The general effects of the main parameters upon various features of the motion have been summarised in Table 6.

8.1. *Effect of span.*—It appears that, given the velocities of aeroplane and gust, the amplitudes in sideslip and yaw are independent of aeroplane size and loading, as is the angle of bank when the period is short. The effects of shortening the period by change of size or loading are, then, to leave the maximum angles of response constant, to increase the rates of roll and yaw inversely with the period, and the accelerations in roll and yaw inversely with the square of the period. A short period thus has the bad effect of causing a violent motion.

Given the stability derivatives, the period is approximately proportional to $(1/U_e)\,(wb/\sigma)^{1/2}$ and the number of swings to halve amplitude varies as $(w/b\sigma)^{1/2}$. A low wing loading has therefore an unfavourable effect on period but a favourable effect on the damping: high velocity has an

adverse effect on the period but a beneficial effect in reducing the maximum angles of response due to a given gust velocity. A small span however has an unfavourable effect on both period and damping.

It appears then that aeroplanes of small span will be especially liable to a lateral oscillation with a most troublesome short period. The period is approximately proportional to $(C_L b i_C / n_v)^{1/2}$, the square root indicating the difficulty of designing for large changes in the period. The survey of this paper shows that for a typical fighter* with derivatives in the normal ranges, the period is between 2 and 3 secs., and cannot be very materially lengthened without using a value of n_v which would be dangerously small for other reasons. No complaints have been made of the Spitfire, but on some other small aeroplanes pilots complain of an oscillation in azimuth which tends to persist in rough weather and is impossible to control. Besides being uncomfortable this impairs firing accuracy. There seems no reason why the damping in these aeroplanes should be less than in the Spitfire, but the measured periods associated with these adverse reports are of order $1\frac{1}{2}$ to 2 secs. at cruising speed, and so significantly less than for the Spitfire. It may be that these are below the limit at which the pilot can effectively control the motion, and the root of the trouble may be that he feels helpless in passing through a train of gusts in rough weather. The critical period can only be guessed from scanty evidence: it is probably of the order of 2 secs.

In judging the decay of a motion of such a frequency the pilot's unit of time is naturally the period itself, hence the importance of number of swings to halve amplitude.

8.2. *Effect of Speed.*—The analysis has been mainly confined to a C_L of 0·2, but the effects of speed on the motion should be summarised. In the response to a side-gust V_g, the variations of the significant quantities with forward speed are

period	$\propto 1/U_e$
swings to halve amplitude	roughly constant
initial kick in azimuth	$\propto V_g/U_e$
initial kick in lateral acceleration at C.G.	$\propto V_g U_e$

The existence of a critical period below which the pilot cannot control the motion implies a critical speed, dependent upon size, loading, and stability parameters, above which the period is too short for control. At higher speeds the pilot will notice the number of swings to halve amplitude, which is independent of speed, and his impressions will be of an oscillation occurring first at a definite speed and thereafter remaining with unchanged characteristics. It is however true that the decreasing period makes the motion more jerky as speed increases, although the initial disturbance in azimuth is reduced. The discomfort caused by rapid changes in lateral acceleration may also be very unpleasant, as the initial amplitude, growing as U_e, is associated with the shortening period. These effects have not yet been sorted out by measurement on the aeroplanes under criticism.

8.3. *Difficulty of Improvement.*—Ideally, the way out of the difficulties sketched in section 8.1 would be as follows,

(*a*) to decrease the initial kick in azimuth, thereby reducing response irrespective of period,

(*b*) to increase the period above the limit of pilot's effective action, so as to put the pilot in command of the situation, even if the damping is thereby decreased,

(*c*) to increase the damping.

Considering these in turn, (*a*) must be ruled out because the initial kick in azimuth is to a first approximation independent of the derivatives.

* Span 42 ft., wing loading 32 lb./sq. ft., speed 250 m.p.h.

The period can be increased only by decrease of n_v. If this is done in the ordinary way by cutting down rear fin, the damping is decreased through n_v and y_v, and the number of swings to halve amplitude may rise in spite of the increase in period. The only way of satisfying both (*b*) and (*c*) by redistributing the side area is the inconvenient one of adding fin ahead of the C.G. Nevertheless it may pay to decrease rear fin in order at all costs to raise the period above the critical value.

The damping may be increased either by a decrease in dihedral or by an increase in rear fin. As l_v has a negligible effect on the period in the normal range of n_v it should, in the context of this problem, be as small as is consistent with safety at slow speed. To increase n_v is to run into the dilemma already mentioned. This has not yet been fully resolved. There is no doubt however that in designing a small high-speed aeroplane the fin area should if possible be adjusted to raise the period above 2 secs. at cruising speed.

8.4. *Possible Importance of Cockpit Position.*—It seems possible that the pilot's objection to the motion may be partly bound up with the lateral acceleration at his seat, and its phase relation to the azimuth. The initial lateral acceleration at the C.G. is proportional to $\bar{y}_v U_e V_g$; the subsequent "jerk" or rate of change increases as the period shortens ; and the acceleration is in phase with the rate of yaw, so that in response to a side-gust from starboard the pilot feels a maximum force to port as the nose begins to swing to starboard.

If the pilot is seated behind the C.G. the yawing acceleration increases the lateral force at his seat without appreciably altering its phase. But if he is in front of the C.G. the yawing acceleration may reverse the sign of the lateral force, so that the pilot now feels a maximum force to starboard as the nose begins to swing to starboard. It may be significant that in most of the oscillations complained of the pilot was seated in front of the C.G.

PART III

Response to Rolling and Yawing Moments

9. *Introduction.*—In this part we continue our study of lateral response at high speeds, dealing now with the response to applied rolling and yawing moments. The prime interest here is the response of an aeroplane to ailerons, rather than to pure rolling moment, and this has been investigated by calculating, from the differential analyser results, complete new sets of curves, many of which are reproduced here in preference to the original curves showing response to rolling moment. The immediate differential analyser results, therefore, play an apparently small role, but are the basis for the whole of this part of the report.

10. *A Norm for Aileron Response.*—10.1. *Theory.*—In discussing the considerable mass of curves of response to pure rolling moment obtained by the differential analyser, and the even greater mass of curves which can be obtained by combining rolling and yawing moments in varying proportions, the need for some standard of comparison is bound to make itself felt. In considering response in roll, simple rolling theory* may be used, but is very artificial, and gives no indication of response in yaw and sideslip, and is not therefore valuable as an aid to analysis. From the practical point of view, of course, simple rolling theory is a very rapid method of estimating rolling response, and it is therefore of interest to examine how well it approximates the actual curves.

A more hopeful norm can be obtained from the consideration that pilots usually use the rudder, in most normal manœuvres, essentially to check the development of sideslip. Our norm may then be a manœuvre executed without sideslip, and it is natural to take the motion resulting from the same aileron application as in the response curves considered, when the rudder is so manipulated as to keep sideslip zero throughout. Assuming for the present that the rudder is powerful enough, and that rudder hinge moments are light enough, for this manœuvre to be possible, the motion may be obtained mathematically as follows. We want a solution of equations (2.1) for a given $\mathscr{C}_l, \mathscr{C}_n$ being varied in such a way as to keep $\hat{v}$ (and hence $d\hat{v}/d\tau$) zero throughout. This solution can be obtained from equations (2.11), omitting the sideslip terms and the yawing moment equation: the required $\mathscr{C}_n$ is then given by substitution of the solution obtained into the yawing moment equation. The formulae are given in full in Appendix I, and have been used to calculate the norm curves, which are plotted on the appropriate figures.

10.2. *The Norm Curves.*—Since sideslip is suppressed and the required yawing moment provided by the rudder, l_v, n_v and n_r have no effect on the motion. The amount of rudder required to produce the manœuvre is, however, dependent on fin area through its effect on n_r. Thus, for the basic programme, variation of inertias, and variation of μ_2, we obtain only two different results for each of $\hat{p}$, $\hat{r}$, ϕ, ψ, $\hat{y}$, depending upon the inertia coefficient i_A, and these results are shown, multiplied by $0{\cdot}12/i_A$, in Figs. 34–37. The corresponding values of $\mathscr{C}_n(t)$ depend upon more parameters, i_C through n_1 and n_2, and n_{vf} through n_2, and are shown in Figs. 38–41, in each case C_n/C_l being plotted.

The application of a varying yawing moment, so as to suppress sideslip, also suppresses the lateral oscillation, and alters the magnitudes of the other stability roots. When $i_A = 0{\cdot}12$, we find roots $\alpha_1 = -3{\cdot}514$, $\alpha_2 = 0{\cdot}0142$, and when $i_A = 0{\cdot}06$, $\alpha_1 = -7{\cdot}014$, $\alpha_2 = 0{\cdot}0142$. These should be compared with the rolling and spiral roots in Table 3: the change in the rolling root is not important, but the normally stable spiral is converted into a slow divergence. On simple rolling theory, there is only a single real root, $-3{\cdot}5$ and -7 in the two cases, and the response in $\hat{p}$ on simple rolling theory has been calculated and is shown in Fig. 34 for comparison with the true response without sideslip.

---

* The equations of motion are simplified to $d\hat{p}/d\tau + l_1\hat{p} = \mathscr{C}_l$, $d\varphi/d\tau = \hat{p}$, having the solution

$$\hat{p} = \mathscr{C}_l\{1 - \exp(-l_1\tau)\}/l_1, \quad \varphi = \mathscr{C}_l\{\exp(-l_1\tau) - 1 + l_1\tau\}/l_1^2.$$

Examining the curves, the response in roll is seen to be admirable, $\hat{p}$ rising rapidly to a nearly steady value, and subsequently slowly increasing. Simple rolling theory gives a very close approximation to this motion, except for the divergence, but this is too slow to matter. The motion in the other components is not of much interest, and the main feature to be noticed in all the curves is the variation with i_A. A small rolling inertia gives a more rapid response, and makes all quantities slightly greater at any instant than they would be, at the same instant, had i_A been larger. The difference, however, is unimportant except when considering the attainment of the highest possible degree of manœuvrability.

The variation of yawing moment required is of more interest, since we wish to be assured that the yawing moment needed does not exceed the maximum yawing moment that can be applied and that the rudder motion is reasonable and possible to the pilot. Neither question is very suitable for discussion in a general report of this nature, but we note that the rudder motion, initially rapid and then slower in the same direction, is quite reasonable. Slightly larger values of C_n/C_l are needed throughout, for $i_C = 0{\cdot}18$, than for $i_C = 0{\cdot}12$. A small yawing inertia is therefore favourable in allowing this sideslip-free manoeuvre to be carried further with a given rudder.

We shall not touch on hinge moment questions here, but we may briefly consider the magnitude of C_n/C_l. Many ailerons will produce a small adverse yawing moment, $-C_n/C_l$ ranging from 0 to $0{\cdot}1$ at this value of C_L. This will have to be cancelled by the rudder, and the motion given by Figs. 38–41 superimposed, and the values of C_n/C_l required must therefore be increased by from 0 to $0{\cdot}1$. Now let us assume an applied C_l of $0{\cdot}04$ (giving $pb/2U_e$ about $0{\cdot}1$), and a maximum C_n of $\frac{1}{3}n_{vf}$, or $0{\cdot}04$ for $n_r = -0{\cdot}120$, $0{\cdot}024$ for $n_r = -0{\cdot}072$ and $0{\cdot}008$ for $n_r = -0{\cdot}024$. We then see that full aileron may be applied and held on, and sideslip suppressed,

(1) for more than 5 airsecs., with $n_r = -0{\cdot}120$ or $-0{\cdot}072$, for any reasonable degree of adverse yaw from ailerons,

(2) for more than 5 airsecs., with $n_r = -0{\cdot}024$, with no adverse yaw,

(3) for about $\frac{1}{2}$ airsec., with $n_r = -0{\cdot}024$, with $-0{\cdot}1$ adverse yaw.

This indicates simply and clearly how a criterion for rudder size, and hence n_{vf}, is to be obtained but further consideration of this is deferred for the present. The high speed case here examined obviously requires only a small rudder, if $pb/2U_e = 0{\cdot}1$ is to be regarded as sufficient.

11. *Response to Pure Rolling Moment.*—11.1. *Basic Programme.*—11.10. *General.*—The basic programme, as we have mentioned, was intended to give a very full general survey of the effects of changes in the main stability parameters l_v and n_v, for a given set of values of μ_2, inertias, and rotary derivatives, at $C_L = 0{\cdot}2$. The full sets of results are contained in Figs. [S.121–S.168], of which Figs. [S.121–S.144] show the results for a fixed l_v with varying n_v, and Figs. [S.145–S.168] those for fixed n_v and varying l_v.

11.11. *Rolling response in unstable regions.*—The general character of the response to rolling moment of a directionally unstable aircraft is illustrated by Figs. [S.145–S.150], which show $\hat{p}$, $\hat{v}$, $\hat{r}$, ϕ, ψ and $\hat{y}$ as functions of τ for $n_v = -0{\cdot}024$, for $l_v = -0{\cdot}12$, $-0{\cdot}06$, 0, $0{\cdot}06$ and $0{\cdot}12$. In all these cases the stability roots include one rapid divergence, and the corresponding mode is strongly excited, though it varies in character as l_v varies. Response in rate of roll is shown in Fig. 78 (S.145,) and in angle of bank in Fig. 79 (S.148). With all values of l_v, the rate of roll shows the usual rapid initial increase to a value in the neighbourhood of that given by the simple rolling theory or the theory of section 10, in much the time suggested by these theories: the subsequent behaviour, however, depends strongly upon l_v. With positive values of l_v the rapid increase of $\hat{p}$ continues, after a slight check, at a steadily increasing rate, but, with the usual negative l_v, $\hat{p}$ passes through a maximum and diverges negatively, the angle of bank reversing. Motion in the other components does not depend much upon l_v. There is a rapidly increasing

positive sideslip, and a rapidly increasing negative rate of yaw, and very small sideways displacement: these features are adequately illustrated by Fig. 42, showing $\hat{v}$, $\hat{r}$, ψ and $\hat{y}$ for the case $l_v = 0$. The scatter due to variation of l_v is not important.

When the aeroplane is directionally neutral results of a similar character are obtained, as seen in Figs. [S.151–S.156], drawn for $n_v = 0$ and the same five values of l_v. The only change to be noted here is that for negative values of l_v the divergence is replaced by a very strongly excited but fairly slow oscillation, seen best in ϕ, Fig. 80 (S.154). The angle of yaw, Fig. 81 (S.155), still has a negative tendency. It is impossible to tell from inspection of the curves whether the oscillation is stable, but the stability roots (Table 3), show stability with $l_v = -0{\cdot}06$, slight instability if $l_v = -0{\cdot}12$. The special case where n_v and l_v are both zero is of interest. Here the rolling response itself is excellent, rising rapidly to a maximum close to that of the norm and then very slowly decaying, but the aeroplane continues to sideslip and yaw against the bank at a steadily increasing rate. All six components are shown in Fig. 43, with the norm for comparison.

In all the above cases the aeroplane would obviously be uncontrollable, and it is clearly essential for n_v to be positive, though this is not theoretically a necessary condition for stability. On the other hand, though $l_v < 0$ is a necessary condition for stability, there is nothing in the results for positive l_v to suggest any great difficulty, at a low value of C_L. Plots of the six components are given in Figs. [S.121–S.126] for $l_v = 0{\cdot}06$, and for $n_v = -0{\cdot}024$, 0, $0{\cdot}048$ and $0{\cdot}096$. With the positive values of n_v we obtain a response which differs only in degree from that of a fully stable aeroplane. There is a rapid increase of $\hat{p}$ at first, Fig. 77 (S.121), followed by a slow increase with a slight superimposed oscillation: the general value of $\hat{p}$ is rather greater than the norm. The aeroplane sideslips slightly in the positive sense, and after an initial period of yawing against the bank, goes into a steepening turn, roughly true-banked. Considerable sideways displacement takes place once the turning regime has set in.

11.12. *Rolling response in normal stability regions.*—In the more normal stability regions, with positive n_v and negative l_v, the response to rolling moment shows only a slight dependence upon these parameters. The full range of possible variation is shown in Figs. 44–48, showing $\hat{p}$, $\hat{v}$, $\hat{r}$, ϕ, ψ and $\hat{y}$ for four combinations of n_v and l_v, namely each of $n_v = 0{\cdot}024$ and $0{\cdot}096$ with $l_v = 0$ and $-0{\cdot}12$, and with the norm added for comparison. The initial rapid increase in $\hat{p}$ (Fig. 44a) is almost independent of both parameters, but a higher value is reached with small l_v. After this stage a slow increase in $\hat{p}$ takes place for $l_v = 0$, almost independent of n_v, while for $l_v = -0{\cdot}12$ the subsequent motion shows the rate of roll oscillating about a mean value much lower then the equilibrium rate of roll predicted by simple rolling theory: the amplitude of the oscillation is considerable when n_v is small. The curve for $n_v = 0{\cdot}120$, $l_v = 0$ is indistinguishable from the norm. Since the aim of applying rolling moment is to produce as large a steady state of roll as possible, as quickly as possible, the main desideratum from this point of view appears to be a small value of l_v, or if a moderate or large negative l_v must be used for other reasons, as large a value of n_v as possible, With small l_v, however, the value of n_v has practically no effect upon the development of rate of roll.

The effect of varying n_v is more clearly seen in Fig. 47, which shows the motion in angle of yaw, and in which increasing n_v is seen to reduce the duration of the initial period in which the aeroplane yaws against the roll. The curve for the norm again closely resembles that for $n_v = 0{\cdot}120$, $l_v = 0$, but lies above it, as there is no initial stage of adverse yaw. Making l_v more negative reduces the yawing motion in the later stages. This aspect of the motion is not, however, of much importance. Comparison of the curves of sideslip and sideways displacement, Figs. 44b, 48, shows that these quantities and adverse yawing motion go together, so that large n_v and small l_v ensure the minimum duration of adverse yaw, the maximum sideways displacement, and the minimum sideslip. The variations shown are not important enough for these considerations to weigh in choice of n_v and l_v. The possibility of a fin-stall following aileron application should also be mentioned: the smallness of the values of $\hat{v}$ indicates that there is no risk whatever of this taking place, when the ailerons produce no adverse yawing moment.

We saw in the preceding paragraph that there was nothing objectionable in the use of a positive value of l_v. From Figs. 83 (S.163) and 82 (S.157), however, we note that $l_v = 0$ is close to the condition in which the oscillatory component of the motion is absent, and that the excitation of this mode increases as l_v moves to positive or negative values. Thus in high-speed flight, where the rate of spiral divergence can never be great, $l_v = 0$ clearly gives the best overall response to pure rolling moment, the rate of roll rising sharply at first, and then very slowly increasing. The higher general response with positive l_v must be weighed against the more rapid divergence, and the more oscillatory character of the motion: the oscillation is, of course, reasonably well damped with positive l_v.

11.2 *Variation of Inertias.*—The full set of curves [S.169–S.192] shows the effect of varying the inertia coefficients i_A and i_C. When varying the former parameter, the curves calculated by the differential analyser were appropriate to a unit value of $\frac{\mu_2 C_l}{i_A}$, but, as already mentioned, a correction factor has been applied, so that the curves show the response to unit $\frac{\mu_2 C_l}{0{\cdot}12}$, and are directly comparable. Few of these sets of curves are suitable for publication in report form, as the effects of inertia variation are mostly too small to show up clearly. The most important effect, the reduction of the period with reduced i_C, can be inferred from the stability roots: of the other effects, the most noticeable is the way in which reduction of i_A speeds up the rate at which the rolling velocity attains its steady value, in precisely the same way as in the norm. This is seen in Fig. 84 (S.169), which also shows a negligible effect from varying i_C. The increased rapidity of establishing the final rolling velocity, however, takes place in too short a time for the value of ϕ to be appreciably affected, as Fig. 85 (S.172) shows. The only other case in which i_C has a noticeable effect on $\hat{p}$ is for small n_v and large l_v, Fig. 86 (S.175), and here the curves, although distinctly separated, reveal no significant differences.

From an examination of the full set of curves, the effects noticeable are as follows :—

(1) The only important effect is the reduction of period with reduction of i_C.

(2) $\hat{v}$, $\hat{r}$ and ψ depend chiefly on i_C, showing little variation with i_A: their order of magnitude is almost unaffected.

(3) A small variation of $\hat{y}$ with i_A is noticeable, the sideways displacement being greater for smaller rolling inertias.

(4) No effect on $\hat{p}$ other than that mentioned above.

Only the first of these effects is important, and any general conclusions as to desirable values of l_v and n_v, deduced from an examination of results for particular values of i_A and i_C, may be taken to hold for general values of these parameters.

11.3. *Variation of μ_2.*—11.30. *General.*—The curves illustrating the variation of response with μ_2, Figs. [S.193–S.216], can be regarded from two aspects. Most simply, we may ignore the factor μ_2 associated with the unit rolling moment $\mu_2 C_l / i_A$ and compare the response for different values of n_v and l_v, to see whether the general conclusions already drawn for $\mu_2 = 20$ can be confirmed for general values of μ_2.

11.31. *Dependence of response upon n_v and l_v.*—The response to rolling moment is shown in Figs. [S.193–S.216] for the standard combinations of n_v and l_v, and for 5 values of μ_2, viz. 5, 10, 20, 40, 80. This method of plotting does not show clearly how response depends upon n_v and l_v, and we have therefore prepared Figs. 49–59 for this report, showing the response for four pairs of values of n_v and l_v, for $\mu_2 = 5$ and $\mu_2 = 80$: these should be compared with Figs. 44–48 giving the corresponding results for $\mu_2 = 20$. Examination of these figures shows that, whatever the value of μ_2, response to rolling moment is best for small or zero l_v, and large n_v: further, the general trends noted in section 11.11 are all independent of μ_2. Variations from the norm are more pronounced at the lower values of μ_2. It should be noted, however, that the higher μ_2 is, the more pronounced is the excitation of the oscillatory mode, while for $\mu_2 = 80$, $n_v = 0{\cdot}048$,

$l_v = -0{\cdot}12$, it is clearly divergent. The shortening of the period of oscillation as μ_2 increases is one of the most noticeable features, though this change may be only apparent, as for example when the change of μ_2 is due to change of height, when the shortening of the period in airsecs is compensated by lengthening of the airsec. The excitation of this mode by a sharp-edged side-gust has already been examined, and it has been shown that the motion is at best poorly damped and unpleasant to control. In rolling response, however, the oscillation is excited to a troublesome amplitude only for small n_v and large negative l_v, conditions which have already been seen to give a very bad response to a side-gust.

11.32. *Dependence of response upon* μ_2.—The variation of μ_2 curves can now be examined from the point of view of the effect upon response to a given C_l, for given values of n_v and l_v, of changes in μ_2. If we consider firstly the effect at constant true airspeed (*i.e.* comparison of different aeroplanes at the same altitude), so that the time scale bears a fixed relationship to true time, we conclude that :—

(1) $pb/2U_e$ is independent of μ_2, save for the more pronounced excitation of oscillations for high values of μ_2.

(2) The angle of bank attained at any time is proportional to μ_2, *i.e.* inversely proportional to span, as could be inferred from (1).

(3) The sideslip developed has a general magnitude independent of μ_2, and oscillates about this with a frequency increasing as μ_2 increases.

(4) The adverse yaw phase is shortened by increase of μ_2, the maximum adverse yaw being roughly independent of μ_2. The normal turning motion subsequently is very much more rapid for large μ_2.

(5) The sideways displacement is increased more than proportionally to μ_2^2, as μ_2 increases.

When we consider the effect of change of height on a given aircraft we must, in order to obtain a fair comparison, take into account the corresponding change of $\hat{t}$ the unit of aerodynamic time, and compare $pb/2U_e$ and similar quantities for the other components against a time scale which does not change with height. When this is done it is seen that the period of the oscillation is almost independent of height (at the same lift coefficient). Under the same conditions the motion in yaw (in the adverse direction) is almost unchanged, and the variation in magnitude of all components is small.

11.4. *Variation of Rotary Derivatives.*—11.40. *General.*—The variation of response as rotary derivatives are changed is shown in Figs. (S.217–S.240). The variations are so small that the bulk of these figures are unsuitable for report reproduction without a multi-colour technique: nevertheless, certain general trends are noticeable, and appear to be roughly independent of n_v and l_v, in direction if not in magnitude. These more distinct effects are discussed below.

11.41. *Effect of* n_p.—This term, as would be expected, controls the initial adverse yaw developed, and the reduction in n_p from $-0{\cdot}03$ to $-0{\cdot}015$ causes a reduction in adverse yaw to about one-half its original value, and a reduction of the time before positive yaw is developed. The result shown in Fig. 88 (S.225), for $l_v = -0{\cdot}12$, $n_v = 0{\cdot}024$, is typical. This change is accompanied by a reduction in sideslip, and increase in the sideways displacement, and, for large negative values of l_v only, a slight increase in rolling response, which becomes rather steadier, Fig. 87 (S.223).

11.42. *Effect of* l_p.—This term controls the magnitude of the steady rolling velocity developed, and at zero l_v it is the only rotary derivative which has any effect on the response in $\hat{p}$ or ϕ. The reduced response in $\hat{p}$ due to increasing $-l_p$ causes a reduction in all other components: the effect on $\hat{p}$ is adequately shown in Fig. 87.

11.43. *Effect of n_r.*—The change in tail arm from 1 to 0·652 in units of the semispan, with constant body and fin contributions to n_v, corresponds to a reduction in $-n_r$, and has a small but noticeable tendency to reduce $\hat{v}$, when n_v is large, as seen in Fig. 89 (S.236). For small n_v the change in $-n_r$ is smaller, and little effect on $\hat{v}$ is to be seen.

The increase in oscillation damping with increase in n_r, which is shown by the stability roots, is not large enough to be apparent in less than one complete period, which is all the curves show.

11.44. *Effect of n_{v_0}.*—The last change made was an increase in the destabilising body contribution to n_v, without change in the fin contribution, and the general changes are precisely those associated with a reduction in the overall value of n_v.

11.45. *Other effects.*—Alteration in l_r produced no noticeable effect in any case, while the effects of increasing $\bar{y}_v$, very slight reductions in sideslip, motion in yaw, and sideways displacement, are noticeable only when n_v is small.

The effects of these changes on the stability roots, Table 3, should also be noted. It is quite clear that we cannot get any direct correlations between the changes in response and in the stability roots. On the response side the effect of l_p is most important, whereas variations in other parameters bring about much larger changes in the stability roots than does change in l_p. This lack of correlation is, of course, only to be expected: response to rolling moment is mostly a matter of response in the first 1 to 2 airsecs, in which time stability changes do not make themselves felt. Such changes as do occur are, also, too small to be detected by response curves, unless we follow the response for a preposterously long time.

12. *The Effect of Adverse Yawing Moment on Response to Ailerons.*—12.0. *General.*—The previous section has treated in some detail the response to pure rolling moment. The differential analyser results also included curves showing response to pure yawing moment, which are briefly discussed in section 13. These results have been used to calculate a further series of curves, showing the response to ailerons producing adverse yawing moment, the assumed ratio of yawing moment to rolling moment being

$$C_n/C_l = -0{\cdot}1 .$$

Calculations of the response in $\hat{p}$, $\hat{v}$, $\hat{r}$, ϕ and ψ have been made, for the basic conditions, using the four combinations of $n_v = 0{\cdot}024$ and $n_v = 0{\cdot}096$, $l_v = 0$ and $-0{\cdot}12$, as well as for all inertia variations, and for $\mu_2 = 5$ and 80. Some of the results are given in Figs. 60–69, but it has not been considered necessary to publish all the results in full.

12.1. *Basic programme.*—Response curves for the basic programme, for $\mathscr{C}_l = 1$, $C_n/C_l = -0{\cdot}1$, are given in Figs. 60–63, for $n_v = 0{\cdot}024$, and Figs. 64–67, for $n_v = 0{\cdot}096$. In each case four curves are shown, for $l_v = 0$ and $-0{\cdot}12$ with and without adverse yaw.

The most striking fact apparent on studying the response in $\hat{p}$ and ϕ for $n_v = 0{\cdot}024$, Figs. 60, 61, is the way in which l_v affects the answer. For $l_v = 0$ adverse yaw causes almost no reduction in the values of $\hat{p}$ and ϕ, whereas with $l_v = -0{\cdot}12$ a considerable reduction takes place, $\hat{p}$ even reversing its direction for short times: the response in ϕ is much less, being at any time after the first airsec of the order of one-half what it would have been without adverse yaw. For the large n_v, Figs. 64, 65, while the same general trend is observable, the reduction in response is much less marked, of the order of 10 per cent. Since also a large n_v will in general imply a large rudder, it will be possible to cancel out the adverse yaw and produce the sideslip-free motion of section 10, whereas with small n_v this will not be possible, the combination of small n_v and large l_v with appreciable adverse yawing moment is clearly one to be avoided.

Examination of the other components does nothing to weaken this conclusion. The adverse yawing moment shows itself by a considerable increase in the extent and duration of the initial period in which the aircraft yaws against the bank, and with small n_v, large l_v, Fig. 62, practically no turning takes place: the sideslip is also much increased, Fig. 63. With large n_v, Figs. 66, 67, the effects are very much smaller.

12.2 *Effects of Variations of Inertias and* μ_2.—The curves corresponding to those above, for different combinations of inertias, and for $\mu_2 = 5$ and 80, are not worth reproducing, as they all tell exactly the same story, and are in many cases almost identical with the curves for the corresponding basic conditions. The combination of $\mu_2 = 80$, $n_v = 0{\cdot}024$, $l_v = -0{\cdot}12$, however, is more interesting as showing up the effect of adverse yaw in the worst possible light. The lateral oscillation is divergent in this condition, and is excited with great violence, as seen in $\hat{p}$, Fig. 68: the corresponding curve for ϕ, Fig. 69, shows the angle of bank going up almost in steps, its general magnitude being between one-third and one-half of what it would have been without adverse yaw. It is worth noticing, in the same figures, the fact that the effect of adverse yaw is quite negligible for the same μ_2 and n_v, but zero l_v.

13. *Response to Yawing Moment.*—13.0. *General.*—The response of an aircraft to rudder at high speed seems to be much less important than the response to aileron application, and we shall accordingly devote less attention to it.

The rudder is used much more on the ground and at slow speeds than at high speeds, and then it is rarely used, as the aileron is, to start a manoeuvre. Its main use in high-speed flight is to reduce sideslip, and to do this the rudder must be frequently moved and our curves of response to a single application will give little help in analysing this motion. It is true that we could, by combining curves of response to rudder with those of response to sideslip, derive theoretically a motion in which the lateral oscillation and sideslip following a lateral gust were very much reduced. This, however, would depend critically on the time at which rudder was applied (and the phases of the two disturbances must be coincident) so that it has little application in practice.

An examination of the curves of response to yawing moment indicates that a steady displacement of the rudder is not likely to be made, owing to the marked tendency of the rudder to excite the lateral oscillation, well shown in Fig. 70, giving response in rate of yaw for the basic conditions for four pairs of values of n_v and l_v. The oscillatory character of the motion is most marked, and it is seen to be excited to the largest amplitude when oscillation damping is least: the initial response in $\hat{r}$ is almost independent of the parameters l_v and n_v, and the same is true of initial response in $\hat{v}$, as shown in Figs. 90 (S.248) and 91 (S.260). The oscillatory response due to steady rudder application also gives some suggestion of the difficulty of using the rudder to control a lateral oscillation excited by a side-gust. Obviously if the control is used at the right instant and to the right extent, so that the oscillation generated by the rudder is of the same amplitude as that excited by the gust, and in the opposite phase, the oscillation will be neutralised. It appears most unlikely that a pilot will use the rudder in this way, as very delicate timing is obviously called for. If he were to learn to do so, his reaction would become instinctive, and would be easily upset, perhaps altogether disturbed, on changing from one aeroplane to another, particularly if an unconventional pilot's position or other major alteration brought about a change in the phase relationships of the various components in the oscillation. This point obviously has a bearing upon the investigation of the behaviour of small high-speed aeroplanes in side-gusts, discussed earlier in this report.

The full set of curves showing response to applied yawing moment is given in Figs. (S.241–S.360). It is, however, evident that a detailed discussion of these curves, at least over the stability regions where the lateral oscillation exists, would merely reinforce the general conclusions to be drawn from our study of the response to a sharp-edged side-gust. No curves of this set, other than those already mentioned, are therefore reproduced here. Use of these curves has been made, of course, in calculating the curves showing response to ailerons with adverse yaw, already discussed.

13.1. *Tendency to Fin Stall.*—One point which is worth investigation at this stage is the tendency of the fin and rudder to stall as a result of the use of the rudder, or the application of an asymmetric moment due to sudden engine failure, in the case of multi-engined types. In investigating the former point, allowance must be made for the change in yawing moment as fin size is changed. If constant geometrical proportions of fin and rudder are assumed, the maximum rudder yawing moment will be approximately proportional to n_{vf} : for rudders of usual proportions we may take the dimensionless yawing moment due to rudder as $n_\zeta = \frac{2}{3} n_{vf}$, with a maximum rudder displacement $\zeta_{\max.}$ of $\frac{1}{2}$ radian. The appropriate value of $\mathscr{C}_n$ (unity in the basic curves) is then found to be

$$\mathscr{C}_n = \frac{\mu_2 n_\zeta \zeta_{\max.}}{i_C} = \frac{1}{3} \frac{\mu_2}{i_C} n_{vf} .$$

The fin incidence $(\hat{v} - l\hat{r}/\mu_2)$ resulting from the application of a yawing moment of this magnitude has been evaluated for the basic cases

$$i_A = 0{\cdot}12 , \qquad i_C = 0{\cdot}18 , \qquad \mu_2 = 20 ,$$

with all combinations of

$$n_{vf} = 0{\cdot}048, \qquad 0{\cdot}120 ,$$
$$l_v = 0 , \qquad -0{\cdot}12 ,$$

as well as for variation of μ_2 to the values 5 and 80, and variation of inertias to the other three pairs of values taken as standard. The results, shown in Figs. 71–76, further illustrate the desirability of a large value of n_v from the control point of view. In all cases the maximum fin incidence is smaller for increased n_v, in spite of the increased rudder moment. For the rudder moments taken, the fin incidence appears to be large enough to be in the stalling region, even for the larger n_v. We may note also the following points,

(1) l_v has only a very small effect, unless n_{vf} is unreasonably small,

(2) the inertia coefficients i_A and i_C have no noticeable effect,

(3) the magnitude of the maximum fin incidence depends slightly upon μ_2, being greater when μ_2 is greater ; the effect is, however, only small.

When the matter is looked at from the point of view of engine failure, the presence of a rolling moment due to engine failure appears to complicate the matter. This can, however, be safely ignored, as the sideslip due to rolling moment is very small, while the rolling moment due to engine failure is not, at high speed, likely to be large. The results can then be deduced from the foregoing figures 71–76, remembering that the yawing moment concerned is independent of n_v, so that the magnitude of the fin incidence shown for $n_{vf} = 0{\cdot}048$ should be multiplied by the factor 2·5 to bring it to the same scale as that for $n_{vf} = 0{\cdot}120$. The advantage of the large fin is therefore overwhelming when the yawing moment due to engine failure is large enough to matter. If we require a fin which cannot be stalled by rudder application, of course, the fact that the yawing moment from the rudder must exceed that due to engine failure ensures that fin stall will not occur in this case.

14. *Discussion.*—14.0. *General.*—The general conclusions to be drawn from the curves discussed above are so clear cut, and the data themselves so complete, that we have not considered it necessary to attempt to develop an approximate theory of response to rolling and yawing moments at low C_L. It is true, of course, that we have considered such response only for one particular value of C_L, and our results are incomplete in this respect. Further calculations for other values of C_L have been made, and will be discussed in later reports.

14.1. *Good Response to Ailerons Alone.*—We may now summarise the main conclusions drawn from the study of the response curves in sections 11 and 12. These are:—

(1) Moderately large to large values of n_v, say 0·05 upwards, give the best overall response, there being little oscillation excited, and the response being very close to that obtained when sideslip is suppressed.

(2) At moderately large to large values of n_v, response to ailerons is little affected by the value of l_v, or by the presence of any reasonable degree of adverse yawing moment.

(3) At small values of n_v, response is more sensitive to l_v. Response is close to that obtained with sideslip suppressed, when $l_v = 0$, and the excitation of the lateral oscillation is then a minimum and the effect of adverse yaw not very important.

(4) For all values of n_v, increase in dihedral angle reduces the rolling response, particularly if adverse yaw is present, while reduction in dihedral angle increases it.

(5) The effects of changes in i_C are unimportant, but reduction in i_A decreases the time needed to set up the steady rate of roll, so that small values of this parameter are desirable when designing for extreme manœuvrability.

(6) The combination of small n_v with large dihedral gives poor response, and with adverse yawing moment may give rise to the distressing condition when the aeroplane cannot be banked beyond a certain angle. The evil effects of this combination are most noticeable for large values of μ_2 and i_A.

(7) Rotary derivatives have very little effect on response, except for the effect of l_p on the equilibrium rate of roll.

14.2. *Other Indications.*—Other important general features emerging from this part are:—

(1) The necessity for minimising the danger of the fin stalling sets an upper limit to the ratio of rudder size to fin size, or more accurately n_ζ/n_{vf}. The value of 2/3 assumed for this ratio in section 8.1 appears to be about the minimum value at which full rudder certainly stalls the fin, when n_v is large, and slightly above the minimum value for smaller values of n_v. Variations in inertia parameters do not appear to affect this aspect of the problem, but increase in μ_2 slightly increases the tendency to fin stall. We cannot at present hazard a guess as to the effect of speed.

(2) The desirability of being able to carry out rolling manoeuvres without sideslip sets a lower limit to n_{vf} as a function of n_ζ/n_{vf} and the adverse yawing moment ratio $-C_n/C_l$ of the ailerons, as can be inferred from the study of the norm for rolling response in section 10.2.

(3) Though it has not been fully discussed in this report, the engine failure case is worth mentioning in connection with (1) and (2) above. Essentially it is a slow speed condition, setting a lower limit to n_ζ, which with the conditions above will determine a minimum value for n_{vf}.

PART IV

General Conclusions

15. *General Conclusions.*—The work described above gives us a general understanding of the importance of various factors in influencing the behaviour of an aeroplane at the high-speed end of its speed range. It does not appear possible, from a general discussion, to dogmatise about suitable numerical values for the lateral stability parameters l_v and n_v, but sufficient has been done for us to pick out the more important features, at the high-speed end, to which attention should be paid by the designer.

The behaviour of an aeroplane at high speeds is almost independent of the "secondary" stability parameters, and very insensitive to moderate variations of the parameters n_v and l_v, within their normal ranges. Rolling response is good for all but very small values of n_v, and is not significantly dependent upon l_v, save when n_v is small: the combination of small n_v and large dihedral is to be avoided as giving poor rolling response, particularly when the ailerons give an adverse yawing moment. The same combination also leads to a poorly damped, or unstable, lateral oscillation.

The lateral oscillation may give rise to trouble if the period is uncomfortably short, as may be the case with small high-speed aircraft. Here the slowing of the oscillation may be the paramount consideration, so that an upper limit must be set to n_v, and dihedral must be kept small to ensure adequate damping, and a suitable rolling performance.

It is impossible to make more definite recommendations until the state of affairs at the slow end of the speed range has been examined. We may expect conditions here to be more critical, and, pending a general survey of this flight condition, we can only call attention to the criteria which may be developed from the suggestions in section 14.2, or from an application, to the low-speed case, of the norm for aileron response.

REFERENCES

No.	*Author.*	*Title, etc.*
1	Mitchell	A Supplementary Notation for Theoretical Lateral Stability Investigations. R.A.E. Tech. Note No. Aero. 1183. A.R.C. 6797. May, 1943. (Unpublished).
2	Brayant and Gates	Nomenclature for Stability Coefficients. R. & M. 1801. October, 1937.
3	Gandy	The Response of an Aeroplane to the Application of Ailerons and Rudders. Part I—Response in Roll. R. & M. 1915. A.R.C. 7016. September, 1943.
4	Bryant and Hopwood	Calculation of the Damping of the Lateral Oscillation of an Aeroplane. R. & M. 1956. January, 1942.
5	Mitchell and Frayn	Lateral Response Theory. R. & M. 2297. March, 1944.
6	Mitchell and Thorpe	Interim Note on Lateral Response Calculations made with the Differential Analyser at Manchester University. R.A.E. Tech. Note No. Aero. 1251. A.R.C. 7042. August, 1943. (Unpublished.)
7	Fehlner	A Study of the Effects of Vertical Tail Area and Dihedral on the Lateral Manoeuvrability of an Airplane. N.A.C.A. Confidential Report. A.R.C. 5670. March, 1942.
8	Carslaw and Jaeger	*Operational Methods in Applied Mathematics.* Clarendon Press, Oxford. 1941.

APPENDIX I

Approximations to the Lateral Stability Roots

The lateral stability equation is

$$\lambda^4 + B\lambda^3 + C\lambda^2 + D\lambda + E = 0\,, \qquad \text{(A1.1)}$$

where

$$\left.\begin{aligned} B &= l_1 + n_2 + \bar{y}_v \\ C &= l_1 n_2 + l_2 n_1 + (l_1 + n_2)\,\bar{y}_v + \mathscr{N} \\ D &= (l_1 n_2 + l_2 n_1)\,\bar{y}_v + l_1 \mathscr{N} + (n_1 + \tfrac{1}{2}C_L)\,\mathscr{L} \\ E &= \tfrac{1}{2}C_L\,(n_2 \mathscr{L} - l_2 \mathscr{N}) \end{aligned}\right\} \qquad \text{(A1.2)}$$

The root corresponding to the slow spiral motion is very small, and may be approximated to as follows. Denoting it by $\lambda = -r_s$, we re-write (A1.1) as an iteration formula

$$r_s = \frac{E}{D - Cr_s + Br_s^2 - r_s^3}\,.$$

Iterating in the usual way, the second approximation is

$$r_s = \frac{E}{D - CE/D} = \frac{n_2 \mathscr{L} - l_2 \mathscr{N}}{l_1 \mathscr{N} + (n_1 + \tfrac{1}{2}C_L)\,\mathscr{L} + (l_1 n_2 + l_2 n_1)\,\bar{y}_v - CE/D}\,\tfrac{1}{2}C_L.$$

We now simplify by omitting all but the terms in $\mathscr{N}$ and $\mathscr{L}$ in the denominator and express in terms of the standard derivatives to obtain (7.1.1). If r_s is positive, the two terms omitted are small and of opposite signs, so would tend to cancel. On the other hand, if r_s is negative, two positive terms are omitted, so we overestimate the numerical value: that is, the formula is conservative. Failure can occur only when $D^2 - CE$ is small, as happens in a region of the stability diagram, near $D = 0$, where stability characteristics are known to be unfavourable.

To obtain the rolling root is not so simple. We set $\lambda = -r_r$, and re-write (A1.1) as an iteration formula in the form

$$\begin{aligned} r_r &= B - \frac{C}{r_r} + \frac{D}{r_r^2} - \frac{E}{r_r^3} \\ &= l_1 + n_2 + \bar{y}_v - \frac{l_1 n_2 + l_2 n_1 + (l_1 + n_2)\,\bar{y}_v + \mathscr{N}}{r_r} \\ &\quad + \frac{(l_1 n_2 + l_2 n_1)\,\bar{y}_v + l_1 \mathscr{N} + (n_1 + \tfrac{1}{2}C_L)\,\mathscr{L}}{r_r^2} - \frac{\tfrac{1}{2}C_L\,(n_2 \mathscr{L} - l_2 \mathscr{N})}{r_r^3}\,, \end{aligned}$$

and then re-arrange as

$$\begin{aligned} r_r \left\{\left(1 - \frac{n_2}{r_r}\right)\left(1 - \frac{\bar{y}_v}{r_r}\right) + \frac{\mathscr{N}}{r_r^2}\right\} &= l_1 \left\{\left(1 - \frac{n_2}{r_r}\right)\left(1 - \frac{\bar{y}_v}{r_r}\right) + \frac{\mathscr{N}}{r^2}\right\} - \frac{l_2 n_1}{r_r}\left(1 - \frac{\bar{y}_v}{r_r}\right) \\ &\quad + \frac{n_1 + \tfrac{1}{2}C_L\left(1 - \dfrac{n_2}{r_r}\right)}{r_r^2}\,\mathscr{L} + \frac{l_2 C_L \mathscr{N}}{2r_r^3}\,. \end{aligned}$$

Dividing out the factor in curly brackets,

$$r_r = l_1 - \frac{\frac{l_2 n_1}{r_r}\left(1 - \frac{\bar{y}_v}{r_r}\right) - \frac{l_2 C_L}{2 r_r^3}\mathscr{N} - \left\{n_1 + \tfrac{1}{2}C_L\left(1 - \frac{n_2}{r_r}\right)\right\}\frac{\mathscr{L}}{r_r^2}}{\left(1 - \frac{n_2}{r_r}\right)\left(1 - \frac{\bar{y}_v}{r_r}\right) + \frac{\mathscr{N}}{r_r^2}} . \qquad .. \quad (A1.3)$$

Clearly the first approximation is $r_r = l_1$: in the second approximation we take into account the term $l_2 n_1 / r_r$ and the term involving $\mathscr{L}$. The former is small, so that the replacement of the denominator factor r_r by l_1 will cause a negligible error, and we also replace the whole denominator in (A1.3) by unity, from which it does not differ appreciably unless $\mathscr{N}$ is very large. This gives us

$$r_r = l_1 - \frac{l_2 n_1}{l_1} + \frac{(n_1 + \tfrac{1}{2}C_L)\,\mathscr{L}}{r_r^2} .$$

Two iterations and an obvious approximation give the result (7.1.2).

Again, if r_l denotes the damping of the lateral oscillation, we have

$$r_l = \tfrac{1}{2}B - \tfrac{1}{2}r_s - \tfrac{1}{2}r_r ,$$

leading immediately to (7.1.3), when r_r is expressed by (A1.3).

The formula (7.1.4) for the frequency is very simple. The sum of the products three at a time of the roots of (A1.1), or $-D$, is approximately equal to $-r_r(r_l^2 + f_l^2)$, and hence to $-r_r f_l^2$, owing to the smallness of the spiral damping. Ignoring all but the terms in $\mathscr{N}$ and $\mathscr{L}$ in D gives the result at once.

APPENDIX II

The Norm for Aileron Response

Omitting sideslip terms, and the yawing moment equation, the system of equations to be satisfied is

$$\left.\begin{aligned} \hat{r} - k\phi &= 0 \\ \frac{d\hat{p}}{d\tau} + l_1\hat{p} - l_2\hat{r} &= \mathscr{C}_l \\ -\hat{p} + \frac{d\phi}{d\tau} &= 0 \\ -\hat{r} + \frac{d\psi}{d\tau} &= 0 \\ -\psi + \frac{d\hat{y}}{d\tau} &= 0 \end{aligned}\right\} . \qquad .. \quad (A2.1)$$

This can be solved most conveniently by using operational methods founded upon the theory of the Laplace transformation[8]. The Laplace transform of (A.1) is

$$\left.\begin{aligned} \bar{r} - k\bar{\phi} &= 0 \\ (p + l_1)\,\bar{p} - l_2\,\bar{r} &= \bar{\mathscr{C}}_l + \hat{p}_0 \\ -\bar{p} + p\bar{\phi} &= \phi_0 \\ -\bar{r} + p\bar{\psi} &= \psi_0 \\ -\bar{\psi} + p\bar{y} &= \hat{y}_0 \end{aligned}\right\} , \qquad .. \quad (A2.2)$$

where $\bar{p}$, $\bar{r}$, $\bar{\phi}$, $\bar{\psi}$, $\bar{y}$ denote the Laplace transforms of $\hat{p}$, $\hat{r}$, ϕ, ψ, $\hat{y}$, and $\hat{p}_0$, ϕ_0, ψ_0, $\hat{y}_0$ their initial

values, and where p is the Laplace operator. Solving this system of equations, we obtain the Laplace transforms in the form

$$\left.\begin{aligned}
\bar{p} &= \frac{p\,(\bar{\mathscr{C}}_l + \hat{p}_0) + kl_2\phi_0}{p^2 + l_1 p - kl_2} \\
\bar{r} &= \frac{k\,(\bar{\mathscr{C}}_l + \hat{p}_0) + k\,(p + l_1)\,\phi_0}{p^2 + l_1 p - kl_2} \\
\bar{\phi} &= \frac{\bar{\mathscr{C}}_l + \hat{p}_0 + (p + l_1)\,\phi_0}{p^2 + l_1 p - kl_2} \\
\bar{\psi} &= \frac{1}{p}\,\psi_0 + \frac{1}{p}\,\bar{r} \\
\bar{y} &= \frac{1}{p}\,\hat{y}_0 + \frac{1}{p}\,\bar{\psi}
\end{aligned}\right| \quad . \quad .. \quad .. \quad .. \quad .. \quad .. \quad \text{(A2.3)}$$

Now let us factorise the denominator in the form

$$p^2 + l_1 p - kl_2 \equiv (p - \alpha_1)\,(p - \alpha_2)\,. \quad .. \quad .. \quad .. \quad .. \quad \text{(A2.4)}$$

The interpretation of (A.3) is then given by the equations (for constant $\mathscr{C}_l$)

$$\left.\begin{aligned}
\hat{p} &= \frac{\alpha_1\hat{p}_0 + kl_2\phi_0}{\alpha_1 - \alpha_2}\,e^{\alpha_1\tau} + \frac{\alpha_2\hat{p}_0 + kl_2\phi_0}{\alpha_2 - \alpha_1}\,e^{\alpha_2\tau} \\
&\quad + \frac{\alpha_1}{\alpha_1 - \alpha_2}\,\mathscr{C}_l\,\frac{1 - e^{\alpha_1\tau}}{-\alpha_1} + \frac{\alpha_2}{\alpha_2 - \alpha_1}\,\mathscr{C}_l\,\frac{1 - e^{\alpha_2\tau}}{-\alpha_2} \\
\hat{r} &= \frac{k\hat{p}_0 + k\,(\alpha_1 + l_1)\,\phi_0}{\alpha_1 - \alpha_2}\,e^{\alpha_1\tau} + \frac{k\hat{p}_0 + k\,(\alpha_2 + l_1)\,\phi_0}{\alpha_2 - \alpha_1}\,e^{\alpha_2\tau} \\
&\quad + \frac{k}{\alpha_1 - \alpha_2}\,\mathscr{C}_l\,\frac{1 - e^{\alpha_1\tau}}{-\alpha_1} + \frac{k}{\alpha_2 - \alpha_1}\,\mathscr{C}_l\,\frac{1 - e^{\alpha_2\tau}}{-\alpha_2} \\
\phi &= \frac{\hat{p}_0 + (\alpha_1 + l_1)\,\phi_0}{\alpha_1 - \alpha_2}\,e^{\alpha_1\tau} + \frac{\hat{p}_0 + (\alpha_2 + l_1)\,\phi_0}{\alpha_2 - \alpha_1}\,e^{\alpha_2\tau} \\
&\quad + \frac{1}{\alpha_1 - \alpha_2}\,\mathscr{C}_l\,\frac{1 - e^{\alpha_1\tau}}{-\alpha_1} + \frac{1}{\alpha_2 - \alpha_1}\,\mathscr{C}_l\,\frac{1 - e^{\alpha_2\tau}}{-\alpha_2} \\
\psi &= \frac{k\hat{p}_0 + k\,(\alpha_1 + l_1)\,\phi_0}{\alpha_1 - \alpha_2}\,\frac{1 - e^{\alpha_1\tau}}{-\alpha_1} + \frac{k\hat{p}_0 + k\,(\alpha_2 + l_1)\,\phi_0}{\alpha_2 - \alpha_1}\,\frac{1 - e^{\alpha_2\tau}}{-\alpha_2} \\
&\quad + \frac{k}{\alpha_1 - \alpha_2}\,\mathscr{C}_l\,\frac{e^{\alpha_1\tau} - 1 - \alpha_1\tau}{\alpha_1^{\,2}} + \frac{k}{\alpha_2 - \alpha_1}\,\mathscr{C}_l\,\frac{e^{\alpha_2\tau} - 1 - \alpha_2\tau}{\alpha_2^{\,2}} \\
\hat{y} &= \frac{k\hat{p}_0 + k\,(\alpha_1 + l_1)\,\phi_0}{\alpha_1 - \alpha_2}\,\frac{e^{\alpha_1\tau} - 1 - \alpha_1\tau}{\alpha_1^{\,2}} + \frac{k\hat{p}_0 + k\,(\alpha_2 + l_1)\,\phi_0}{\alpha_2 - \alpha_1}\,\frac{e^{\alpha_2\tau} - 1 - \alpha_2\tau}{\alpha_2^{\,2}} \\
&\quad + \frac{k}{\alpha_1 - \alpha_2}\,\mathscr{C}_l\,\frac{1 + \alpha_1\tau + \frac{1}{2}\alpha_1^{\,2}\tau^2 - e^{\alpha_1\tau}}{-\alpha_1^{\,3}} + \frac{k}{\alpha_2 - \alpha_1}\,\mathscr{C}_l\,\frac{1 + \alpha_2\tau + \frac{1}{2}\alpha_2^{\,2}\tau^2 - e^{\alpha_2\tau}}{-\alpha_2^{\,3}}
\end{aligned}\right\} \quad . \quad \text{(A2.5)}$$

Finally, we substitute back in the yawing moment equation of (2.1.1), with $\hat{v} = 0$, to obtain

$$\mathscr{C}_n = \frac{d\hat{r}}{d\tau} + n_1\hat{p} + n_2\hat{r}\,. \quad .. \quad .. \quad .. \quad .. \quad .. \quad .. \quad \text{(A2.6)}$$

APPENDIX III

List of Symbols

A	rolling moment of inertia
b	span of aeroplane (ft.)
B	coefficient of cubic term in stability equation
C	coefficient of square term in stability equation
C	yawing moment of inertia
C_l	rolling moment coefficient
C_L	lift coefficient
C_n	yawing moment coefficient
$\mathscr{C}_l$	$\mu_2 C_l / i_A$
$\mathscr{C}_n$	$\mu_2 C_n / i_C$
$\bar{\mathscr{C}}_l$	Laplace transform of $\mathscr{C}_l$
$\bar{\mathscr{C}}_n$	Laplace transform of $\mathscr{C}_n$
D	coefficient of linear term in stability equation
E	product of inertia constant term in stability equation
f_l	dimensionless frequency
g	acceleration due to gravity (ft./sec.^{2})
i_A	rolling inertia coefficient
i_C	yawing inertia coefficient
k	$\frac{1}{2}C_L$
l	fin arm (dimensionless) distance of pilot's seat ahead of C.G.
l_p	rolling moment due to rate of roll
$\bar{l}_p$	$-l^p$
l_r	rolling moment due to rate of yaw
l_v	rolling moment due to sideslip
$\bar{l}_v$	$-l_v$
l_1	$-l_p/i_A$
$\bar{l}_2$	l_r/i_A
$\mathscr{L}$	$-\mu_2 l_v/i_A$
n	acceleration of pilot (in units of g) at C.G.
n'	acceleration of pilot (in units of g) in general position
n_v	yawing moment due to rate of roll

$\bar{n}_p$ — n_p

n_r yawing moment due to rate of yaw

$\bar{n}_r$ — n_r

n_v yawing moment due to sideslip

n_{v0} body contribution to n_v

n_{vf} fin contribution to n_v

n_ζ yawing moment due to rudder

n_1 — n_p/i_C

n_2 — n_r/i_C

$\mathcal{N}$ $\mu_2 n_v/i_C$

p rate of roll in radians per second

Laplace operator

$\hat{p}$ rate of roll in radians per airsec.

$\hat{p}_0$ initial value of $\hat{p}$

$\bar{p}$ Laplace transform of $\hat{p}$

p_i modal amplitude in rate of roll

r rate of yaw in radians per true second

$\hat{r}$ rate of yaw in radians per airsec

$\hat{r}_0$ initial value of $\hat{r}$

$\bar{r}$ Laplace transform of $\hat{r}$

r_i modal amplitude in rate of yaw

r_l damping of lateral oscillation

r_r damping of rolling subsidence

r_s damping of spiral subsidence

S wing area

t time in seconds

$\hat{t}$ unit of aerodynamic time (airsec)

U_e steady velocity of aircraft

$\hat{v}$ angle of sideslip in radians

v_i modal amplitude in sideslip

$\hat{v}_0$ initial value of $\hat{v}$

V_g gust velocity

w wing loading

W weight

y sideways displacement, ft.

$\hat{y}$ sideways displacement, in units $U_e\hat{t}$

$\hat{y}_0$	initial value of $\hat{y}$
$\bar{y}$	Laplace transform of $\hat{y}$
y_v	sideforce due to sideslip
$\bar{y}_v$	$-y_v$ stability
α_1, α_2	roots of stability equation for response with sideslip suppressed
α_{iv}	modal response coefficient to initial sideslip
γ_e	angle of climb in steady motion
ε_A	$-E/A$
ε_C	$-E/C$
$\zeta_{\max.}$	maximum rudder angle (radians)
λ_i	roots of stability equation
μ_2	lateral relative density
ρ	air density (slugs/ft.^{3})
ρ_0	air density at sea level
σ	density ratio, ρ/ρ_0
τ	time in airsecs
ϕ	angle of bank
ϕ_0	initial value of ϕ
$\bar{\phi}$	Laplace transform of ϕ
ϕ_i	modal amplitude in bank
ψ	angle of yaw (azimuth)
ψ_0	initial value of ψ
$\bar{\psi}$	Laplace transform of ψ

TABLE 1

Index of Runs Made on the Differential Analyser

Response to Side-gust

Stage of programme	n_{vf}	l_v			
		0·06	0	−0·06	−0·12
Basic	0	47*, 48*, 49*, 50†, 77	78	46*, 79	80
	0·024	76	74, 75	73	72
	0·048	—	82	—	81
	0·072	68	69	70	71
	0·120	67	66	65	63, 64 ($\dot{v}$)

Variation of inertias	n_{vf}	l_v	$i_A = 0·12$ $i_G = 0·18$	$i_A = 0·12$ $i_G = 0·12$	$i_A = 0·06$ $i_G = 0·12$	$i_A = 0·06$ $i_G = 0·18$
	0·048	0	82	91	105	121
	0·048	−0·12	81	92	104	120
	0·120	0	66	94*, 102	103	119
	0·120	−0·12	63	93*, 101	99*, 100	118

Variation of μ_2	n_{vf}	l_v	$\mu_2 = 5$	$\mu_2 = 10$	$\mu_2 = 20$	$\mu_2 = 40$	$\mu_2 = 80$
	0·048	0	175	161	82	148	136
	0·048	−0·12	174	162*, 164	81	147	135
	0·120	0	176	160	66	149	137
	0·120	−0·12	177	159*, 163	63	150	138

Variation of rotaries	n_{vf}	l_v	Rotary derivatives changed (cumulative)						
			Basic	n_p	l_r	l_p	y_v	l	n_{vo}
	0·048	0	175	188	201	212	217	236	258
	0·048	−0·12	174	187	202	211	218	235	260
	0·120	0	176	189	200	213	216	237	265
	0·120	−0·12	177	190	199	214	215	238	266

Notes.—* Runs so marked were erroneous, for various reasons.

† Non-stop check run.

($\dot{v}$) Check run for initial $\dot{v}$ to check the initial settings for initial v.

Otherwise, where two runs are made with the same conditions, one was intended to check the other.

TABLE 2

Index of Runs made on the Differential Analyser

Response to Rolling and Yawing Moments

I. *Basic programme*

n_{vf}	l_v				
	0·12	0·06	0	−0·06	−0·12
Response to rolling moment					
0	5[s], 6[s], 9	24	23	2[s], 3[s], 10	55[s], 56[s], 57
0·024	26	25	18[s], 19[s], 20	15[s], 16[s], 17	54
0·048			83		84
0·060					52
0·072	11	12	13	14	53
0·096	1	21*, 22, 62	7	4, 8	51
Response to yawing moment					
0	42	43	44	45	58
0·024	41	40	38[s], 39	36[s], 37	59
0·048			86		85
0·060	32				
0·072	27	28	29	30	60
0·096	31	33	34	35	61

II. *Variation of inertias*

i_A	i_C	Rolling moment				Yawing moment			
		$n_{vf} = 0·048$		$n_{vf} = 0·120$		$n_{vf} = 0·048$		$n_{vf} = 0·120$	
		$l_v = 0$	$l_v = -0·12$	$l_v = 0$	$l_v = -0·12$	$l_v = 0$	$l_v = -0·12$	$l_v = 0$	$l_v = -0·12$
0·12	0·18	83	84	7	51	86	85	34	62
0·12	0·12	90	89	95	96	87	88	98	97
0·06	0·12	106	107	109	108	113	112	110	111
0·06	0·18	126	124*, 125	123	122	114	115	117	116

III. *Variation of* μ_2

μ_2	Rolling moment				Yawing moment			
	$n_{vf} = 0·048$		$n_{vf} = 0·120$		$n_{vf} = 0·048$		$n_{vf} = 0·120$	
	$l_v = 0$	$l_v = -0·12$	$l_v = 0$	$l_v = -0·12$	$l_v = 0$	$l_v = -0·12$	$l_v = 0$	$l_v = -0·12$
5	167	168	166	165	171	169[s], 170	172	173
10	153	154	152	151	156	155	157	158
20	83	84	7	51	86	85	34	61
40	141	142	140	139	144	143	145	146
80	129	130	128	127	132	131	133	134

TABLE 2—*contd.*

IV. *Variation of rotaries*

Rotaries changed (Cumulative)	Rolling moment				Yawing moment			
	$n_{vf} = 0{\cdot}048$		$n_{vf} = 0{\cdot}120$		$n_{vf} = 0{\cdot}048$		$n_{vf} = 0{\cdot}120$	
	$l_v = 0$	$l_v = -0{\cdot}12$	$l_v = 0$	$l_v = -0{\cdot}12$	$l_v = 0$	$l_v = -0{\cdot}12$	$l_v = 0$	$l_v = -0{\cdot}12$
Basic	167	168	166	165	171	170	172	173
n_p	181	182	180	179	184	183	186	185
l_r	196	195	197	198	193	194	192	191
l_p	204	203	205	206	209	210	208	207
y_v	220	219	221	222	225	226	224	223
l	233	234	232	231	228	227	229	230
n_{v0}	248	246	242	240	249	251	255	257

Notes.—* Runs so marked were erroneous, for various reasons.

s Runs cut short by scale difficulties.

Otherwise, where two runs are made with the same conditions, one was intended to check the other.

TABLE 3

Roots of Stability Equation

I. *Basic programme*

n_v	l_v	Spiral root λ_1		Rolling root λ_2		Oscillatory roots λ_3 (λ_4)		No. of swings to halve amplitude (Exact)
		Exact	Approx.	Exact	Approx.	Exact	Approx.	
0·096	−0·12	−0·01865	−0·01875	−3·725	−3·828	−0·3115 + 3·379i	−0·3179 + 3·385i	1·19
	−0·06	−0·00330	−0·00333	−3·613	−3·672	−0·3751 + 3·324i	−0·3762 + 3·300i	0·97
	0	0·01403	0·01428	−3·494	−3·476	−0·4434 + 3·269i	−0·4435 + 3·277i	0·81
	0·06	0·03369	0·03461	−3·366	−3·223	−0·5172 + 3·212i	−0·5198 + 3·279i	0·68
	0·12	0·05609		−3·228		−0·5973 + 3·289i		0·61
0·048	−0·12	−0·02210	−0·02222	−3·781	−3·828	−0·1486 + 2·522i	−0·1513 + 2·504i	1·87
	−0·06	−0·00618	−0·00625	−3·642	−3·672	−0·2259 + 2·424i	−0·2268 + 2·410i	1·18
	0	0·01398	0·01429	−3·487	−3·476	−0·3134 + 2·317i	−0·3135 + 2·317i	0·81
	0·06	0·04014	0·04167	−3·310	−3·223	−0·4148 + 2·201i	−0·4186 + 2·228i	0·58
	0·12	0·07499		−3·103		−0·5360 + 2·073i		0·43
0·036	−0·12	−0·02400		−3·798		−0·1056 + 2·260i		2·35
	0·12	0·09123		−3·050		−0·5973 + 1·681i		0·31
0·024	−0·12	−0·02711		−3·818		−0·0610 + 1·965i		3·54
	0	0·01389		−3·482		−0·2492 + 1·641i		0·72
0	−0·12	−0·04948	−0·05000	−3·863	−3·828	0·0396 + 1·180i	0·0434 + 1·180i	−3·28
	−0·06	−0·04896	−0·05000	−3·689	−3·672	−0·0479 + 0·858i	−0·0464 + 0·852i	1·97
	0	0	0	−3·475	−3·476	−0·2, − 0·1583	−0·179, − 0·179	*
	0·06	−0·05105	−0·05000	−3·184	−3·223	−1·252, + 0·655	−1·205, 0·614	*
	0·12	−0·05052		−2·525		−2·205, 0·948		*
−0·024	−0·12	0·03299	0·03333	−3·919	−3·828	−0·927, 1·113	−0·916, 1·128	*
	−0·06	0·01994	0·02000	−3·724	−3·672	−1·338, 1·342	−1·341, 1·354	*
	0	0·01427	0·01429	−3·464	−3·476	−1·772, 1·522	−1·764, 1·513	*
	0·06	0·01111	0·01111	−2·972	−3·223	−2·413, 1·674	−2·224, 1·615	*
	0·12	0·00911		−2·757 + 0·710i		1·805		0·03

* Indicates that there is no oscillatory mode.

TABLE 3—*continued*

II. *Variation of Inertia*

i_A	i_C	Spiral root λ_1		Rolling root λ_2		Oscillatory root λ_3 (λ_4)		No. of swings to halve amplitude (Exact)
		Exact	Approx.	Exact	Approx.	Exact	Approx.	
$n_v = 0{\cdot}024$, $l_v = 0$								
0·06	0·12	0·01392	0·01429	−6·966	−6·964	−0·3238 + 2·005i	−0·3240 + 2·005i	0·68
	0·18	0·01392	0·01429	−6·977	−6·976	−0·2516 + 1·638i	−0·2518 + 1·636i	0·72
0·12	0·12	0·01390	0·01429	−3·475	−3·464	−0·3194 + 2·010i	−0·3197 + 2·010i	0·69
	0·18	0·01389	0·01429	−3·482	−3·476	−0·2492 + 1·642i	−0·2494 + 1·639i	0·72
$n_v = 0{\cdot}024$, $l_v = -0{\cdot}12$								
0·06	0·12	−0·02832	−0·02857	−7·232	−7·231	−0·1698 + 2·415i	−0·1697 + 2·312i	1·56
	0·18	−0·02705	−0·02727	−7·184	−7·182	−0·1277 + 2·025i	−0·1272 + 2·021i	1·74
0·12	0·12	−0·02840	−0·02857	−3·880	−3·901	−0·0958 + 2·332i	−0·0967 + 2·326i	2·68
	0·18	−0·02711	−0·02727	−3·818	−3·828	−0·0610 + 1·965i	−0·0617 + 1·957i	3·54
$n_v = 0{\cdot}096$, $l_v = 0$								
0·06	0·12	0·01406	0·01429	−6·974	−6·964	−0·6200 + 3·992i	−0·6201 + 4·010i	0·71
	0·18	0·01406	0·01429	−6·982	−6·976	−0·4495 + 3·266i	−0·4496 + 3·271i	0·80
0·12	0·12	0·01403	0·01429	−3·492	−3·476	−0·6110 + 3·994i	−0·6109 + 4·020i	0·72
	0·18	0·01403	0·01429	−3·494	−3·476	−0·4434 + 3·268i	−0·4435 + 3·277i	0·81
$n_v = 0{\cdot}096$, $l_v = -0{\cdot}12$								
0·06	0·12	−0·01890	−0·01905	−7·201	−7·321	−0·4903 + 4·171i	−0·4910 + 4·118i	0·94
	0·18	−0·01861	−0·01875	−7·166	−7·182	−0·3411 + 3·447i	−0·3411 + 3·447i	1·11
0·12	0·12	−0·01895	−0·01905	−3·743	−3·901	−0·4693 + 4·087i	−0·4734 + 3·965i	0·96
	0·18	−0·01865	−0·01875	−3·725	−3·828	−0·3115 + 3·379i	−0·3179 + 3·385i	1·19

TABLE 3—*continued*

III. *Variation of* μ_2

μ_2	Spiral root λ_1		Rolling root λ_2		Oscillatory roots λ_3 (λ_4)		No. of swings to halve amplitude (Exact)
	Exact	Approx.	Exact	Approx.	Exact	Approx.	
$n_v = 0{\cdot}024,\ l_v = 0$							
5	0·01298	0·01429	−3·476	−3·476	−0·2516 + 0·822i	−0·2506 + 0·818i	0·36
10	0·01357	0·01429	−3·479	−3·476	−0·2508 + 1·162i	−0·2500 + 1·158i	0·51
20	0·01389	0·01429	−3·482	−3·476	−0·2492 + 1·641i	−0·2494 + 1·639i	0·72
40	0·01406	0·01429	−3·488	−3·476	−0·2466 + 2·319i	−0·2477 + 2·317i	1·03
80	0·01414	0·01429	−3·494	−3·476	−0·2433 + 3·276i	−0·2459 + 3·277i	1·48
$n_v = 0{\cdot}024,\ l_v = -0{\cdot}12$							
5	−0·02626	−0·02727	−3·586	−3·580	−0·1772 + 1·015i	−0·1754 + 1·012i	0·63
10	−0·02682	−0·02727	−3·676	−3·672	−0·1318 + 1·418i	−0·1307 + 1·413i	1·18
20	−0·02711	−0·02727	−3·818	−3·828	−0·0610 + 1·965i	−0·0617 + 1·957i	3·54
40	−0·02726	−0·02727	−4·017	−4·062	0·0386 + 2·703i	0·0333 + 2·687i	−7·70
80	−0·02734	−0·02727	−4·266	−4·352	0·1632 + 3·701i	0·1518 + 3·672i	−2·49
$n_v = 0{\cdot}096,\ l_v = 0$							
5	0·01347	0·01429	−3·480	−3·476	−0·4500 + 1·625i	−0·4455 + 1·639i	0·40
10	0·01384	0·01429	−3·486	−3·476	−0·4470 + 2·308i	−0·4446 + 2·317i	0·57
20	0·01403	0·01429	−3·494	−3·476	−0·4434 + 3·269i	−0·4435 + 3·277i	0·81
40	0·01413	0·01429	−3·501	−3·476	−0·4399 + 4·623i	−0·4424 + 4·634i	1·16
80	0·01418	0·01429	−3·506	−3·476	−0·4372 + 6·536i	−0·4416 + 6·554i	1·64
$n_v = 0{\cdot}096,\ l_v = -0{\cdot}12$							
5	−0·01811	−0·01875	−3·580	−3·580	−0·3845 + 1·714i	−0·3797 + 1·726i	0·49
10	−0·01847	−0·01875	−3·646	−3·672	−0·3513 + 2·412i	−0·3497 + 2·410i	0·76
20	−0·01865	−0·01875	−3·725	−3·828	−0·3115 + 3·379i	−0·3179 + 3·385i	1·19
40	−0·01879	−0·01875	−3·805	−4·062	−0·2716 + 4·729i	−0·2814 + 4·584i	1·42
80	−0·01879	−0·01875	−3·871	−4·352	−0·2384 + 6·628i	−0·2524 + 6·263i	3·06

TABLE 3—*continued*

IV. *Variation of rotary derivatives*

n	l_v	Quantities changed (Cumulative)						Spiral root λ_1		Rolling root λ_2		Oscillatory roots λ_3 (λ_4)		No. of swings to halve amplitude (Exact)
		n_p	l_r	l_p	$\bar{y}_v$	l	n_{v0}	Exact	Approx.	Exact	Approx.	Exact	Approx.	
0·024	0	—0·03	0·06	—0·42	0·2	1	—0·024	0·01298	0·01429	—3·476	—3·476	—0·2516+0·822i	—0·2506+0·818i	0·36
		—0·015						0·01302	0·01429	—3·489	—3·488	—0·2455+0·821i	—0·2461+0·818i	0·37
			0·052					0·01131	0·01238	—3·490	—3·490	—0·2439+0·820i	—0·2445+0·818i	0·37
				—0·54				0·00883	0·00963	—4·492	—4·492	—0·2417+0·819i	—0·2421+0·817i	0·37
					0·233			0·00872	0·00963	—4·492	—4·492	—0·2581+0·819i	—0·2586+0·817i	0·35
						0·652		0·00899	0·00963	—4·492	—4·492	—0·2118+0·819i	—0·2121+0·817i	0·43
							—0·033	0·00865	0·00963	—4·492	—4·492	—0·2117+0·648i	—0·2117+0·646i	0·34
0·024	—0·12	—0·03	0·06	—0·42	0·2	1	—0·024	—0·02626	—0·02727	—3·586	—3·580	—0·1772+1·015i	—0·1754+1·012i	0·63
		—0·015						—0·02961	—0·03077	—3·564	—3·560	—0·1867+0·955i	—0·1826+0·955i	0·56
			0·052					—0·03096	—0·03214	—3·565	—3·562	—0·1853+0·955i	—0·1847+0·955i	0·57
				—0·54				—0·02551	—0·02667	—4·538	—4·537	—0·2014+0·928i	—0·2009+0·929i	0·51
					0·233			—0·02528	—0·02667	—4·539	—4·537	—0·2178+0·929i	—0·2172+0·929i	0·47
						0·652		—0·01426	—0·01482	—4·538	—4·537	—0·1771+0·930i	—0·1768+0·929i	0·58
							—0·033	—0·02350	—0·02467	—4·539	—4·537	—0·1723+0·785i	—0·1717+0·785i	0·50
0·096	0	—0·03	0·06	—0·42	0·2	1	—0·024	0·01347	0·01429	—3·480	—3·476	—0·4500+1·625i	—0·4455+1·639i	0·40
		—0·015						0·01348	0·01429	—3·492	—3·488	—0·4442+1·623i	—0·4446+1·636i	0·40
			0·052					0·01170	0·01238	—3·493	—3·490	—0·4428+1·622i	—0·4432+1·636i	0·40
				—0·54				0·00912	0·00963	—4·493	—4·492	—0·4413+1·620i	—0·4416+1·634i	0·40
					0·233			0·00905	0·00963	—4·493	—4·492	—0·4577+1·623i	—0·4580+1·634i	0·39
						0·652		0·00923	0·00963	—4·494	—4·492	—0·3417+1·634i	—0·3419+1·634i	0·53
							—0·033	0·00919	0·00963	—4·493	—4·492	—0·3417+1·555i	—0·3420+1·556i	0·50
0·096	—0·12	—0·03	0·06	—0·42	0·2	1	—0·024	—0·01811	—0·01875	—3·580	—3·580	—0·3845+1·714i	—0·3797+1·726i	0·49
		—0·015						—0·01883	—0·01923	—3·558	—3·560	—0·3948+1·687i	—0·3946+1·697i	0·47
			0·052					—0·02054	—0·02094	—3·559	—3·562	—0·3934+1·681i	—0·3933+1·697i	0·47
				—0·54				—0·01623	—0·01686	—4·537	—4·537	—0·4069+1·671i	—0·4066+1·687i	0·45
					0·233			—0·01611	—0·01686	—4·537	—4·537	—0·4233+1·673i	—0·4230+1·687i	0·43
						0·652		—0·00763	—0·00788	—4·536	—4·537	—0·3118+1·686i	—0·3117+1·687i	0·59
							—0·033	—0·00923	—0·00955	—4·537	—4·537	—0·3109+1·610i	—0·3107+1·612i	0·57

TABLE 4

Periods and Times to Halve Amplitude, in Seconds, for the Typical Aeroplanes of Section 3

I. *Basic Programme—Span 42·25 ft.*

n_v	l_v	Lateral oscillation		Spiral root
		Period	Time to halve amplitude	Time to halve amplitude
0·096	−0·12	2·129	2·548	42·6
	−0·06	2·164	2·116	240·6
	0	2·201	1·790	−56·6
	0·06	2·240	1·535	−23·6
0·048	−0·12	2·852	5·341	35·9
	−0·06	2·968	3·515	128·5
	0	3·104	2·533	−56·8
	0·06	3·268	1·914	−19·8
0	−0·12	6·094	−20·061	16·0
	−0·06	8·385	16·587	16·2
	0	*	5·024	Neutral
	0·06	*	− 1·215	15·6
−0·024	−0·12	*	− 0·714	− 24·1
	−0·06	*	− 0·592	− 39·8
	0	*	− 0·522	− 55·6
	0·06	*	− 0·475	− 71·5

* Indicates that there is no oscillation : the time to halve amplitude then entered is that corresponding to the most unstable mode.

II. *Variation of inertia—Span 42·25 ft.*

n_v	l_v	i_A	i_C	Lateral oscillation		Spiral root
				Period	Time to halve amplitude	Time to halve amplitude
0·024	0	0·06	0·12	3·588	2·451	−57·0
		0·06	0·18	4·392	3·155	−57·0
		0·12	0·12	3·579	2·485	−57·1
		0·12	0·18	4·382	3·186	−57·2
0·024	−0·12	0·06	0·12	2·979	4·675	28·0
		0·06	0·18	3·552	6·216	29·3
		0·12	0·12	3·085	8·284	28·0
		0·12	0·18	3·661	13·020	29·3
0·096	0	0·06	0·12	1·802	1·280	−56·5
		0·06	0·18	2·203	1·766	−56·5
		0·12	0·12	1·801	1·300	−56·6
		0·12	0·18	2·201	1·790	−56·6
0·096	−0·12	0·06	0·12	1·725	1·619	42·0
		0·06	0·18	2·087	2·328	42·7
		0·12	0·12	1·760	1·692	41·9
		0·12	0·18	2·229	2·548	42·6

TABLE 4—*continued*

III. *Variation of* μ_2

n_v	l_v	μ_2	Span	Height ft.	Lateral oscillation		Spiral root
					Period	Time to halve amplitude	Time to halve amplitude
0·024	0	5	169	Sea level	8·752	3·155	— 61·2
		10		20,000	8·758	4·476	— 82·7
		20		40,000	8·765	6·372	—114·3
		20	42·25	Sea level	4·382	3·186	— 57·2
		40		20,000	4·387	4·553	— 79·8
		80		40,000	4·391	6·526	—112·3
0·024	—0·12	5	169	Sea level	7·086	4·479	30·2
		10		20,000	7·174	8·515	41·9
		20		40,000	7·322	26·040	58·6
		20	42·25	Sea level	3·661	13·020	29·3
		40		20,000	3·764	—29·077	41·2
		80		40,000	3·888	— 9·727	58·1
0·096	0	5	169	Sea level	4·426	1·764	— 58·9
		10		20,000	4·408	2·511	— 81·1
		20		40,000	4·402	3·581	—113·2
		20	42·25	Sea level	2·201	1·790	— 56·6
		40		20,000	2·201	2·552	— 79·5
		80		40,000	2·201	3·631	—112·0
0·096	—0·12	5	169	Sea level	4·197	2·065	43·8
		10		20,000	4·218	3·195	60·8
		20		40,000	4·258	5·096	85·1
		20	42·25	Sea level	2·129	2·548	42·6
		40		20,000	2·151	4·133	59·9
		80		40,000	2·171	6·661	84·5

TABLE 5

Check of Approximate Formulae for Rates of Roll and Yaw due to Side-Gust

Basic conditions

	$n_v = 0{\cdot}024$		$n_v = 0{\cdot}048$		$n_v = 0{\cdot}096$	
	Theory	Meas.	Theory	Meas.	Theory	Meas.
$\hat{p}$						
$l_v = 0{\cdot}06$	2·6	—	2·4	2·1	2·1	1·8
0	0	0·2	0	0·3	0	0·4
−0·06	2·6	—	2·4	1·7	2·1	1·5
−0·12	5·2	3·7	4·8	3·4	4·2	3·0
$\hat{r}$						
$l_v = 0{\cdot}06$	1·6	—	2·3	2·3	3·3	3·3
0	1·6	1·7	2·3	2·3	3·3	3·3
−0·06	1·6	—	2·3	2·2	3·3	3·2
−0·12	1·6	1·6	2·3	2·2	3·3	3·1

TABLE 6

Summary of the Principal Factors affecting the Character of the Motion due to Side-Gust

Quantity increased	Effect of increase on the lateral oscillation				
	Period	No. of swings to halve amplitude	Amplitude in yaw		Force on pilot at C.G.
			Rate.	Acceleration.	
Wing loading ..	Incr.	Incr.	Decr.	Decr.	Decr.
Span	Incr.	Decr.	Decr.	Decr.	Nil
Velocity ..	Decr.	Nil	Nil	Incr.	Incr.
Inertia in yaw ..	Incr.	Var.	Decr.	Decr.	Nil
Fin area ..	Decr.	Var.	Incr.	Incr.	Nil
Dihedral ..	Small	Incr.	Nil	Nil	Nil
Body side area..	Nil	Decr.	Nil	Nil	Incr.

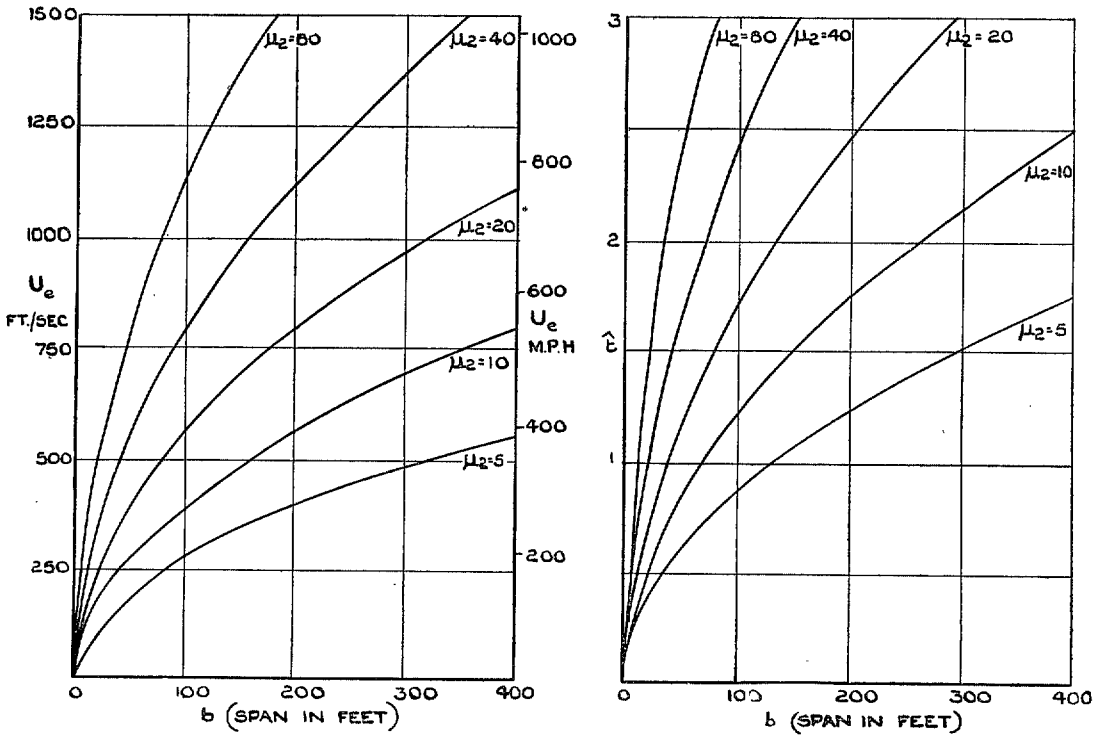

FIG. 1. Curves for determining $\hat{t}, \bar{U}_e$ ($\mu_2 = 5$, 10, 20, 40, 80, and $C_L = 0{\cdot}2$).

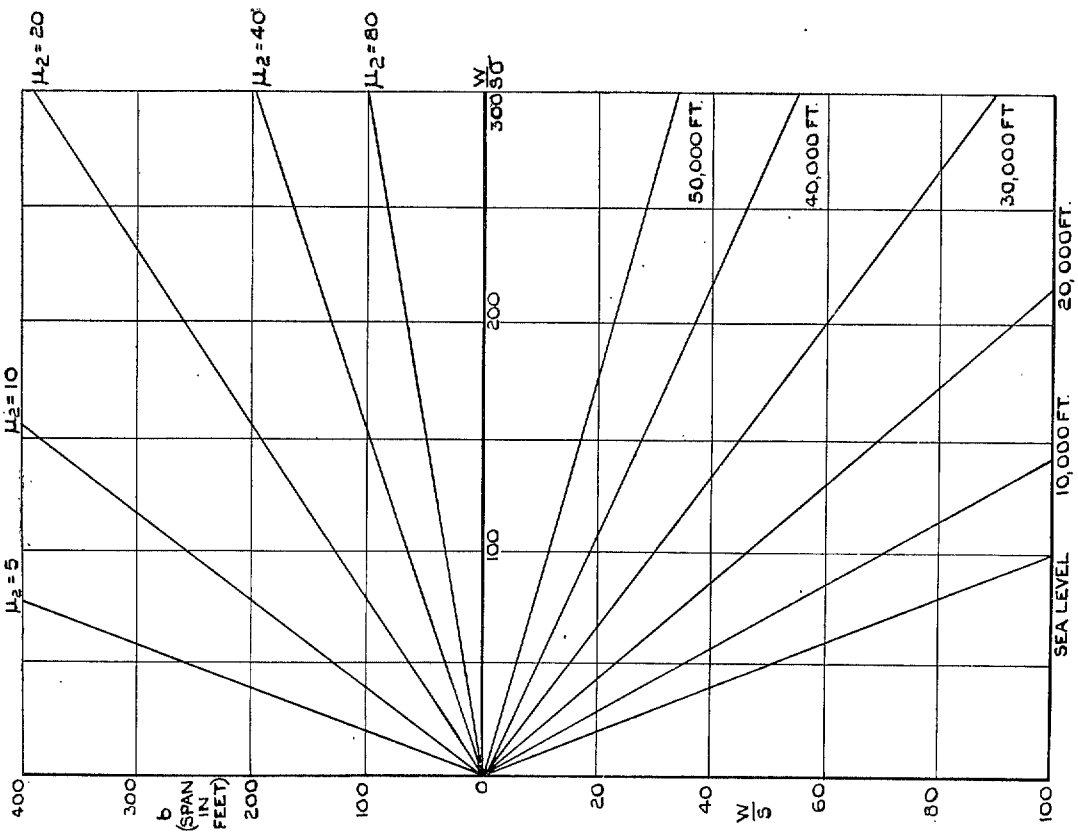

FIG. 2. Curves for determining $W/S\sigma$ and W/S ($\mu_2 = 5$, 10, 20, 40, 80, and $C_L = 0{\cdot}2$).

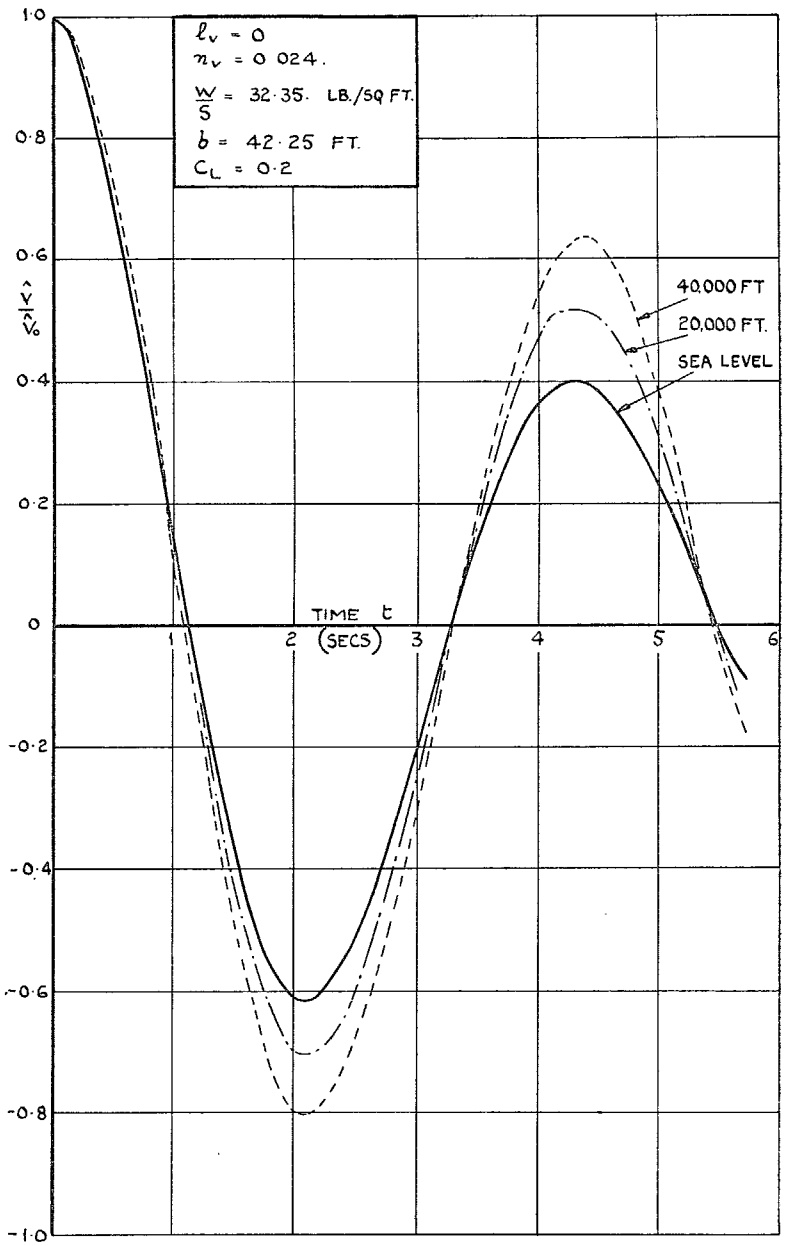

FIG. 3. Response to a side-gust. Variation with height.

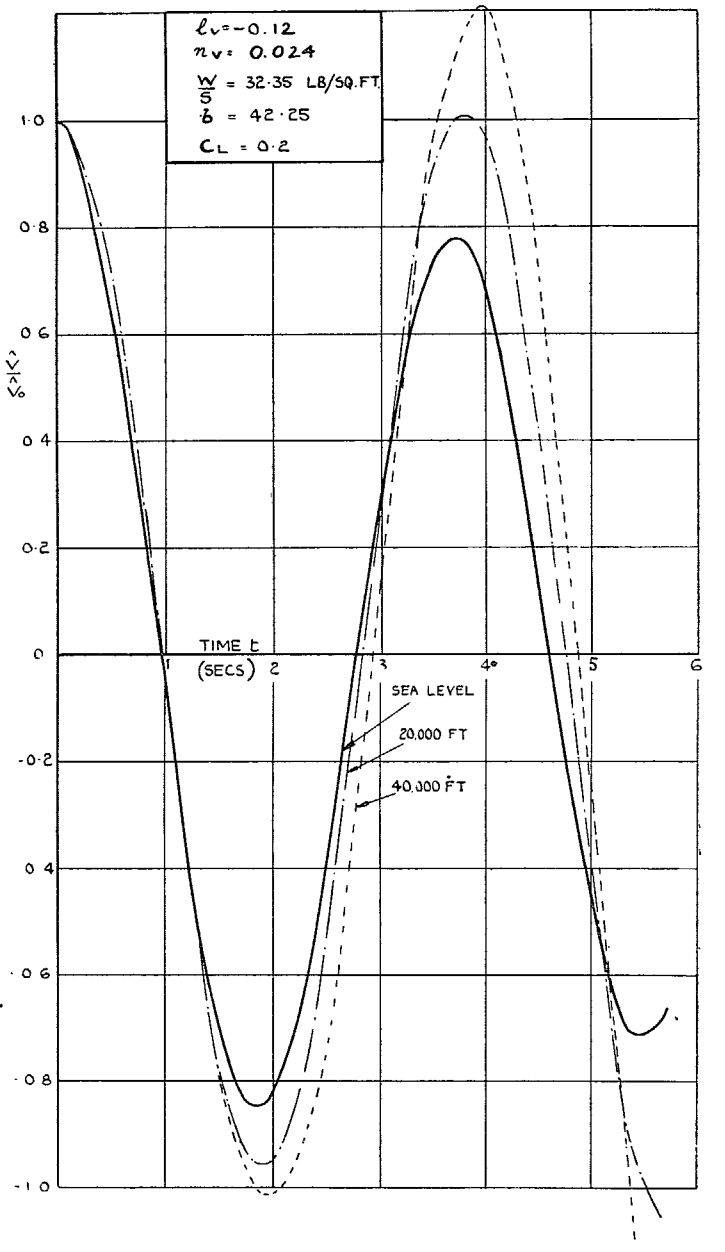

FIG. 4. Response to a side-gust. Variation with height.

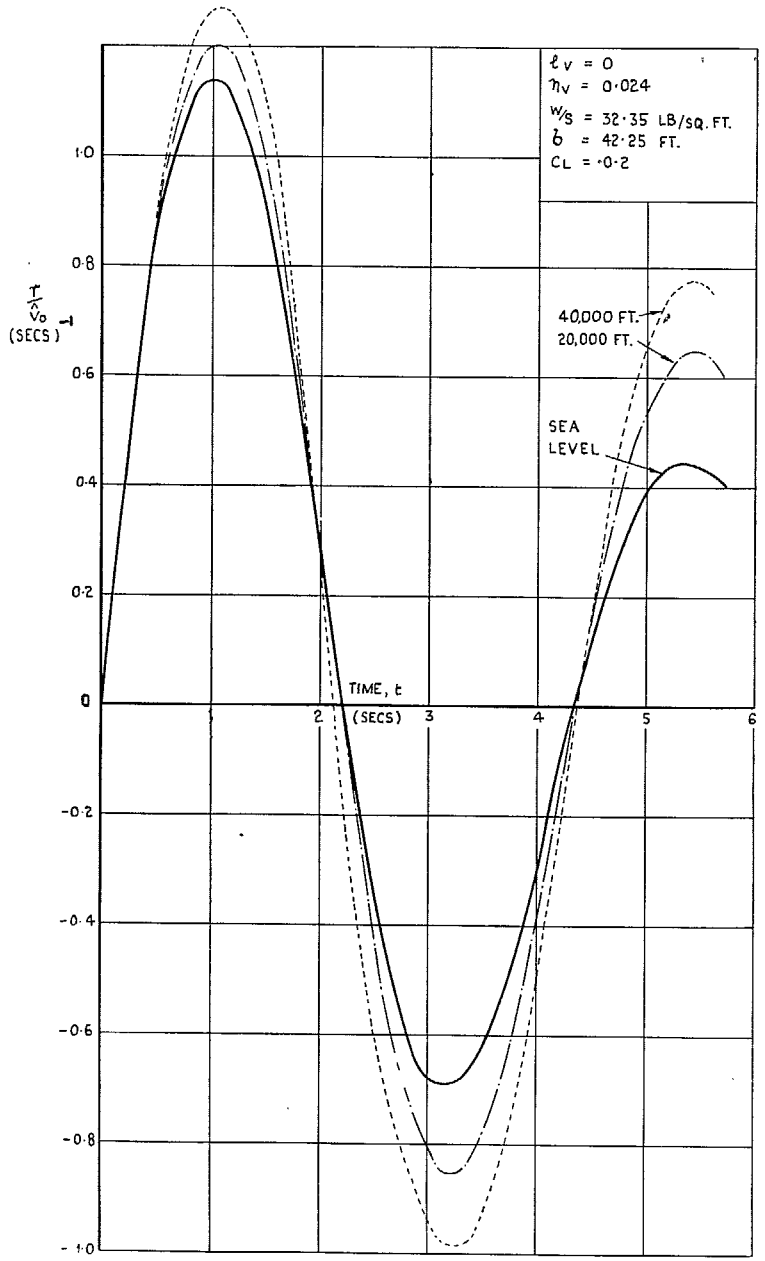

FIG. 5. Rate of yaw due to side-gust. Variation with height.

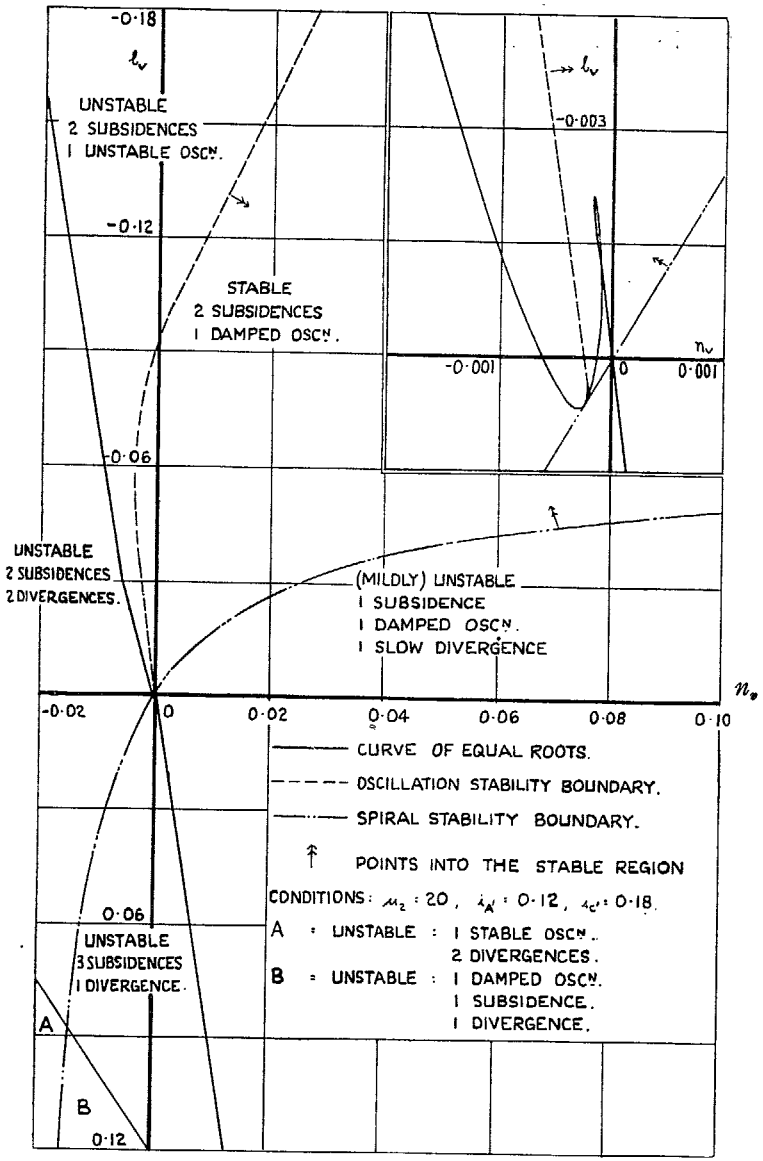

FIG. 6. Stability Diagram for Basic Conditions.

The spiral and oscillation boundaries and the curve of equal roots demarcate various regions in the (l_v, n_v) diagram, having the characteristics shown. The inset figure shows the curves near the origin.

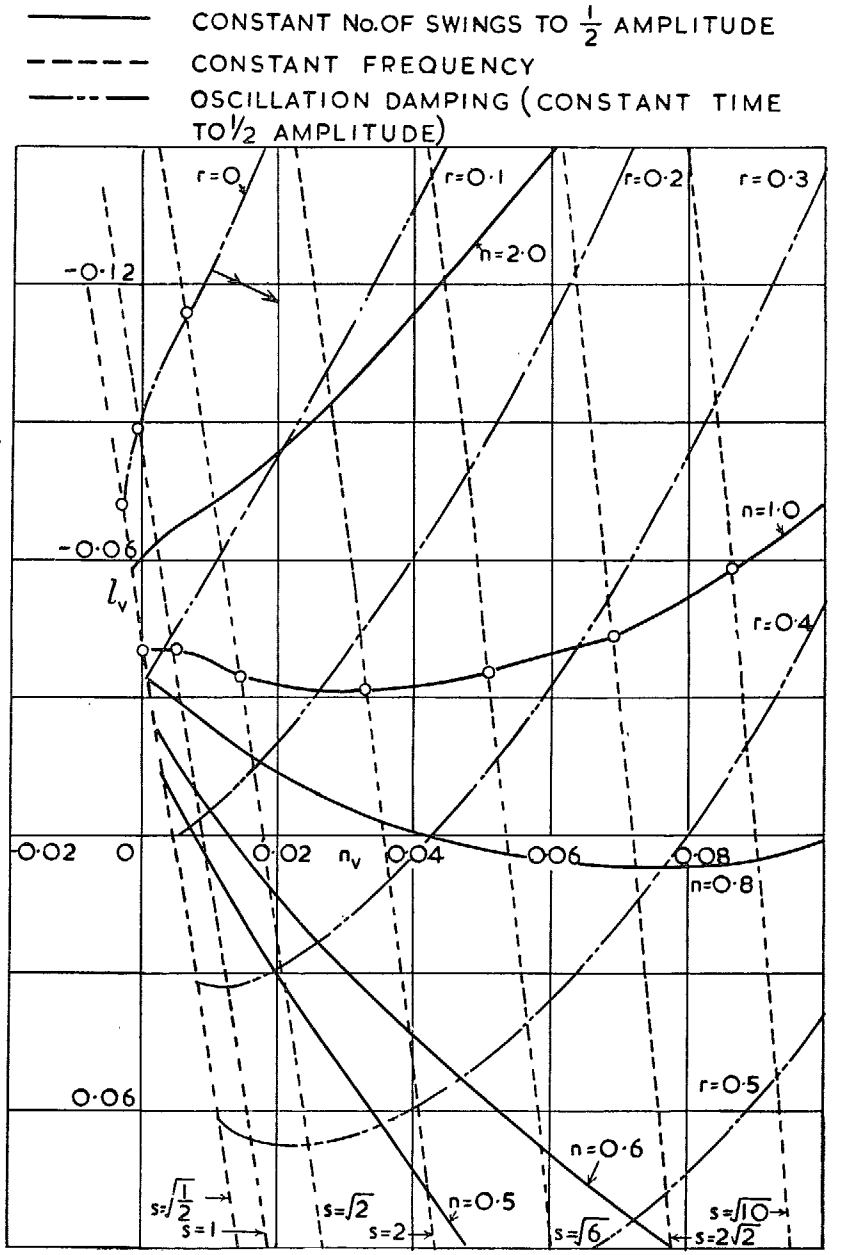

FIG. 7. Stability diagram for basic conditions showing curves of constant oscillation damping (r), constant number of swings to half amplitude (n) and constant frequency (s).

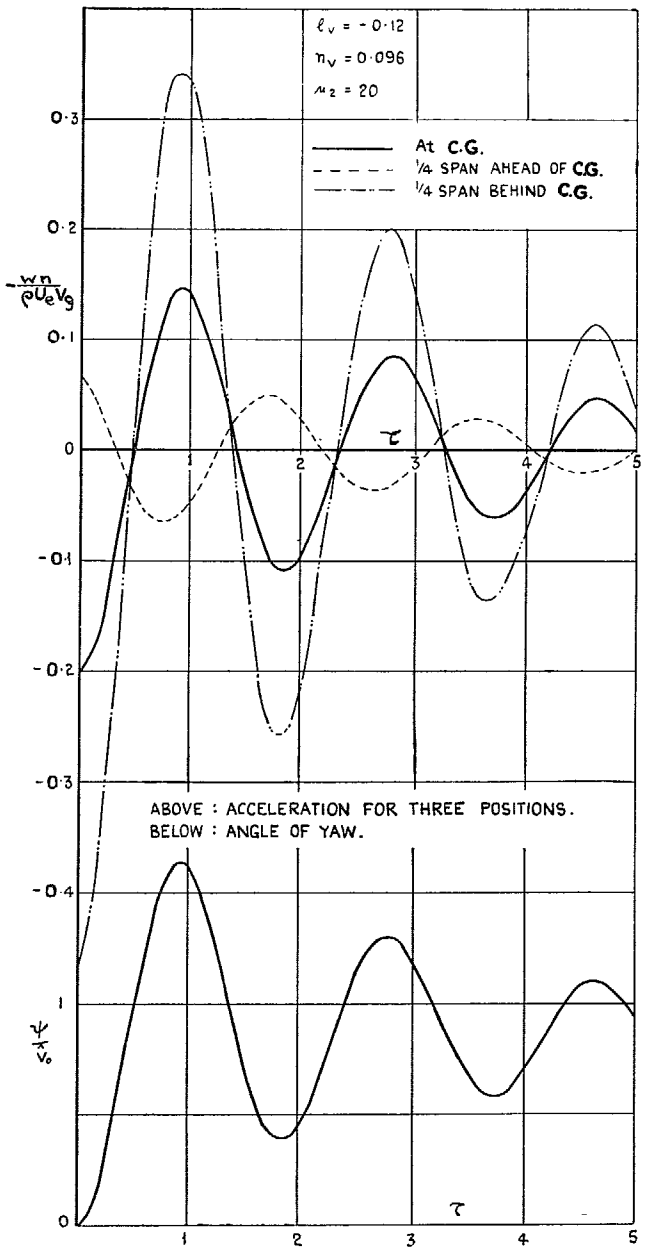

FIG. 8. Effect of pilot's position on the acceleration at pilot's seat.

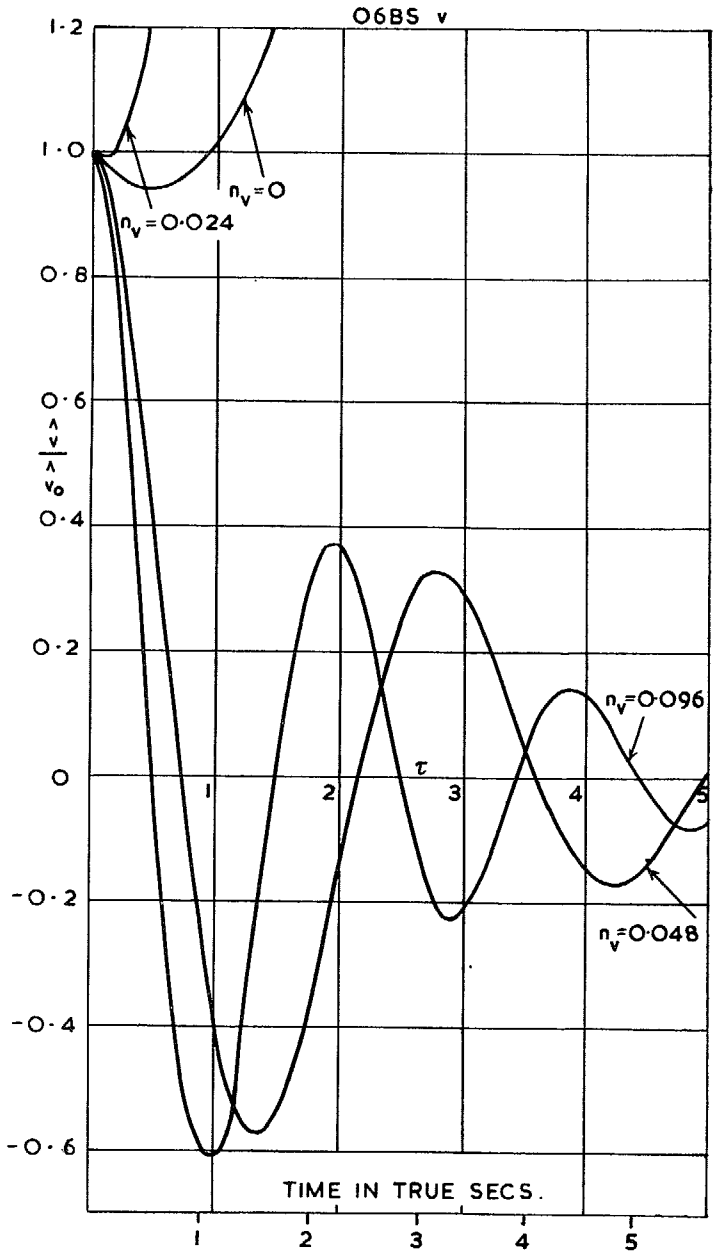

FIG. 9 (S.2). Response to initial sideslip. Angle of sideslip for $l_v = 0{\cdot}06$ and $\mu_2 = 20$. Effect of varying n_v.

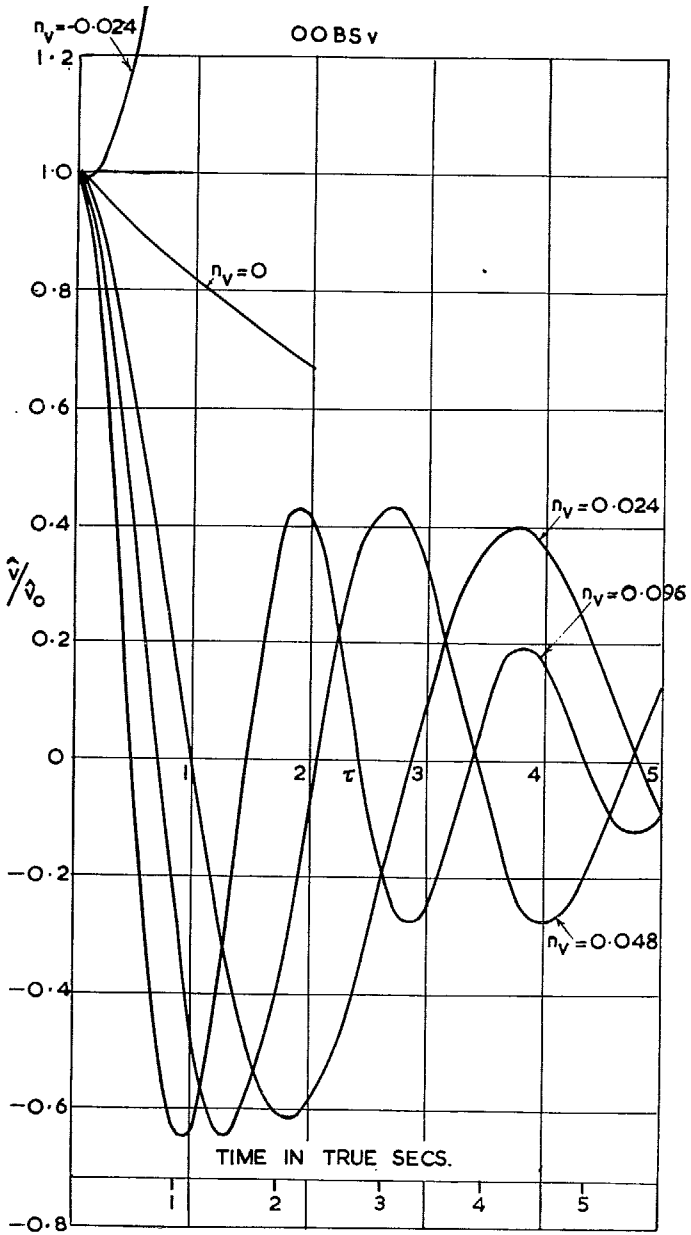

FIG. 10 (S.8). Response to initial sideslip. Angle of sideslip for $l_v = 0$ and $\mu_2 = 20$. Effect of varying n_v.

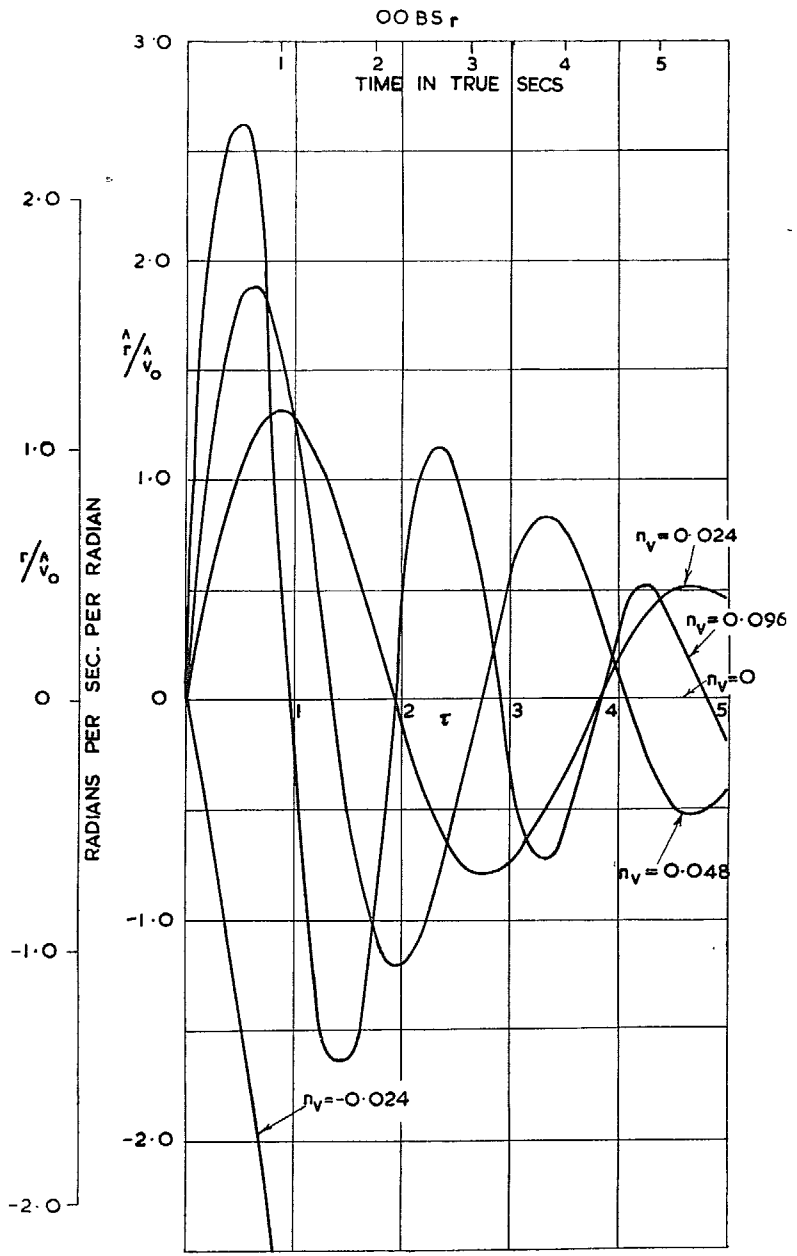

FIG. 11 (S.9). Response to initial sideslip. Rate of yaw for $l_v = 0$ and $\mu_2 = 20$. Effect of varying n_v.

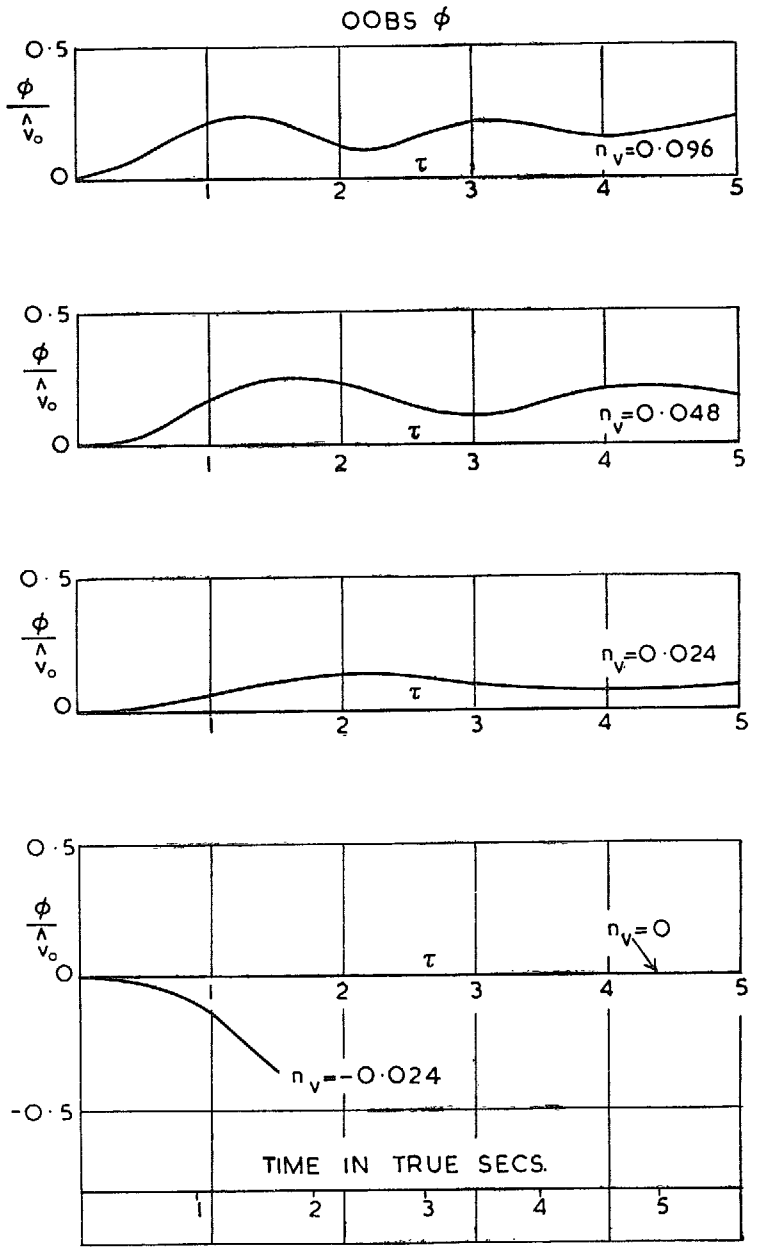

FIG. 12 (S.10). Response to initial sideslip. Angle of bank for $l_v = 0$ and $\mu_2 = 20$. Effect of varying n_v.

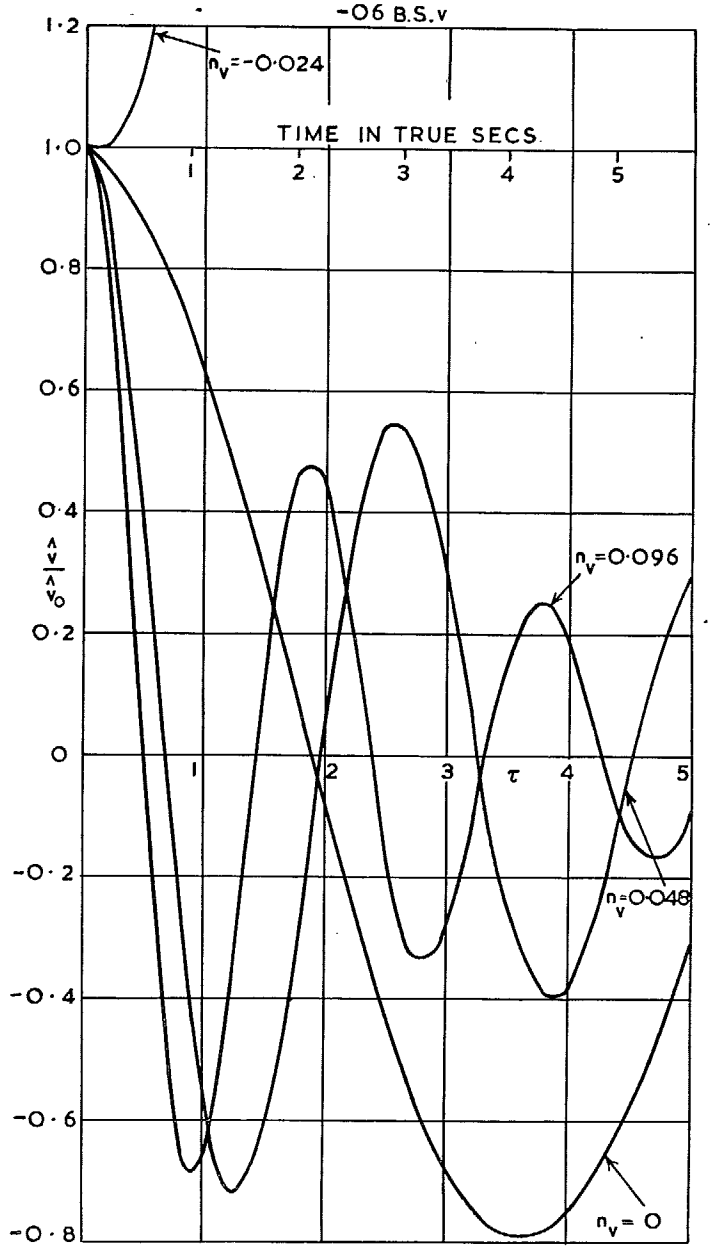

FIG. 13 (S.14). Response to initial sideslip. Angle of sideslip for $l_v = -0{\cdot}06$ and $\mu_2 = 20$. Effect of varying n_v.

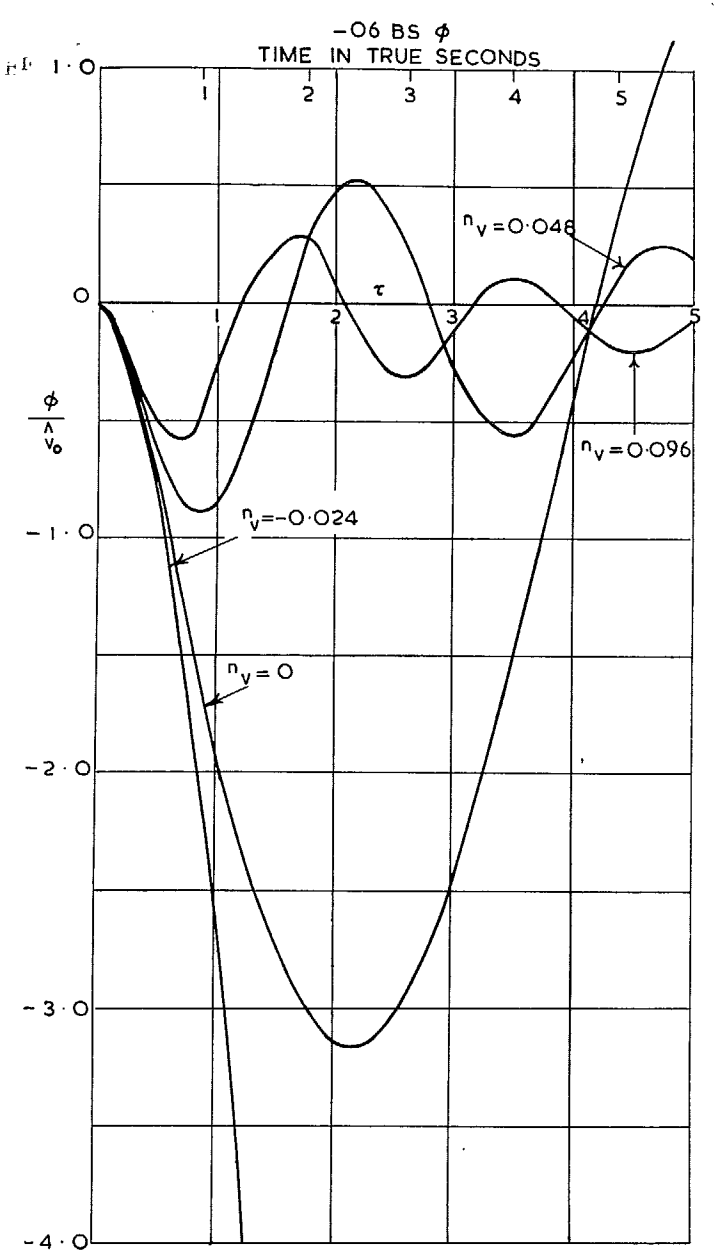

FIG. 14 (S.16). Response to initial sideslip. Angle of bank for $l_v = -0{\cdot}06$ and $\mu_2 = 20$. Effect of varying n_v.

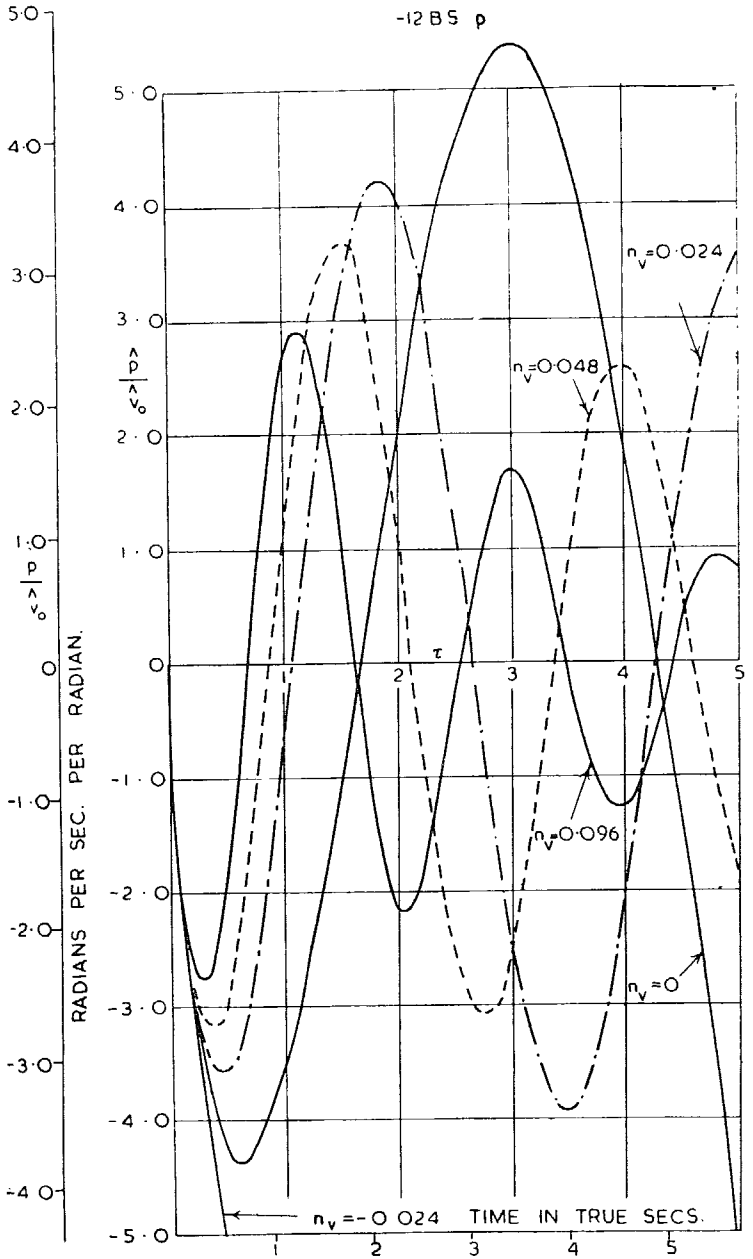

FIG. 15 (S.19). Response to initial sideslip. Rate of roll for $l_v = -0{\cdot}12$ and $\mu_2 = 20$. Effect of varying n_v.

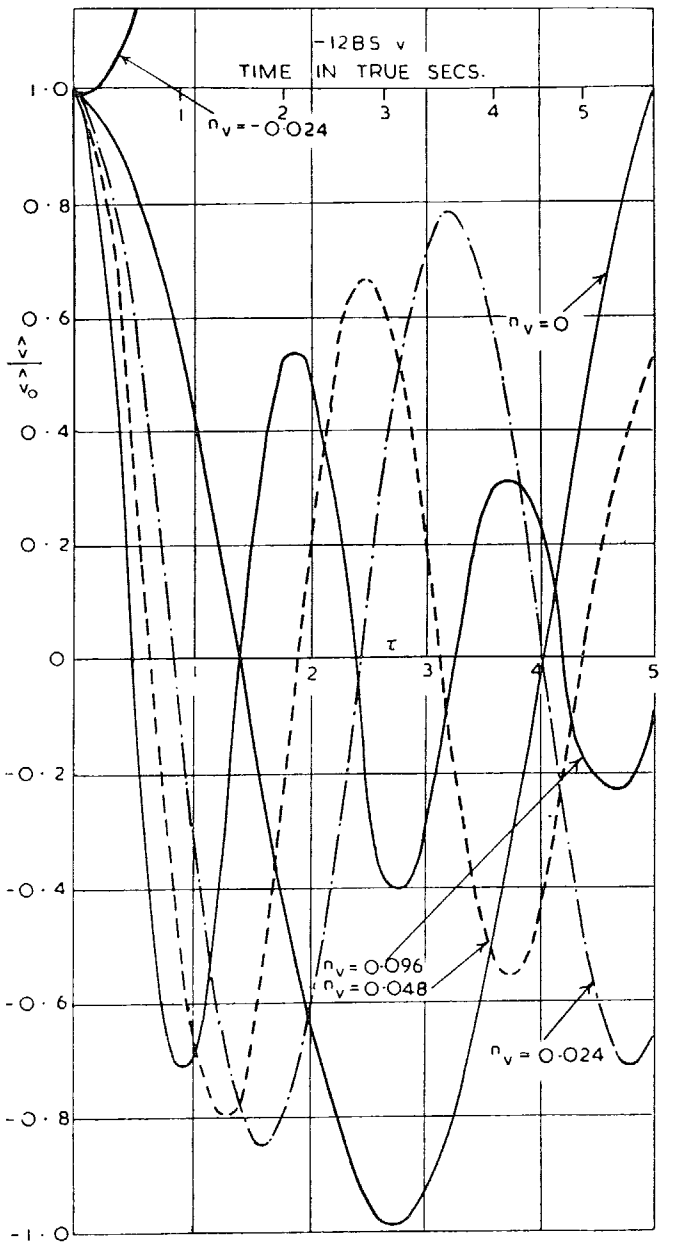

FIG. 16 (S.20). Response to initial sideslip. Angle of sideslip for $l_v = -0{\cdot}12$ and $\mu_2 = 20$. Effect of varying n_v.

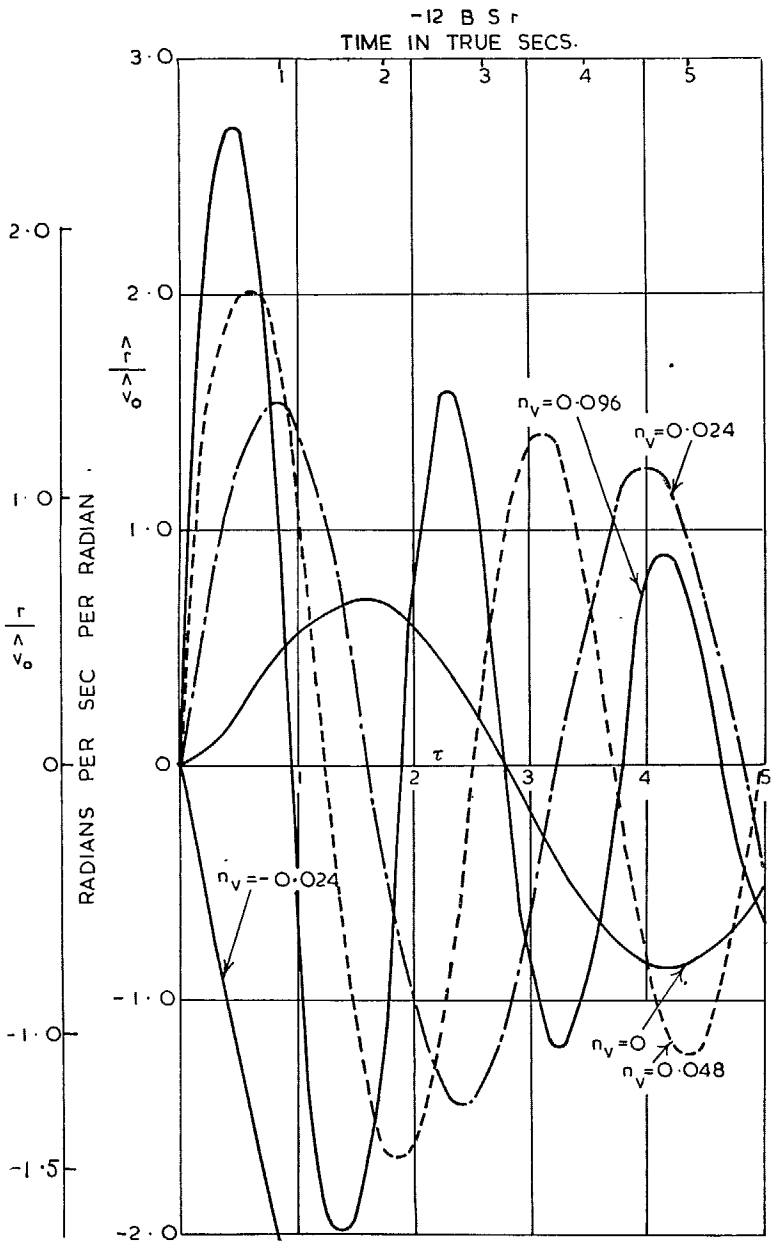

FIG. 17 (S.21). Response to initial sideslip. Rate of yaw for $l_v = -0{\cdot}12$ and $\mu_2 = 20$. Effect of varying n_v.

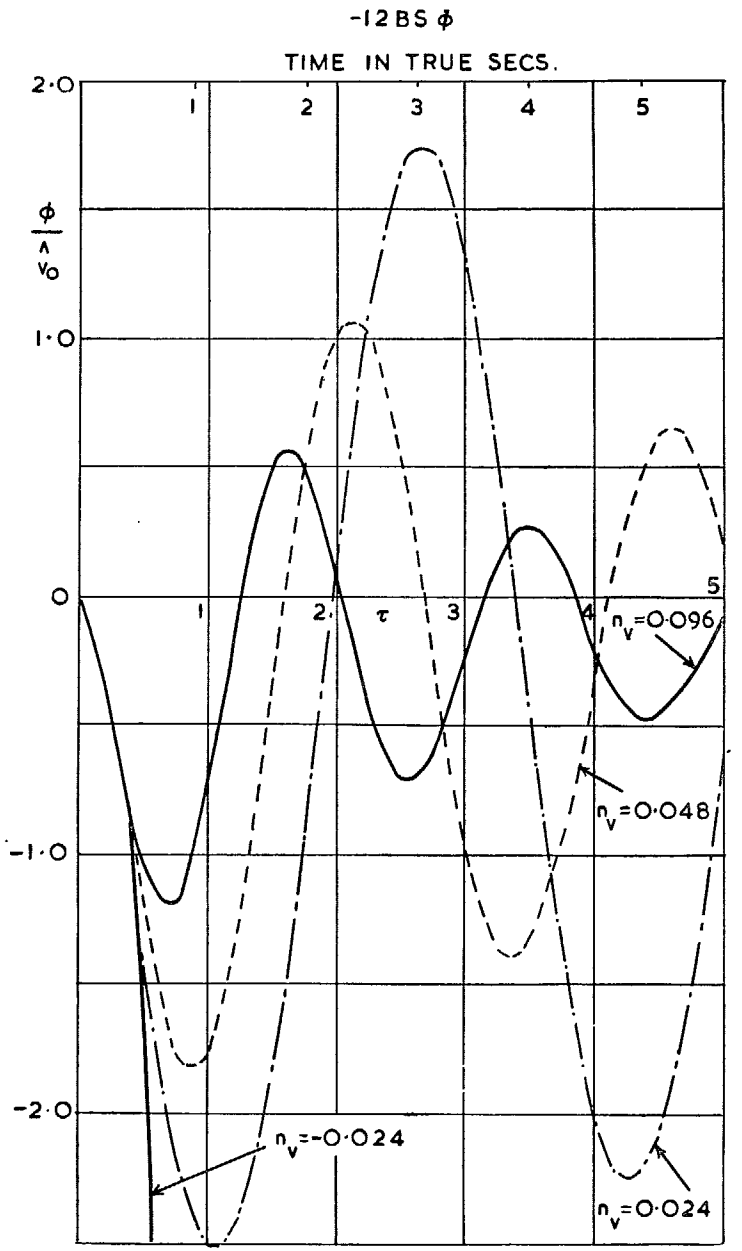

FIG. 18 (S.22). Response to initial sideslip. Angle of bank for $l_v = -0{\cdot}12$ and $\mu_2 = 20$. Effect of varying n_v.

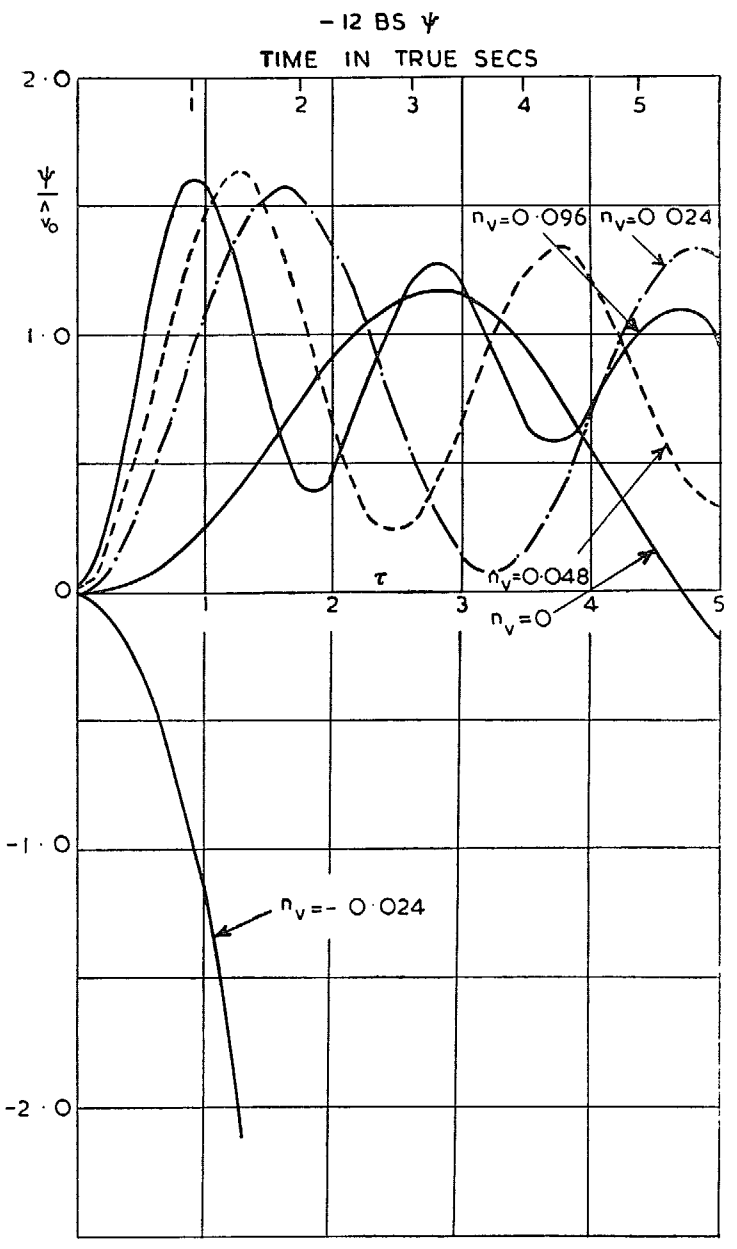

FIG. 19 (S.23). Response to initial sideslip. Angle of yaw for $l_v = -0{\cdot}12$ and $\mu_2 = 20$. Effect of varying n_v.

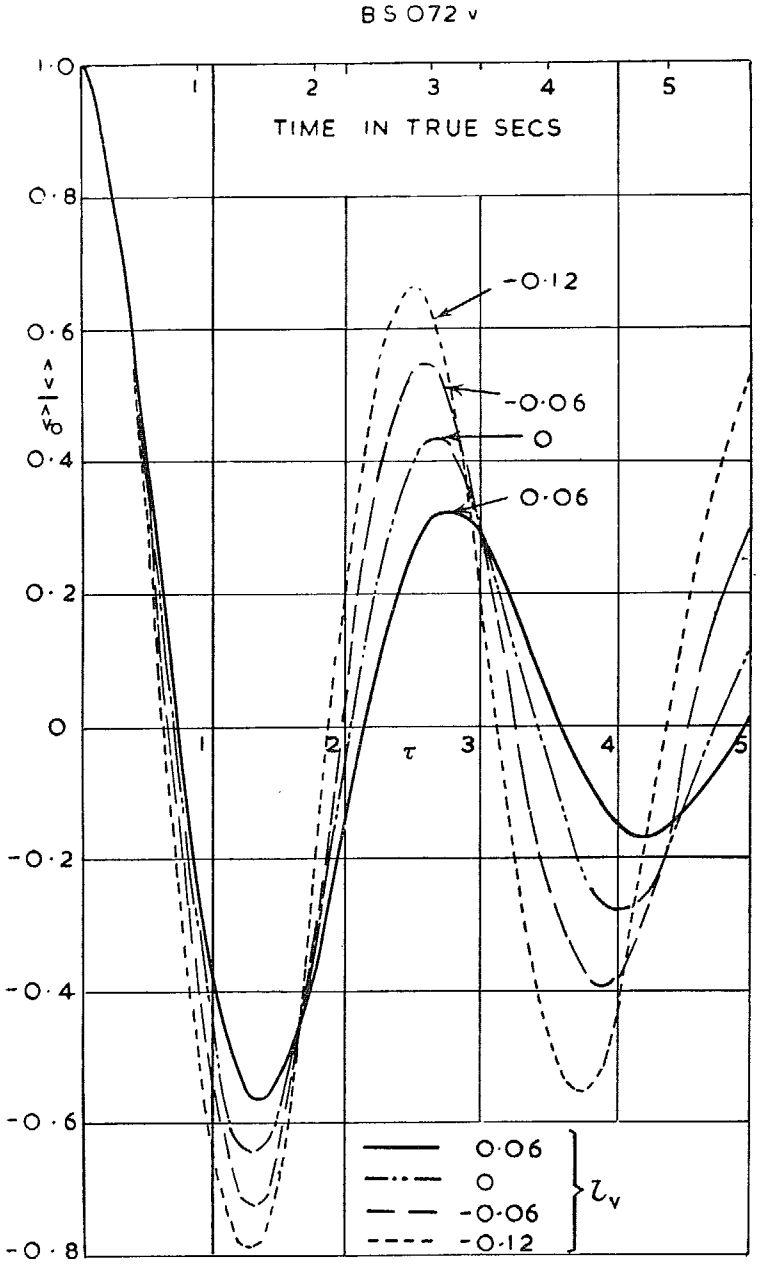

FIG. 20 (S.38). Response to initial sideslip. Angle of sideslip for $n_v = 0{\cdot}048$ and $\mu_2 = 20$. Effect of varying l_v.

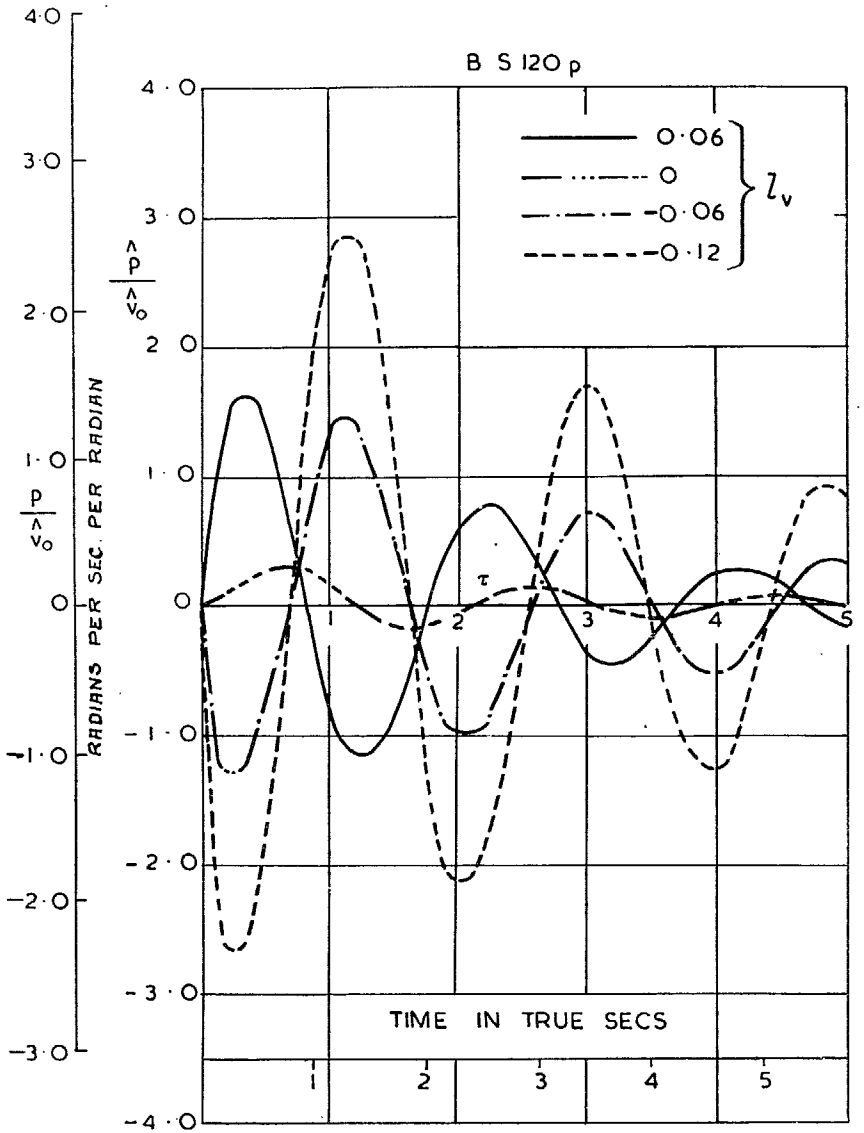

FIG. 21 (S.43). Response to initial sideslip. Rate of roll for $n_v = 0{\cdot}096$ and $\mu_2 = 20$. Effect of varying l_v.

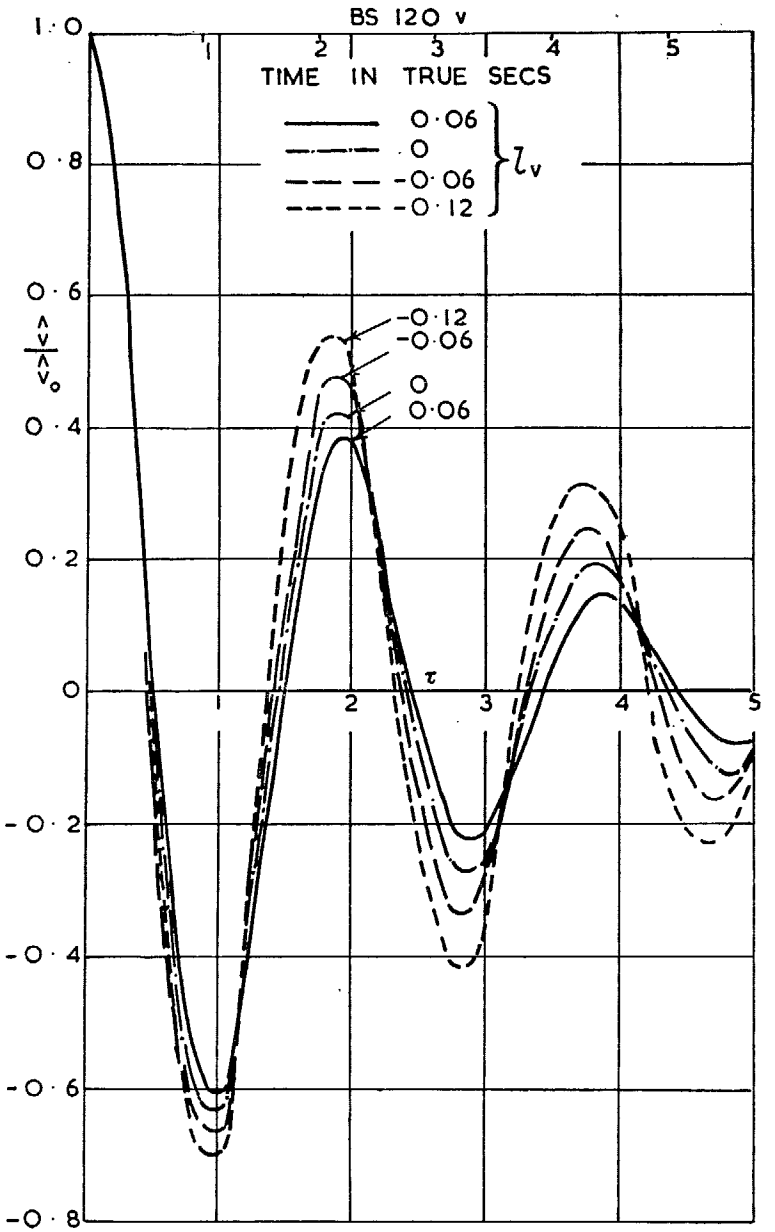

FIG. 22 (S.44). Response to initial sideslip. Angle of sideslip for $n_v = 0{\cdot}096$ and $\mu_2 = 20$. Effect of varying l_v.

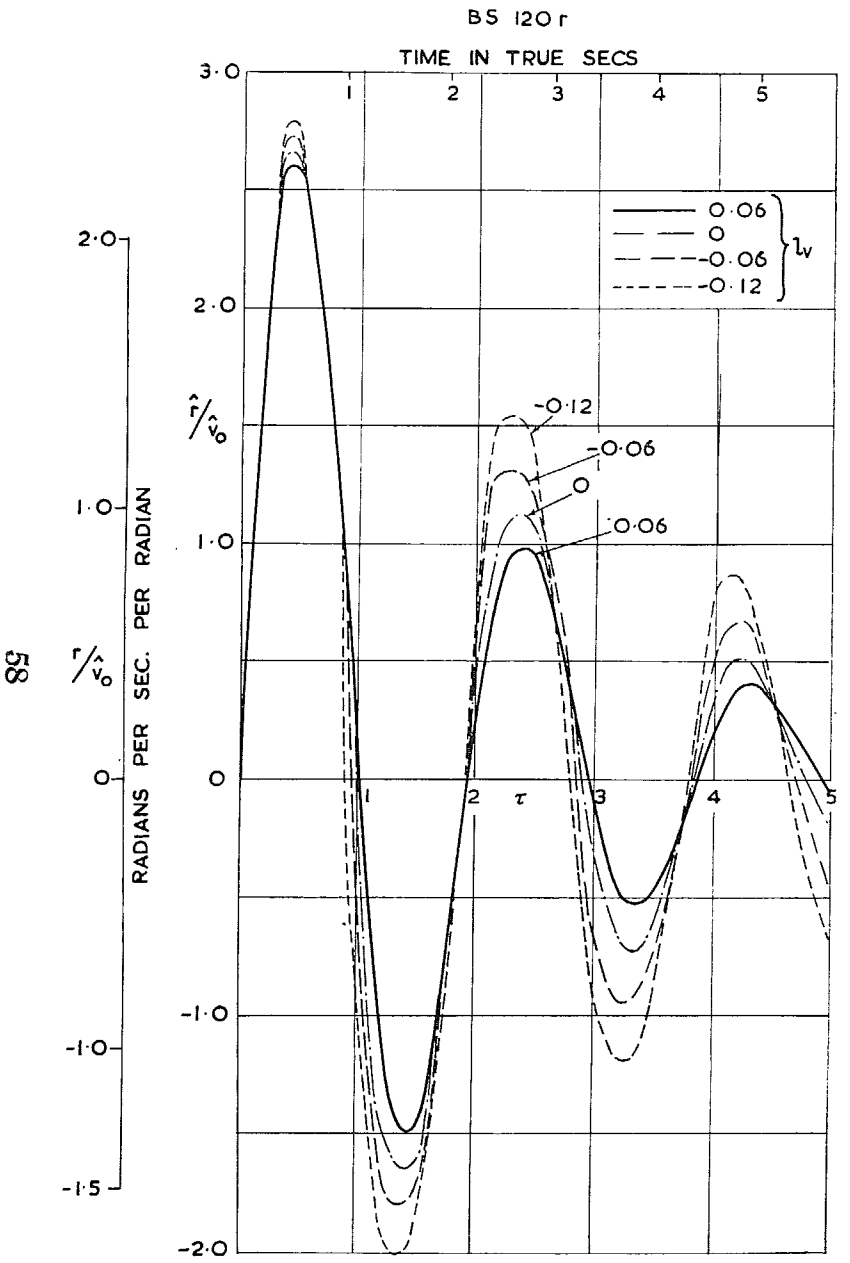

FIG. 23 (S.45). Response to initial sideslip. Rate of yaw for $n_v = 0{\cdot}096$ and $\mu_2 = 20$. Effect of varying l_v.

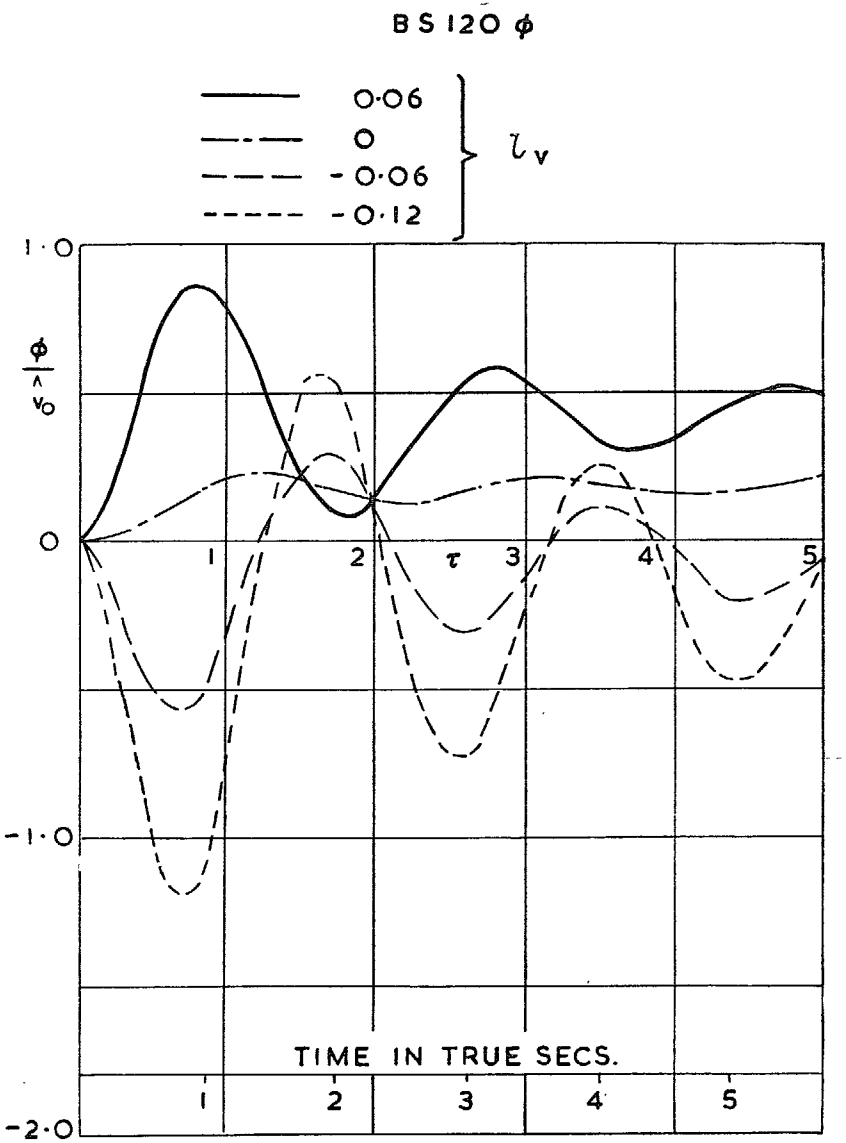

FIG. 24 (S.46). Response to initial sideslip. Angle of bank for $n_v = 0{\cdot}096$ and $\mu_2 = 20$. Effect of varying l_v.

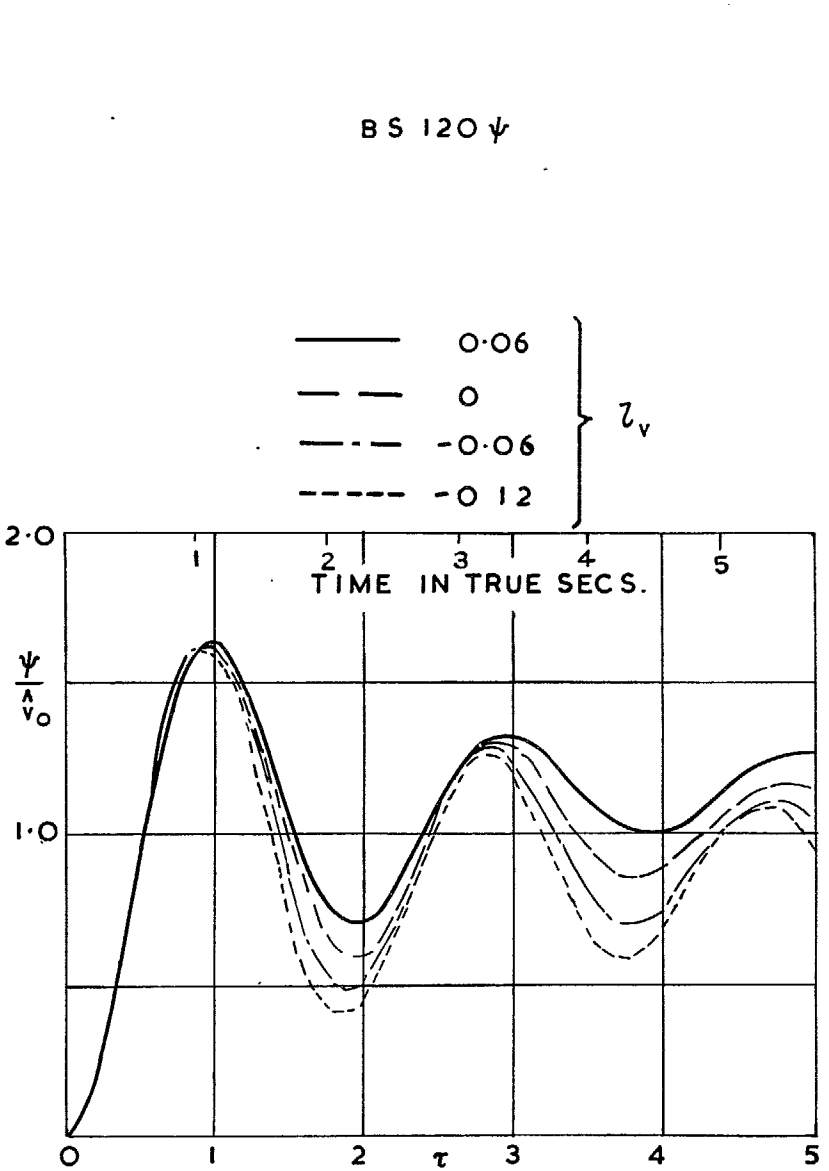

FIG. 25 (S.47). Response to initial sideslip. Angle of yaw for $n_v = 0{\cdot}096$ and $\mu_2 = 20$. Effect of varying l_v.

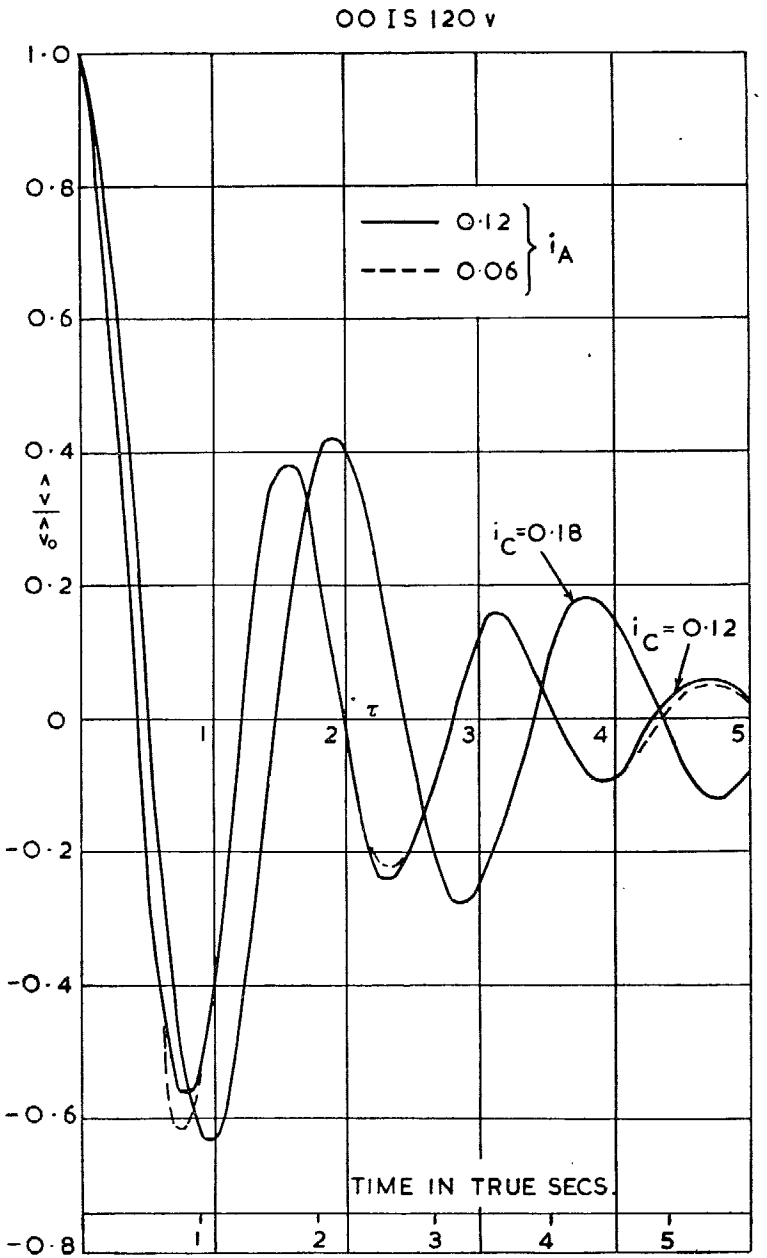

FIG. 26 (S.62). Response to initial sideslip. Angle of sideslip for $n_v = 0{\cdot}096$ and $l_v = 0$. Effect of varying inertia.

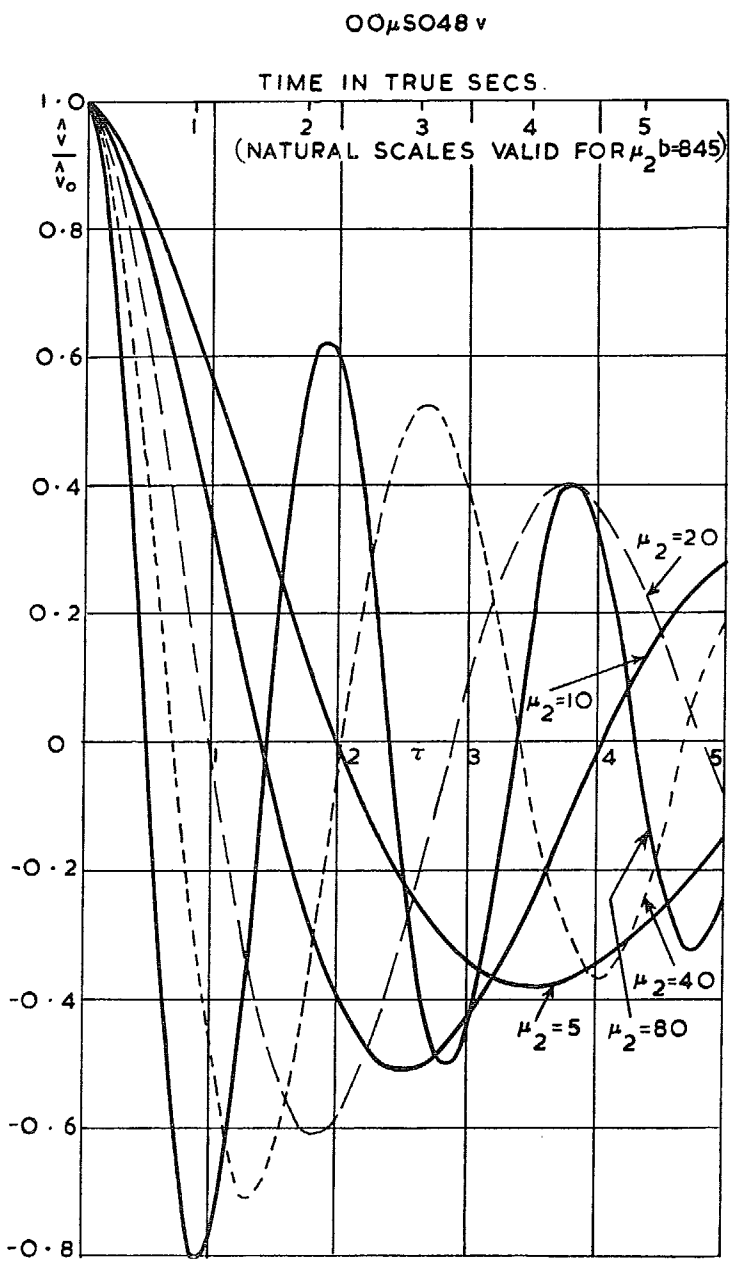

FIG. 27 (S.74). Response to initial sideslip. Angle of sideslip for $l_v = 0$ and $n_v = 0{\cdot}024$. Effect of varying μ_2.

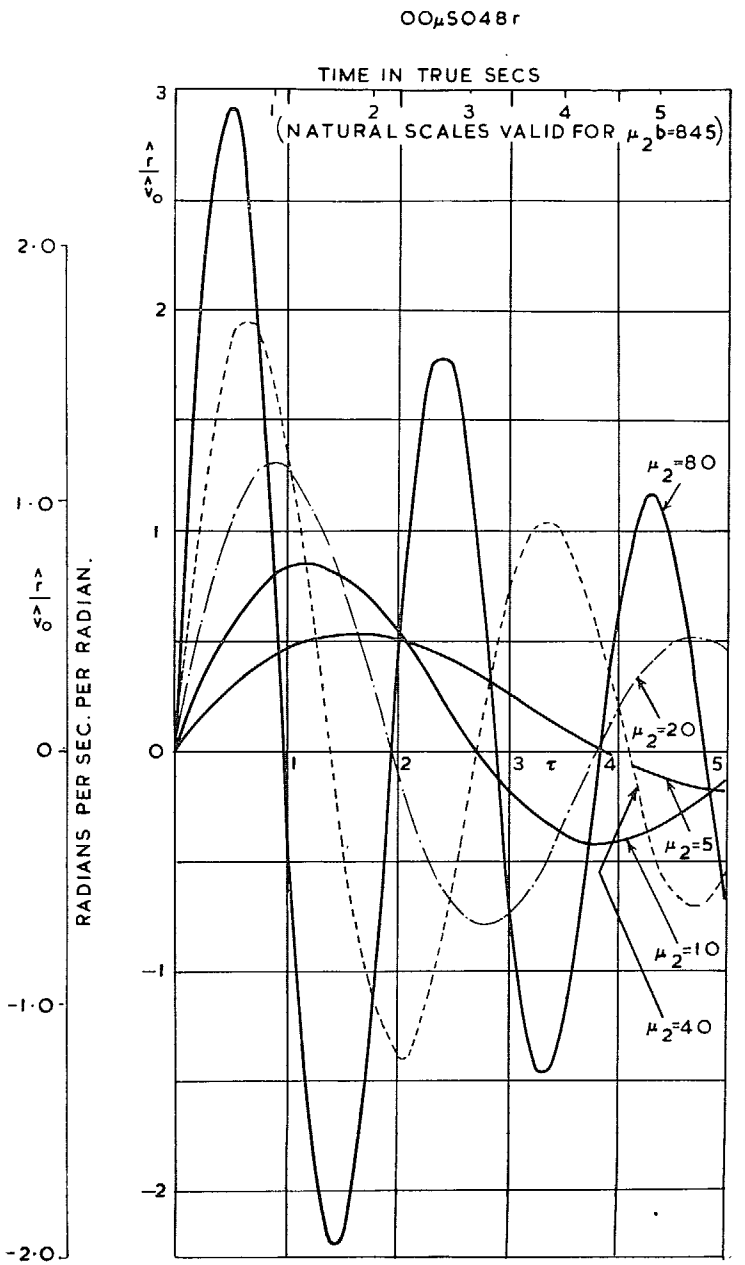

FIG. 28 (S.75). Response to initial sideslip. Rate of yaw for $l_v = 0$, and $n_v = 0{\cdot}024$. Effect of varying μ_2.

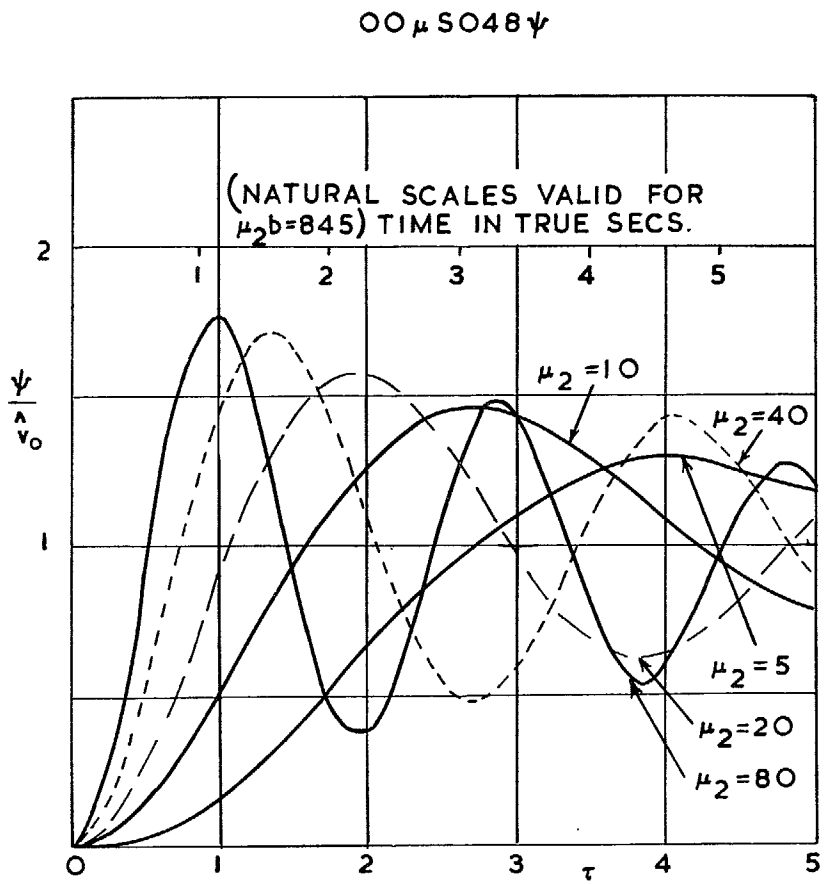

FIG. 29 (S.77). Response to initial sideslip. Angle of yaw for $l_v = 0$ and $n_v = 0{\cdot}024$. Effect of varying μ_2.

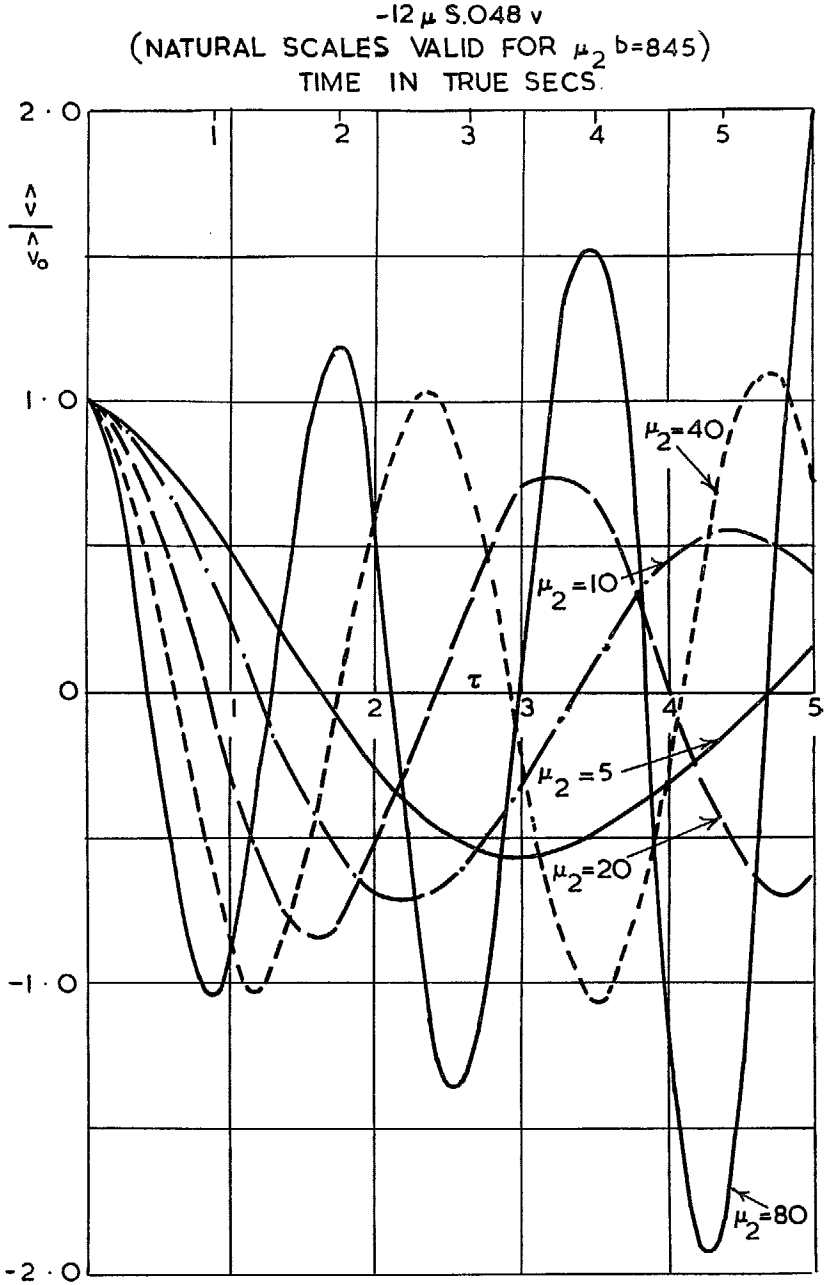

FIG. 30 (S.80). Response to initial sideslip. Angle of sideslip for $l_v = -0{\cdot}12$ and $n_v = 0{\cdot}024$. Effect of varying μ_2.

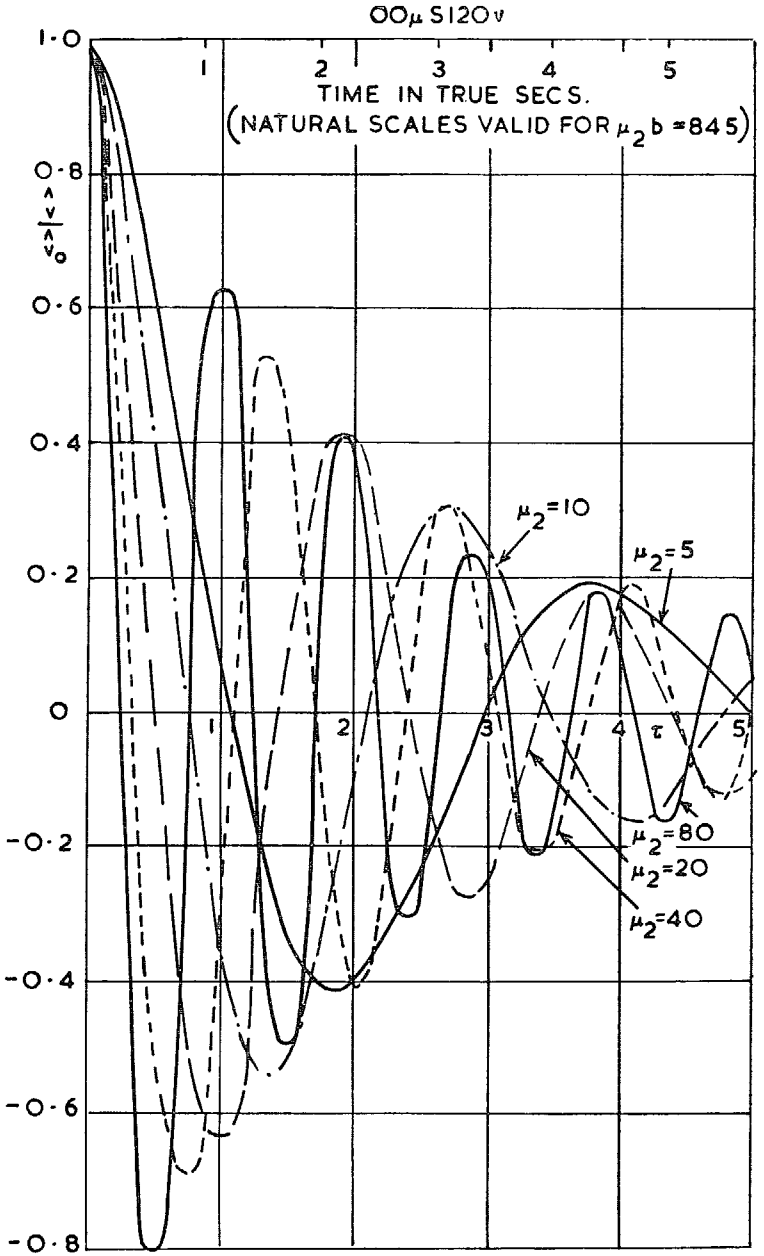

FIG. 31 (S.86). Response to initial sideslip. Angle of sideslip for $l_v = 0$ and $n_v = 0{\cdot}096$. Effect of varying μ_2.

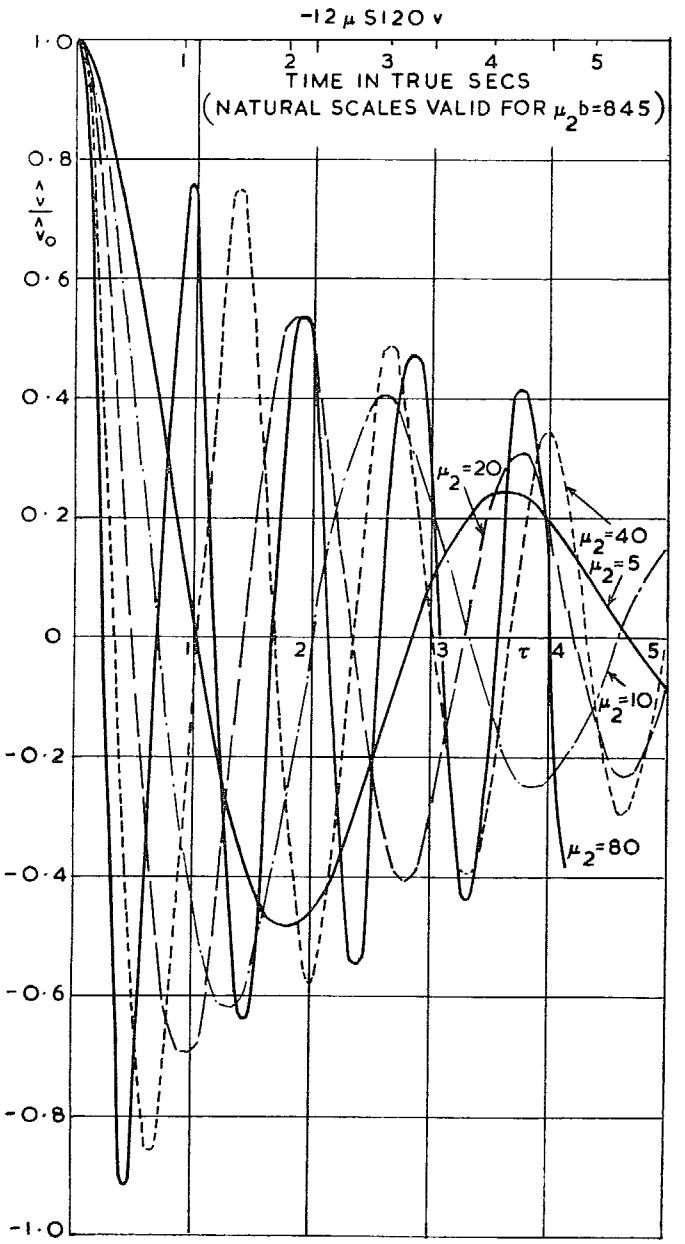

FIG. 32 (S.92). Response to initial sideslip. Angle of sideslip for $l_v = -0{\cdot}12$ and $n_v = 0{\cdot}096$. Effect of varying μ_2.

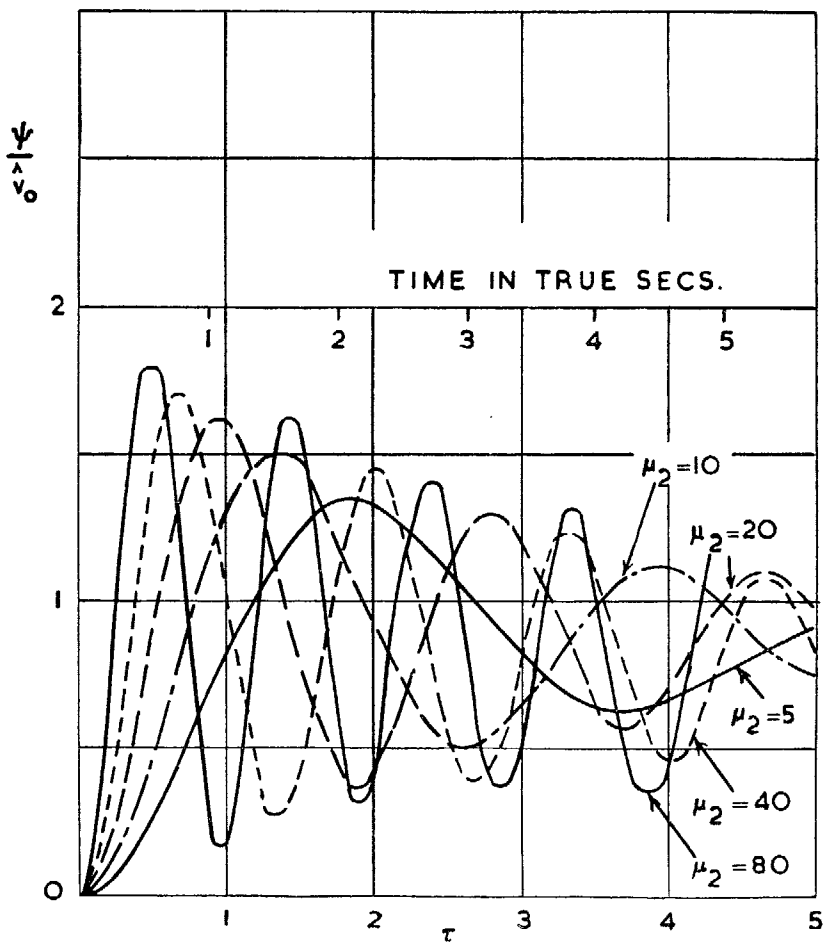

FIG. 33 (S.95). Response to initial sideslip. Angle of yaw for $l_v = -0{\cdot}12$ and $n_v = 0{\cdot}096$. Effect of varying μ_2. (The natural time scale is valid for $\mu_2 b = 845$).

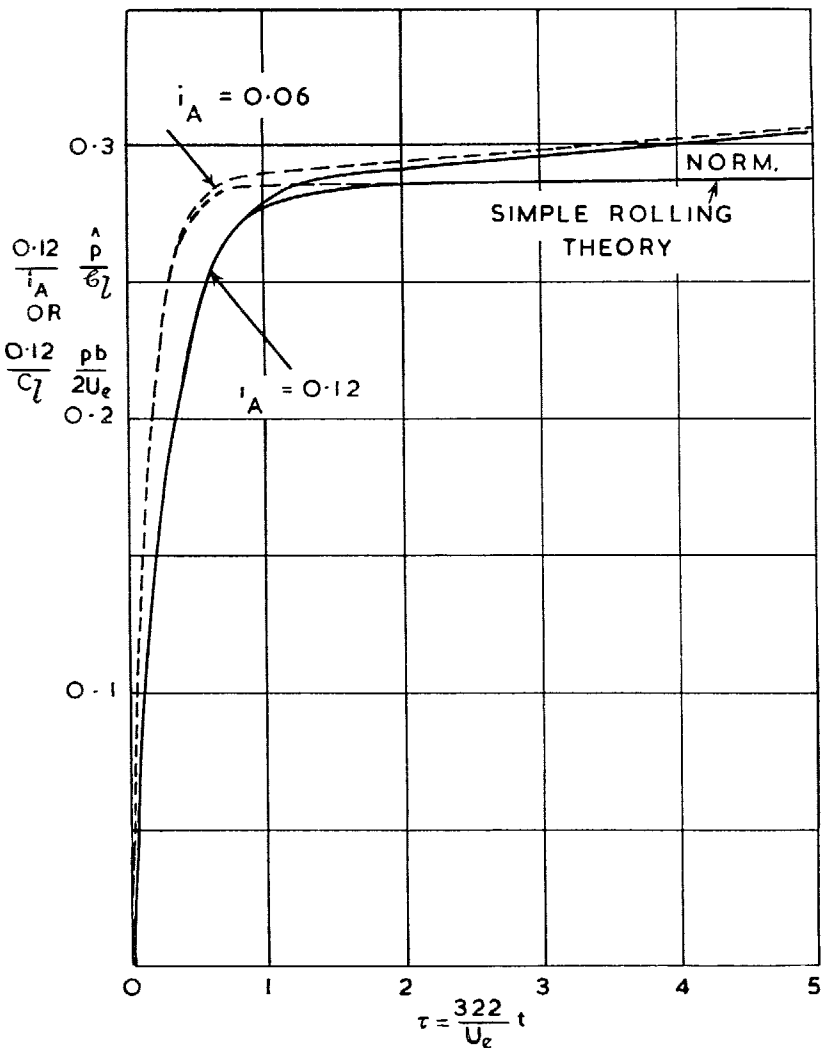

FIG. 34. Aileron response, no sideslip. Rate of roll for varying i_A.

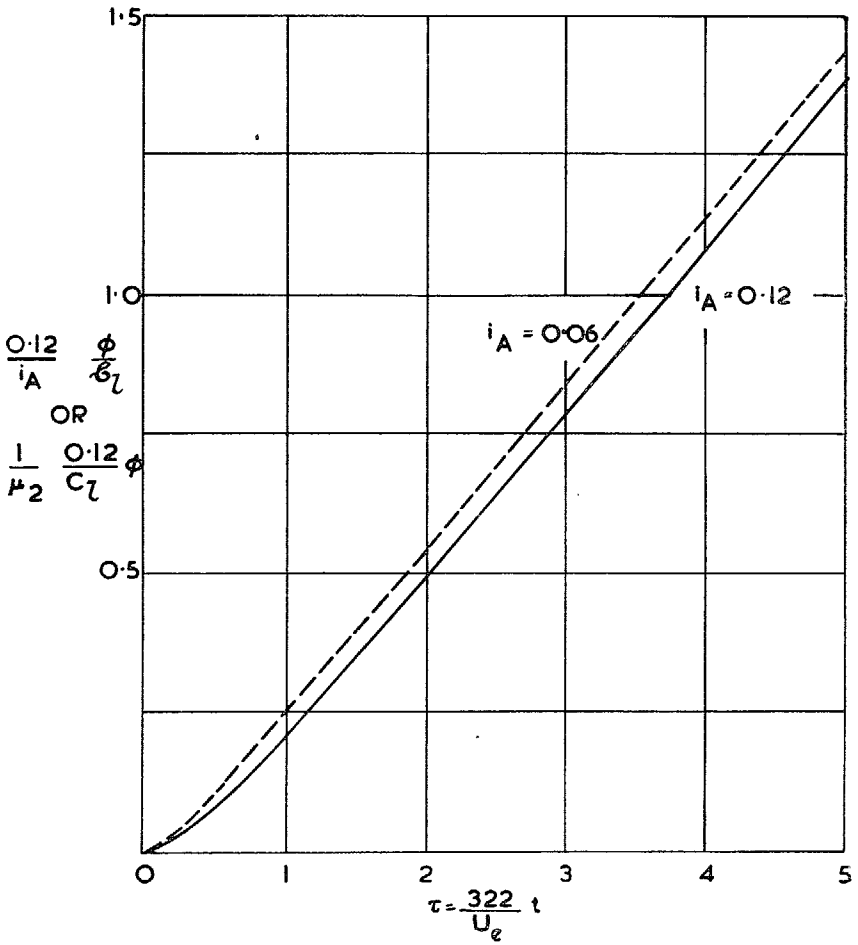

FIG. 35. Aileron response, no sideslip. Angle of bank for varying i_A.

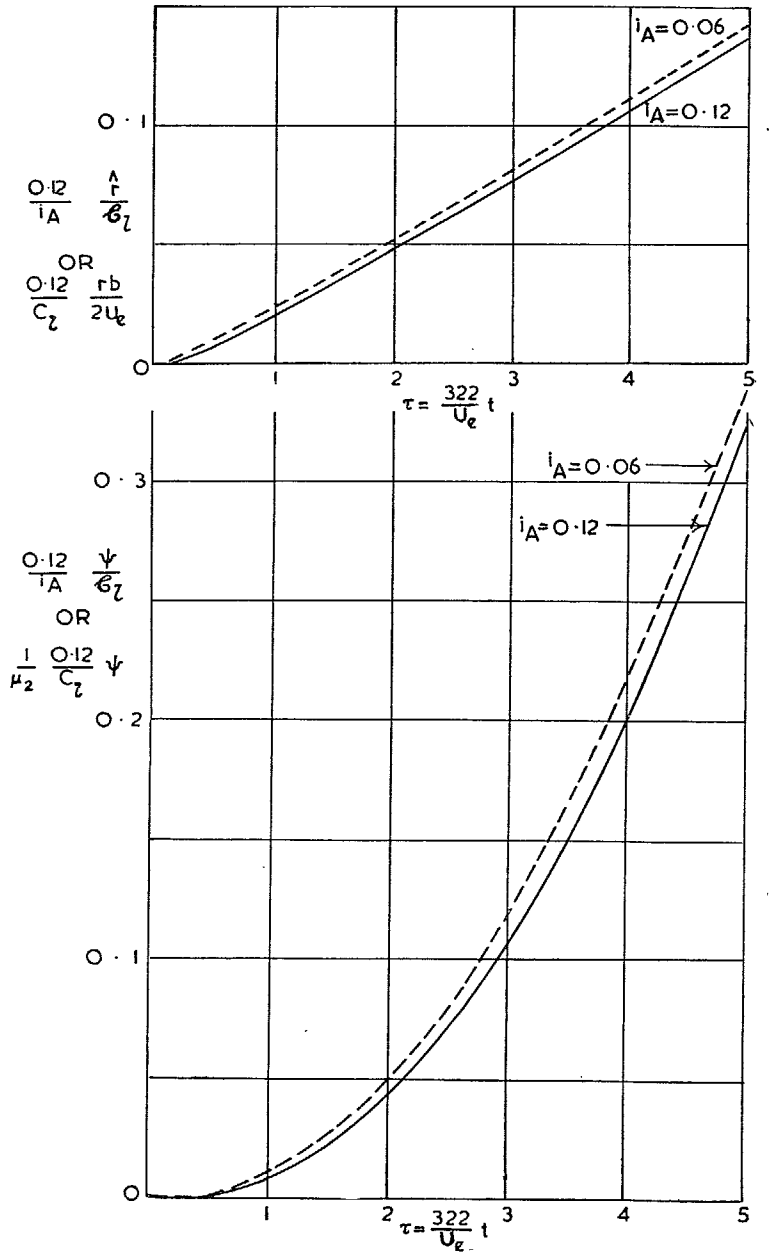

FIG. 36. Aileron response, no sideslip. Rate of yaw, angle of yaw, for varying i_A.

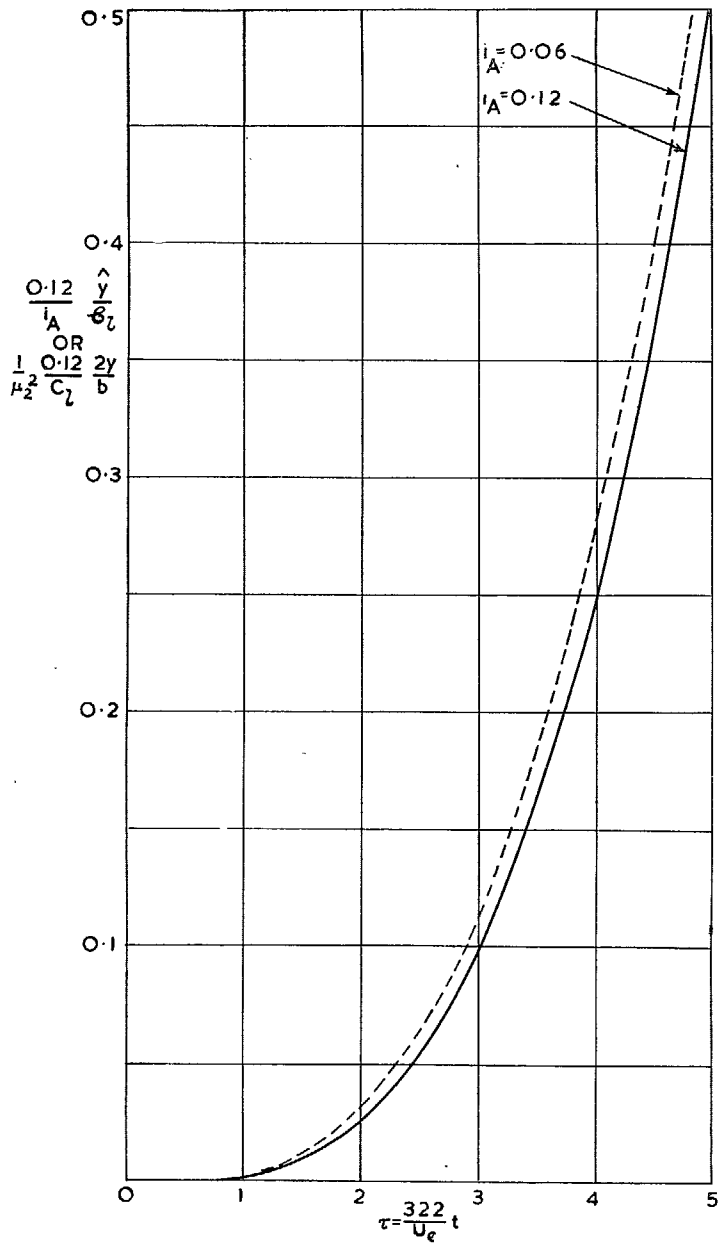

FIG. 37. Aileron response, no sideslip. Sideways displacement for varying i_A.

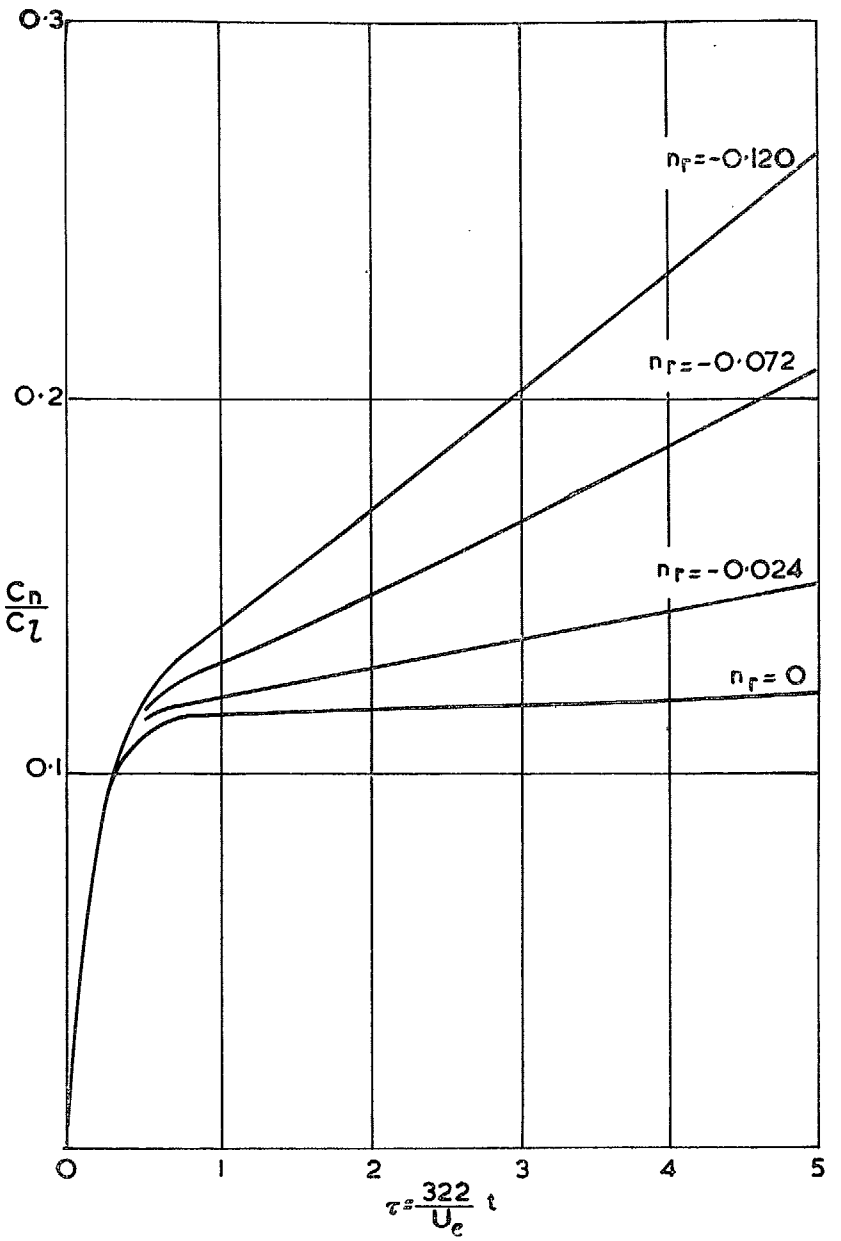

FIG. 38. Aileron response, no sideslip. C_n/C_l for $i_A = 0{\cdot}12$, $i_v = 0{\cdot}18$ and varying n_r.

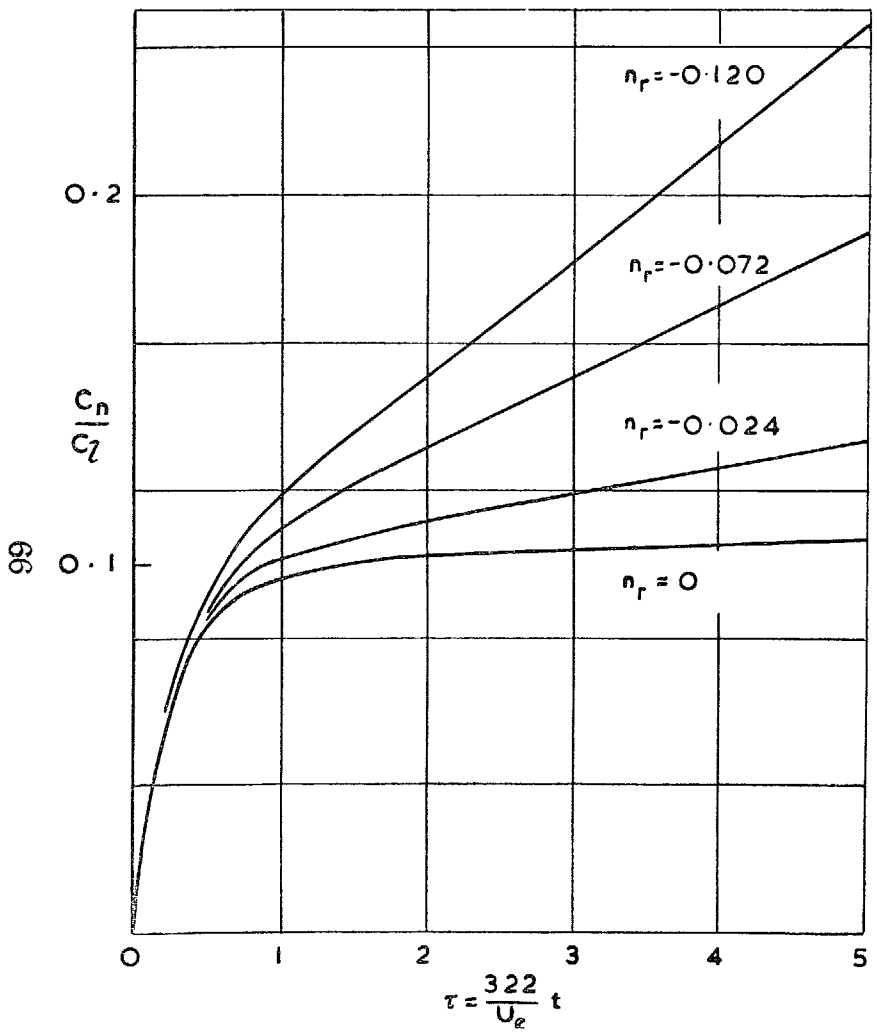

FIG. 39. Aileron response, no sideslip. C_n/C_l for $i_A = 0{\cdot}12$, $i_G = 0{\cdot}12$ for varying n_r.

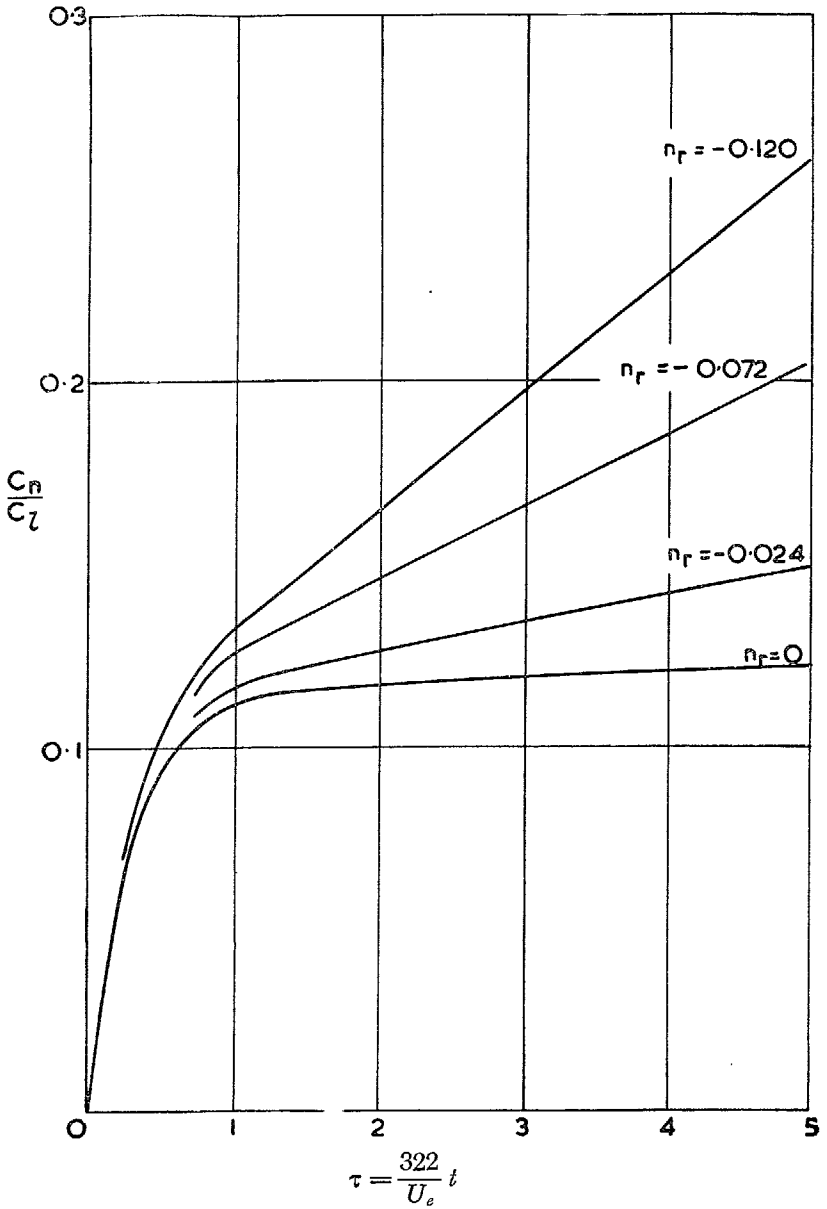

FIG. 40. Aileron response, no sideslip. C_n/C_l for $i_A = 0{\cdot}06$. $i_G = 0{\cdot}18$ and varying n_r.

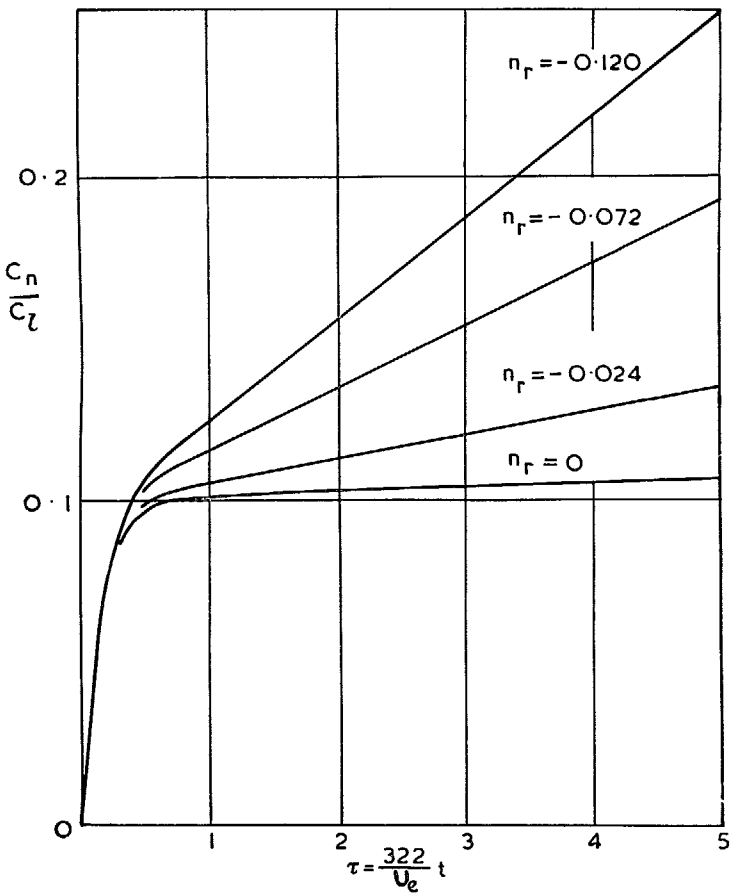

FIG. 41. Aileron response, no sideslip. C_n/C_l for $i_A = 0{\cdot}06$. $i_\sigma = 0{\cdot}12$ and varying n_r.

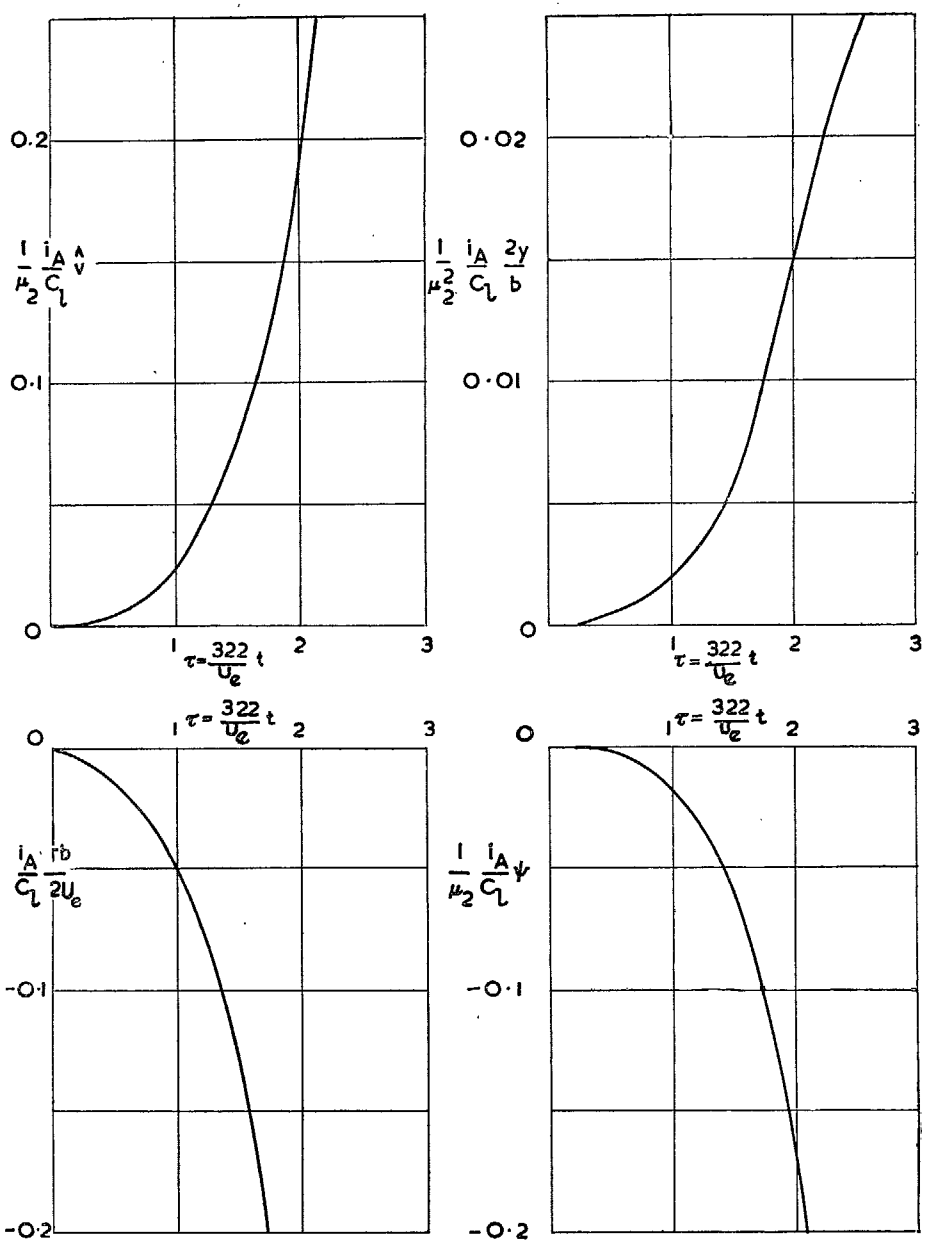

FIG. 42. Response to applied rolling moment. Angles of sideslip and yaw, rate of yaw and sideways displacement for $\mu_2 = 20$, $i_A = 0{\cdot}12$, $i_\sigma = 0{\cdot}18$ and $l_v = 0$, $n_v = 0{\cdot}024$.

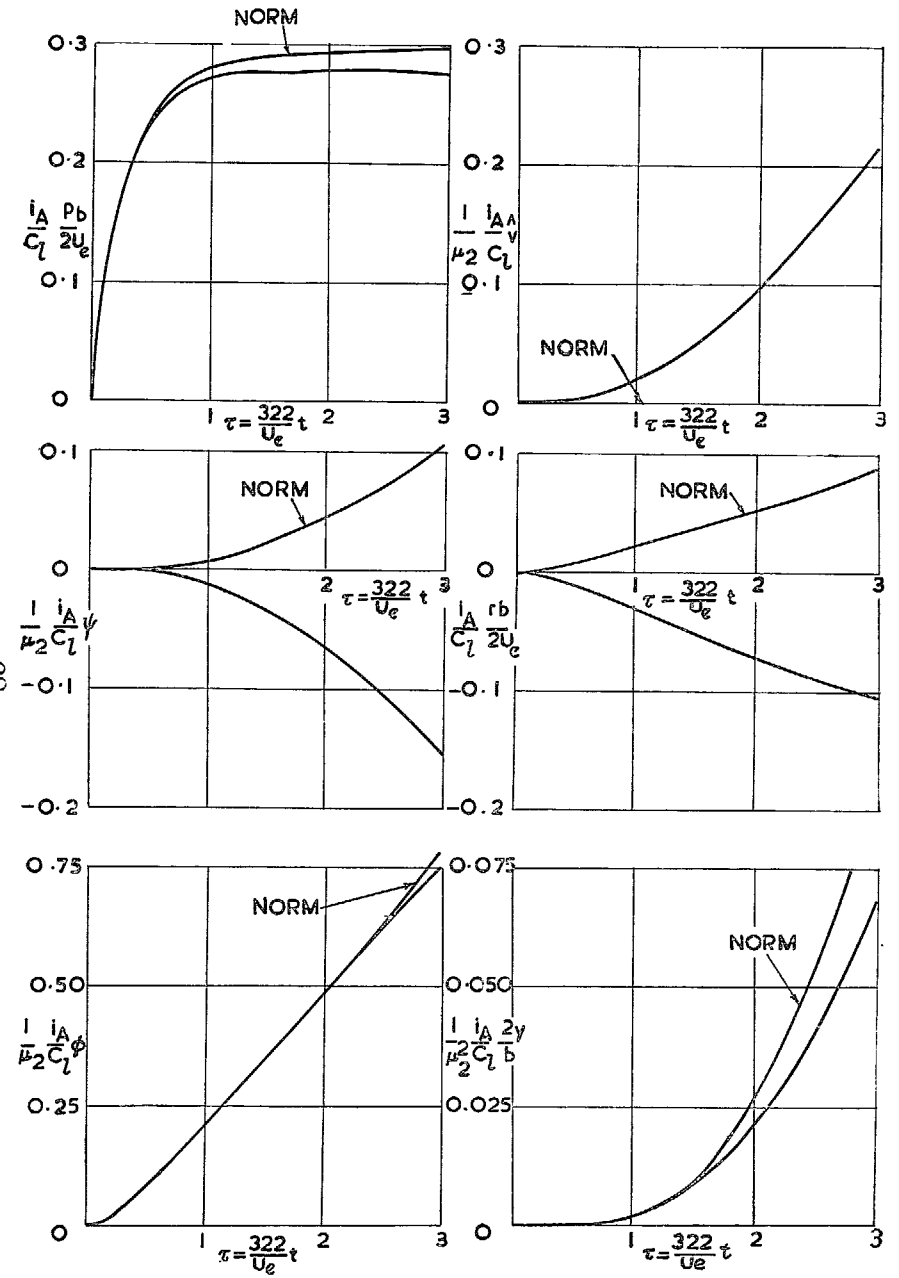

FIG. 43. Response to applied rolling moment in all components for $\mu_2 = 20$, $i_A = 0{\cdot}12$, $i_o = 0{\cdot}18$ and $l_v = 0$, $n_v = 0$.

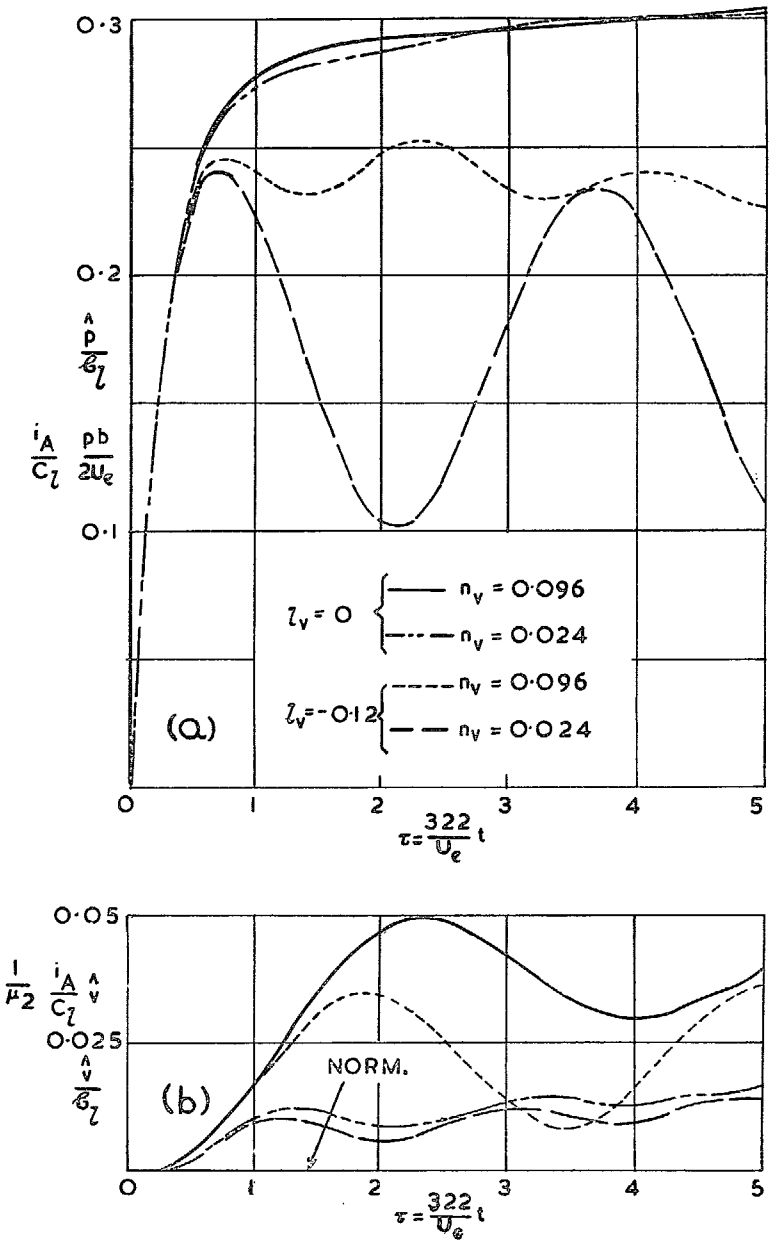

FIG. 44. Response to applied rolling moment. Rate of roll and angle of sideslip for $\mu_2 = 20$, $i_A = 0{\cdot}12$, $i_o = 0{\cdot}18$ and varying l_v, n_v. Norm coincides with $l_v = 0$, $n_v = 0{\cdot}096$ in Fig. 44 (a).

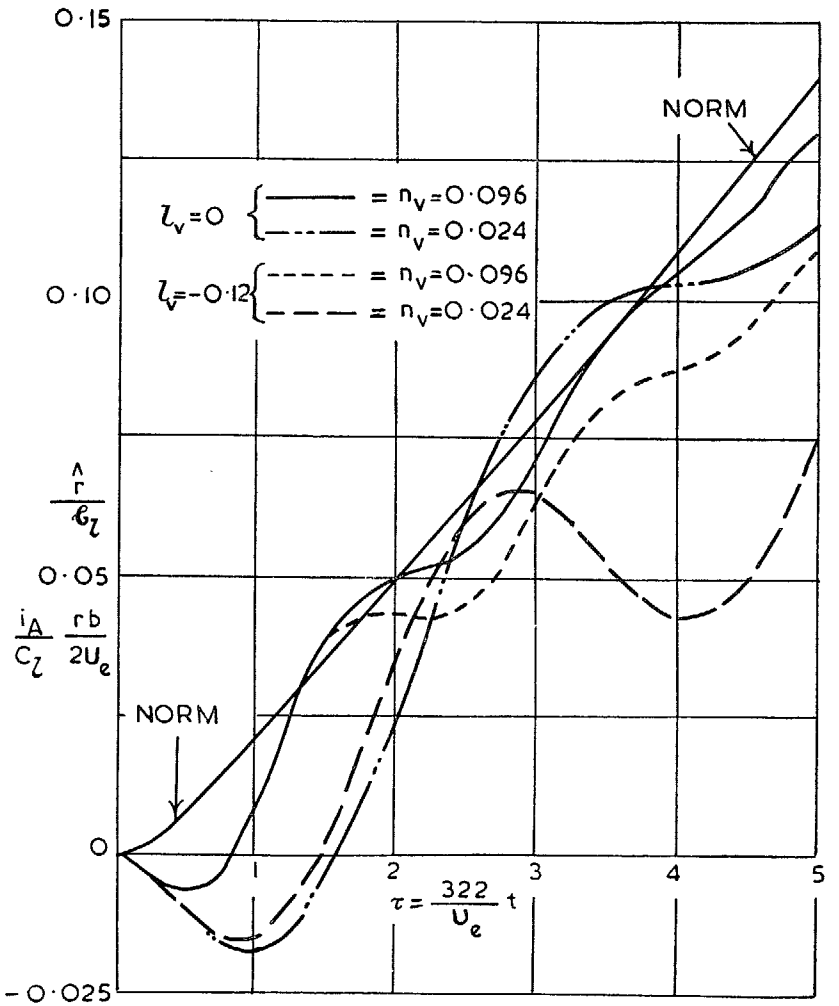

FIG. 45. Response to applied rolling moment. Rate of yaw for $\mu_2 = 20$, $i_A = 0{\cdot}12$, $i_C = 0{\cdot}18$ and varying l_v, n_v.

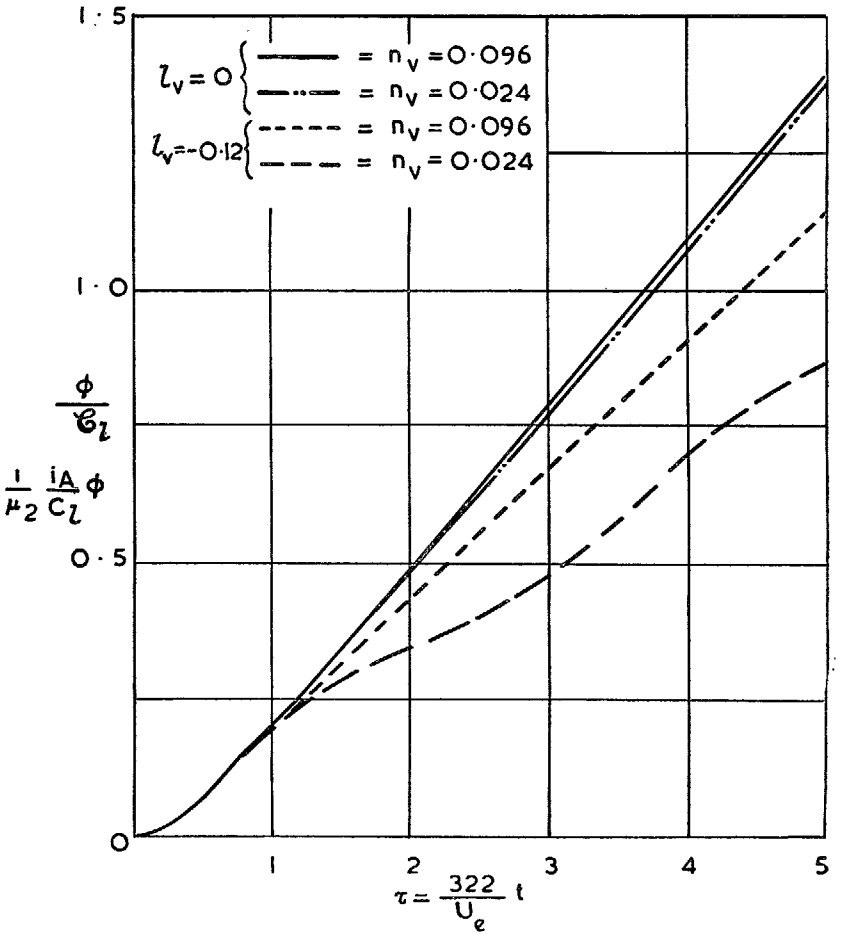

FIG. 46. Response to applied rolling moment. Angle of bank for $\mu_2 = 20$, $i_A = 0{\cdot}12$, $i_C = 0{\cdot}18$ and varying l_v, n_v. Norm coincides with $l_v = 0$, $n_v = 0{\cdot}096$.

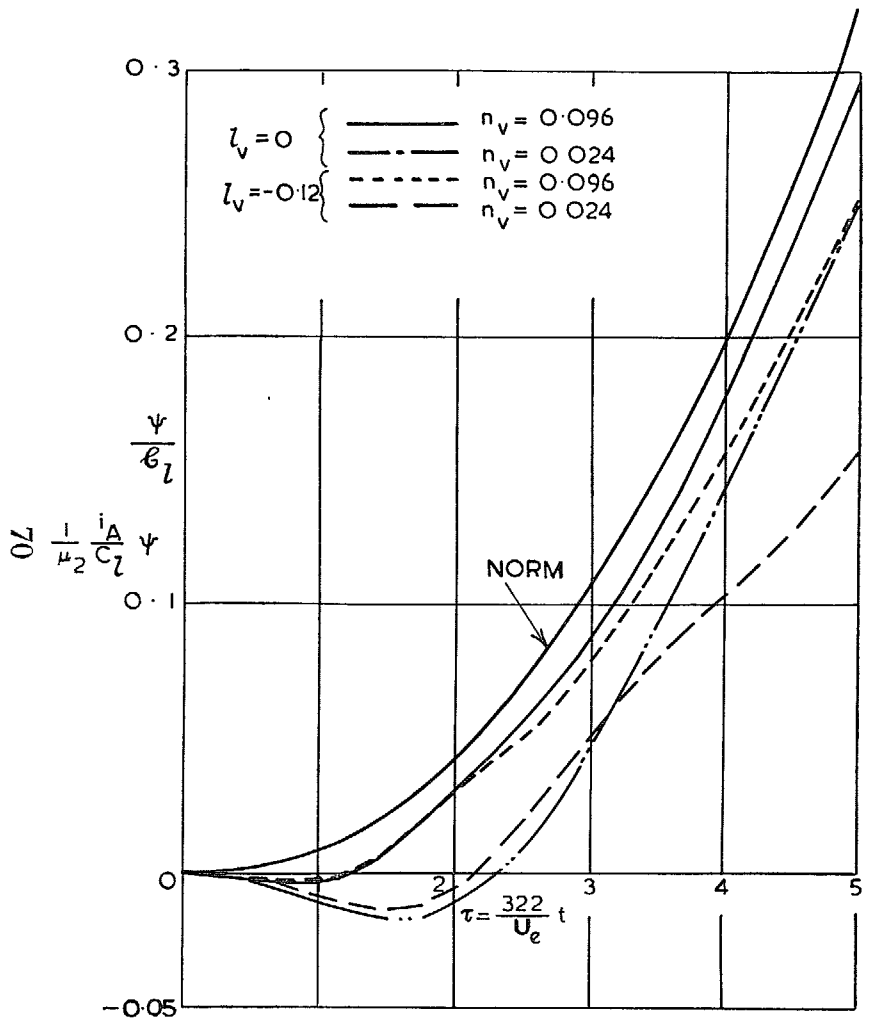

FIG. 47. Response to applied rolling moment. Angle of yaw for $\mu_2 = 20$, $i_A = 0·12$, $i_C = 0·18$ and varying l_v, n_v.

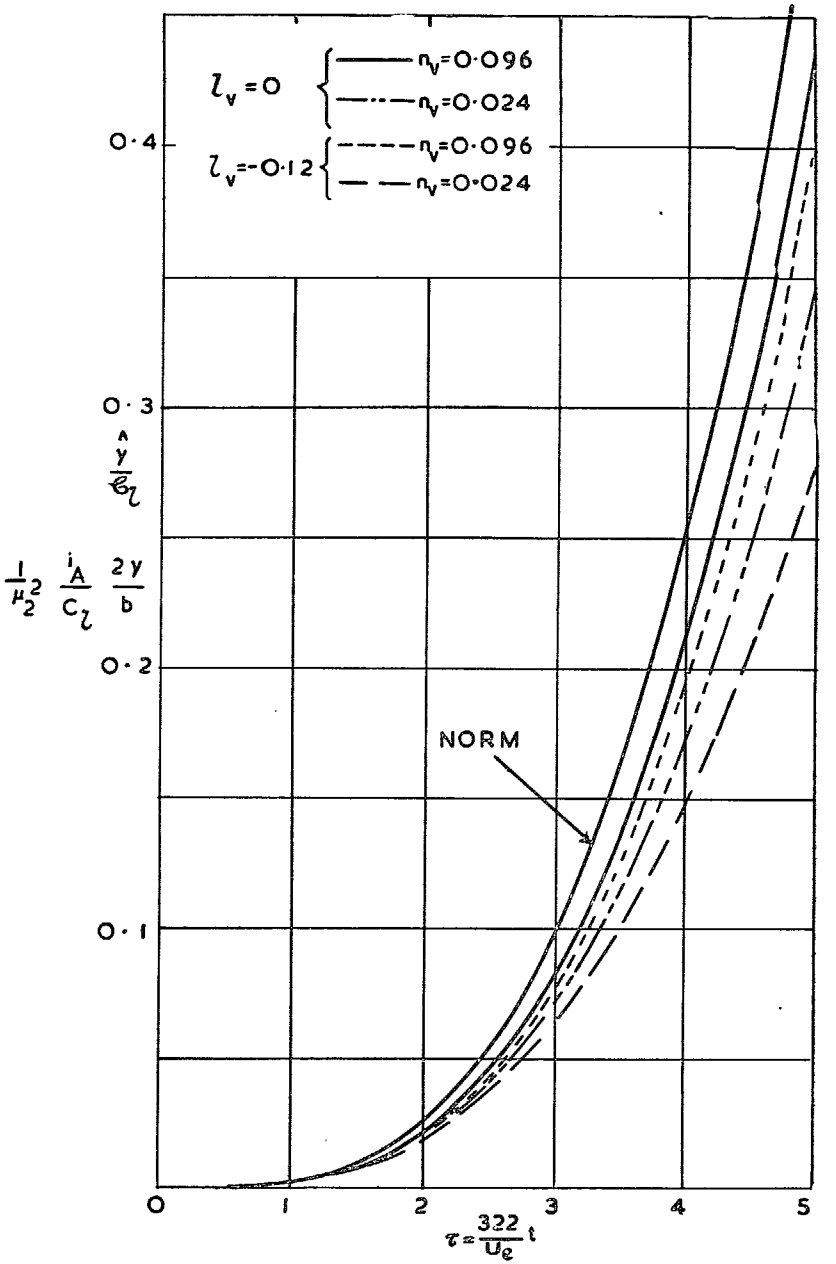

FIG. 48. Response to applied rolling moment. Sideways displacement for $\mu_2 = 20$, $i_A = 0·12$, $i_C = 0·18$ and varying l_v, n_v.

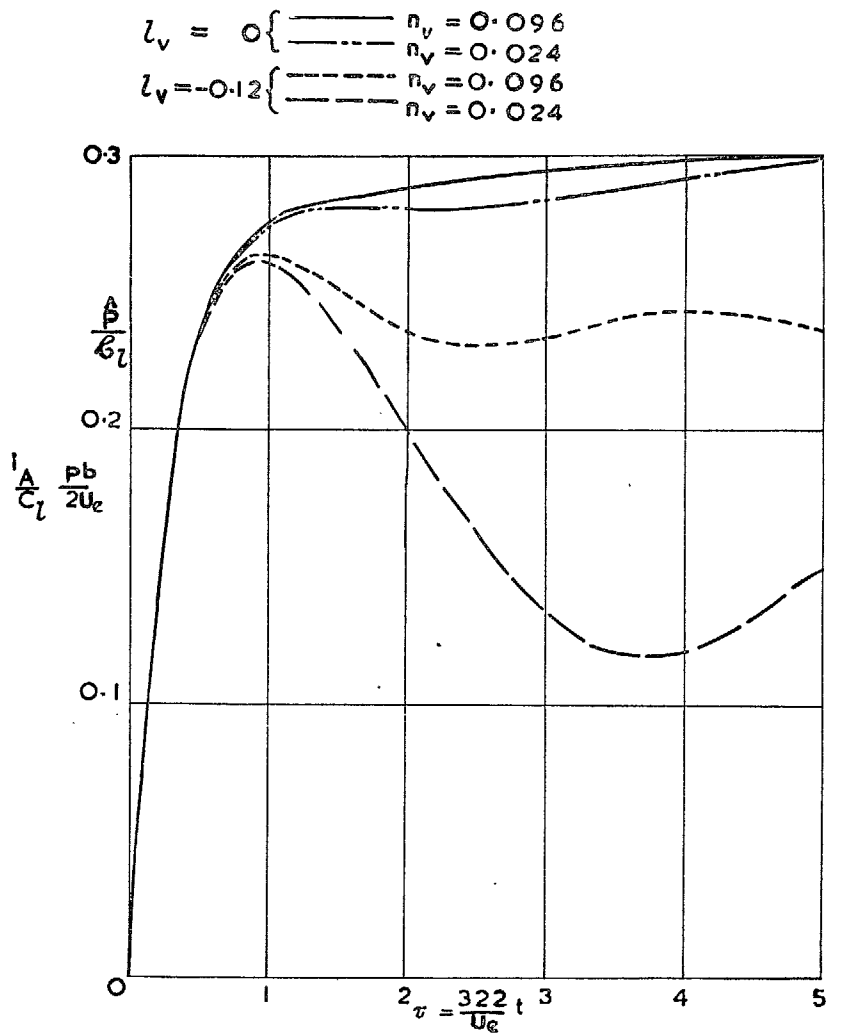

FIG. 49. Response to applied rolling moment. Rate of roll for $\mu_2 = 5$, $i_A = 0{\cdot}12$, $i_0 = 0{\cdot}18$ and varying l_v, n_v. Norm coincides with $l_v = 0$, $n_v = 0{\cdot}096$.

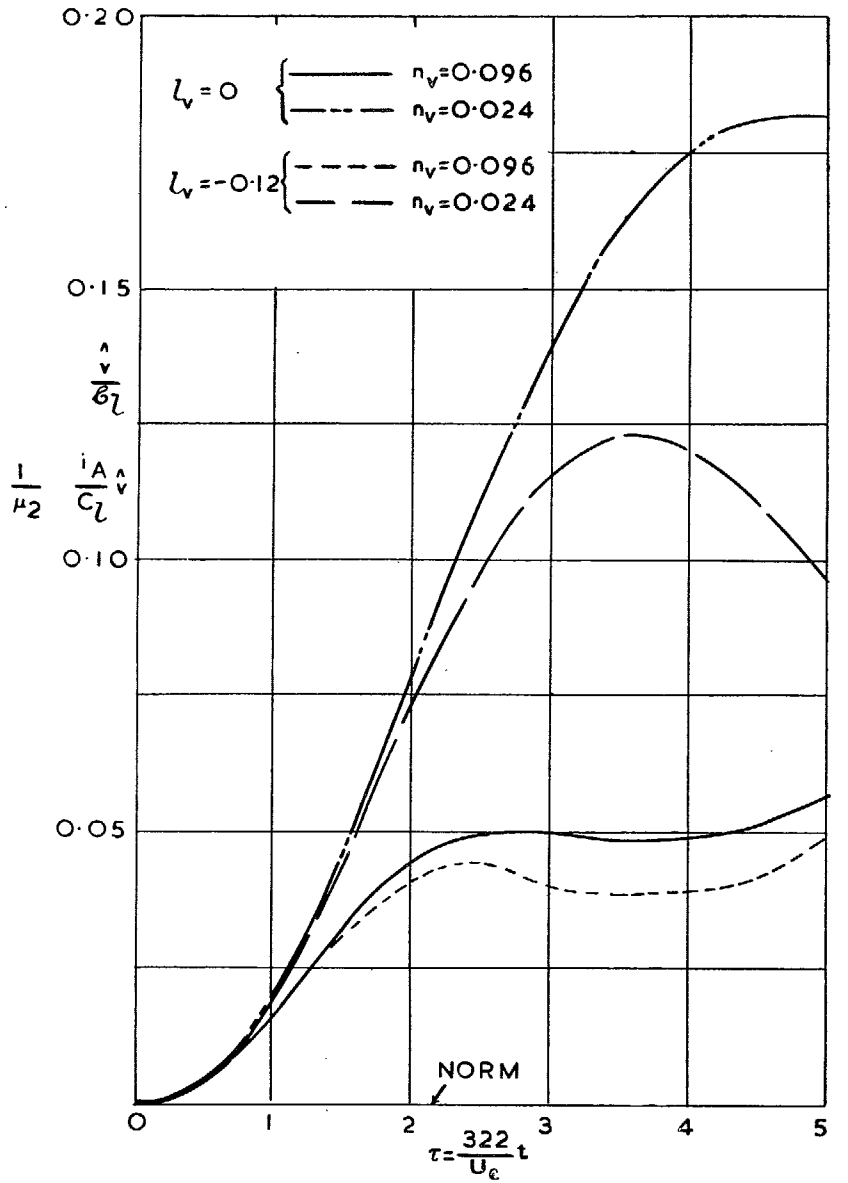

FIG. 50. Response to applied rolling moment. Angle of sideslip for $\mu_2 = 5$, $i_A = 0{\cdot}12$, $i_0 = 0{\cdot}18$ and varying l_v, n_v.

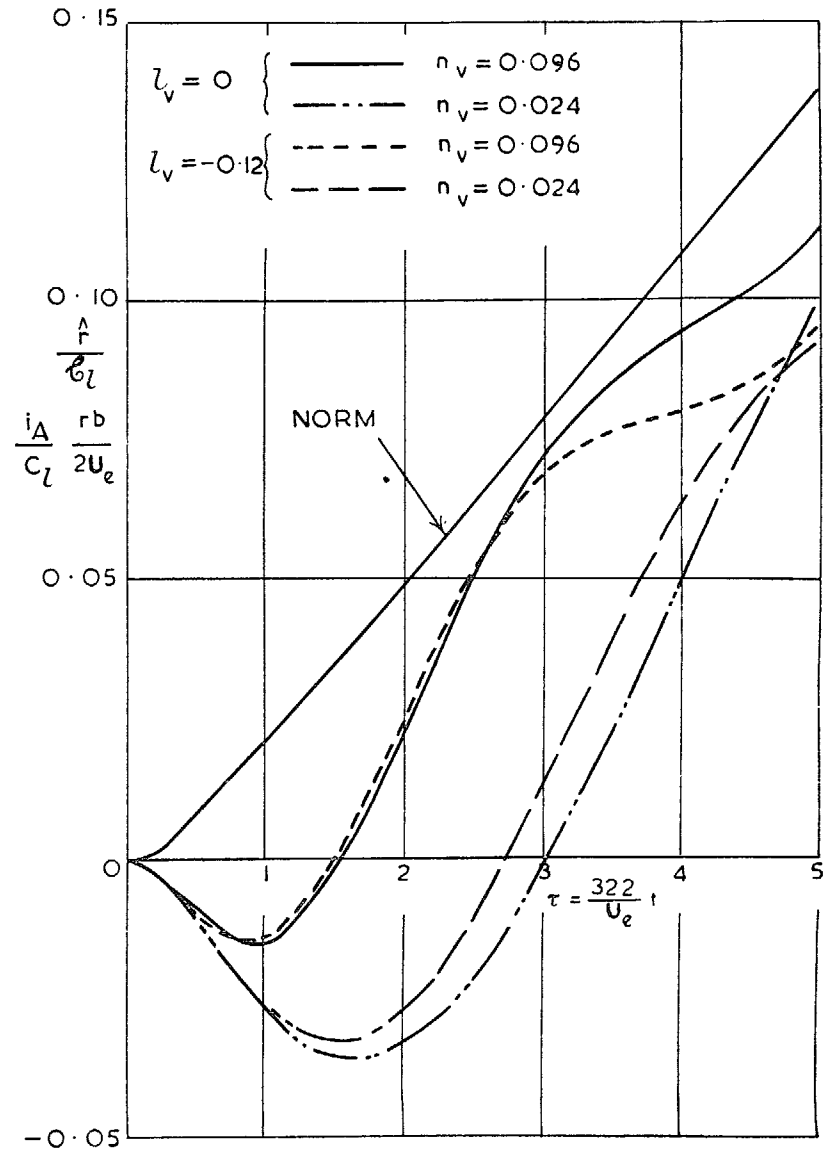

FIG. 51. Response to applied rolling moment. Rate of yaw for $\mu_2 = 5$, $i_A = 0·12$, $i_0 = 0·18$ and varying l_v, n_v.

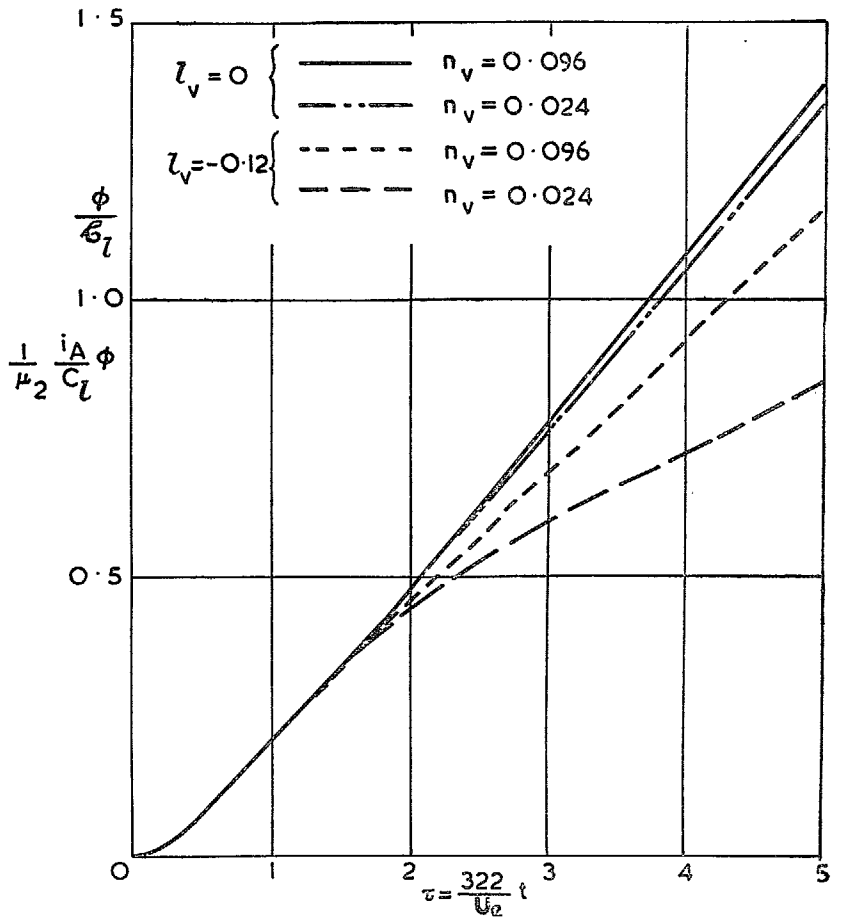

FIG. 52. Response to applied rolling moment. Angle of bank for $\mu_2 = 5$, $i_A = 0·12$, $i_0 = 0·18$ and varying l_v, n_v. Norm coincides with $l_v = 0$, $n_v = 0·096$.

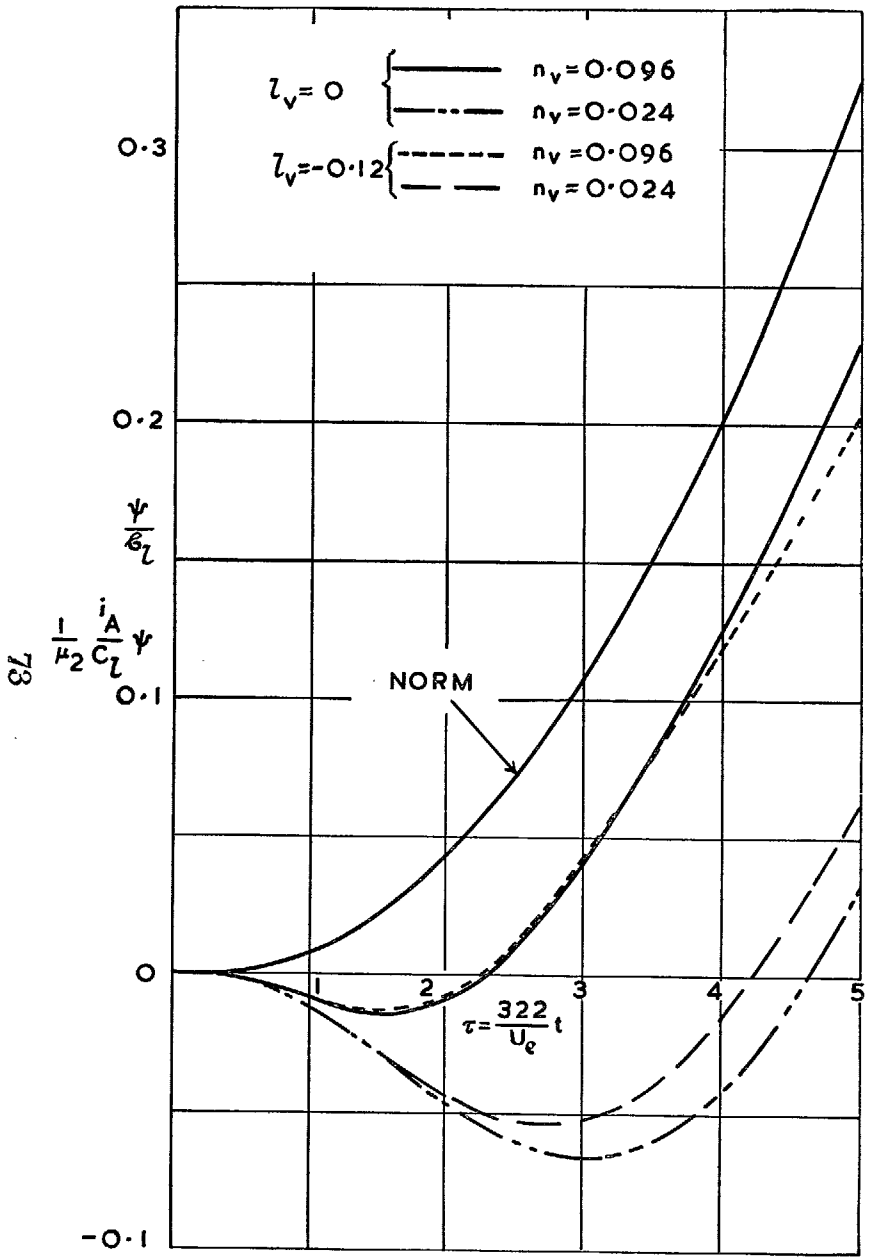

FIG. 53. Response to applied rolling moment. Angle of yaw for $\mu_2 = 5$, $i_A = 0{\cdot}12$, $i_0 = 0{\cdot}18$ and varying l_v, n_v.

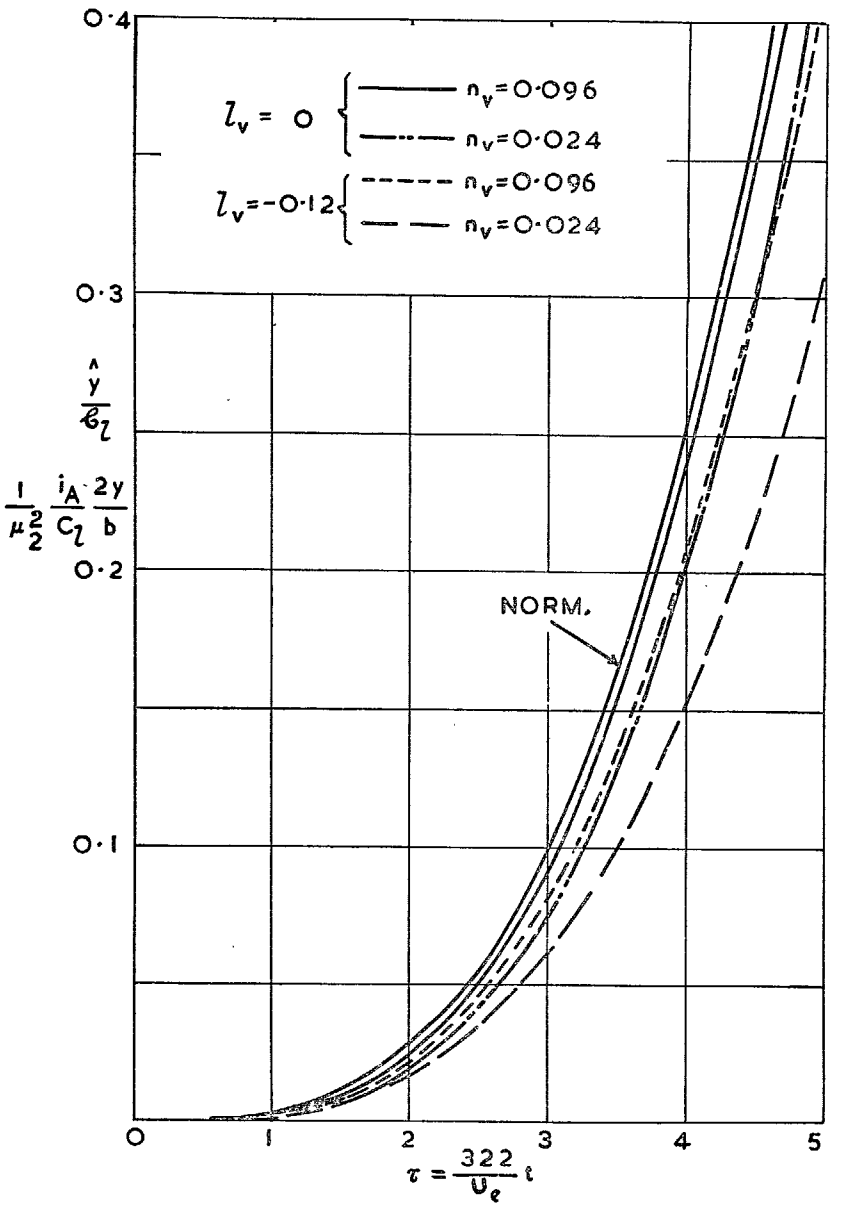

FIG. 54. Response to applied rolling moment. Sideways displacement for $\mu_2 = 5$, $i_A = 0{\cdot}12$, $i_0 = 0{\cdot}18$, and varying l_v, n_v.

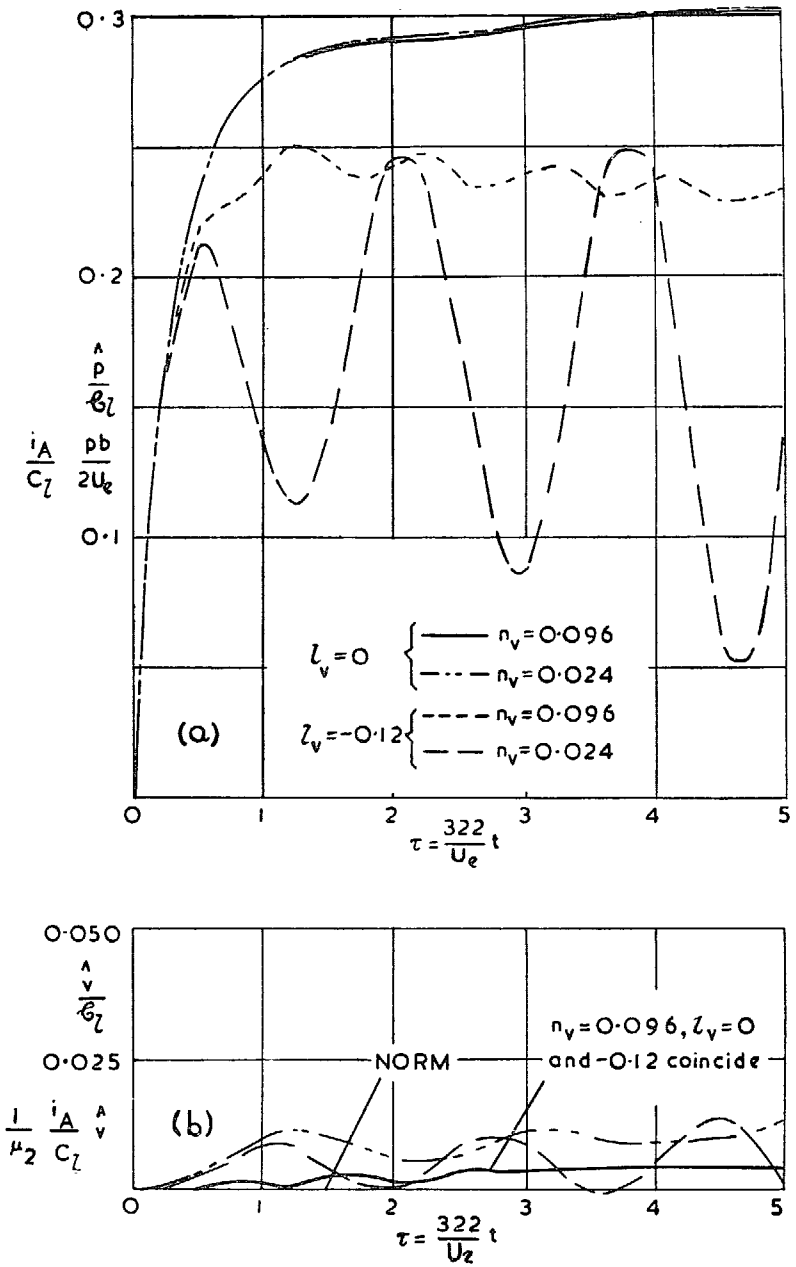

FIG. 55. Response to applied rolling moment. Rate of roll and angle of sideslip for $\mu_2 = 80$, $i_A = 0{\cdot}12$, $i_C = 0{\cdot}18$ and varying l_v, n_v. Norm coincides with $l_v = 0$, $n_v = 0{\cdot}096$ in Fig. 55 (a).

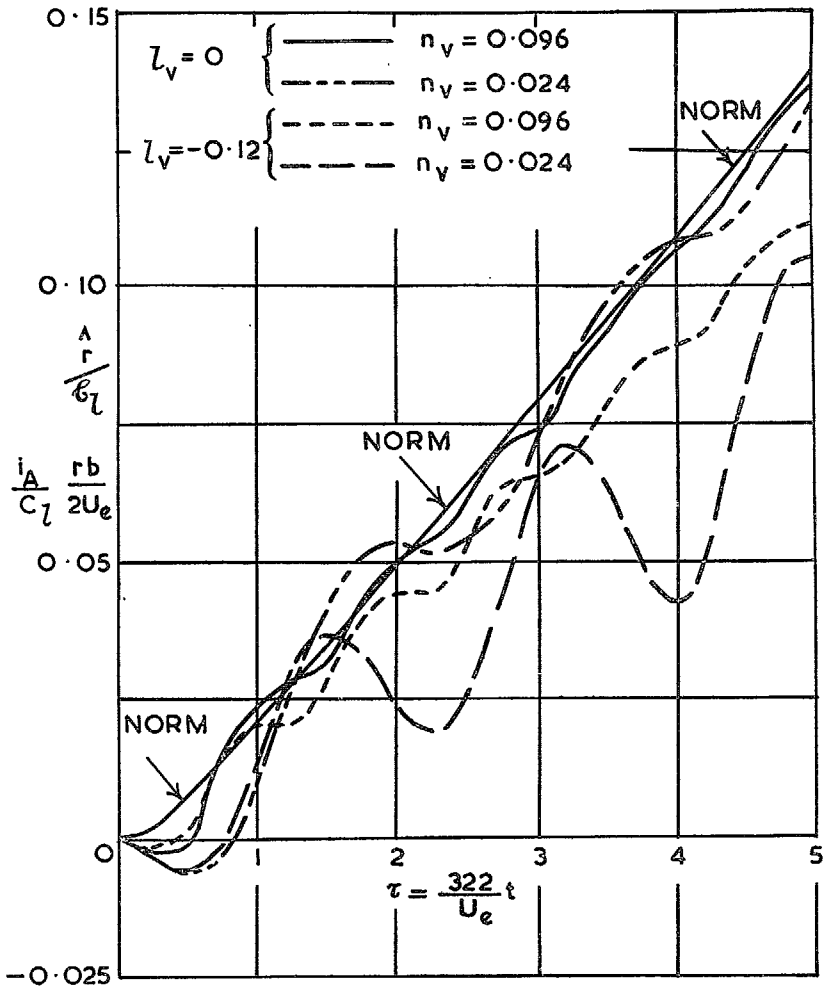

FIG. 56. Response to applied rolling moment. Rate of yaw for $\mu_2 = 80$, $i_A = 0{\cdot}12$, $i_C = 0{\cdot}18$ and varying l_v, n_v.

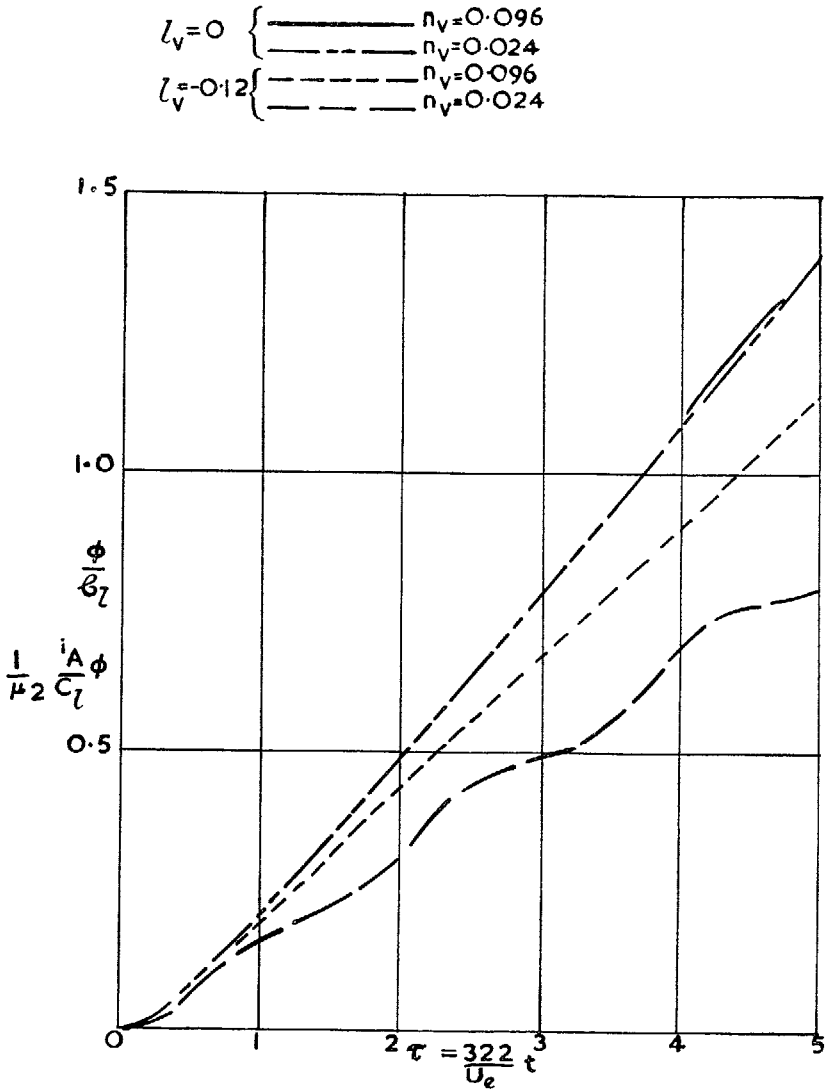

FIG. 57. Response to applied rolling moment. Angle of bank for $\mu_2 = 80$, $i_A = 0\cdot12$, $i_0 = 0\cdot18$, and varying l_v, n_v. Norm coincides with $l_v = 0$, $n_v = 0\cdot096$.

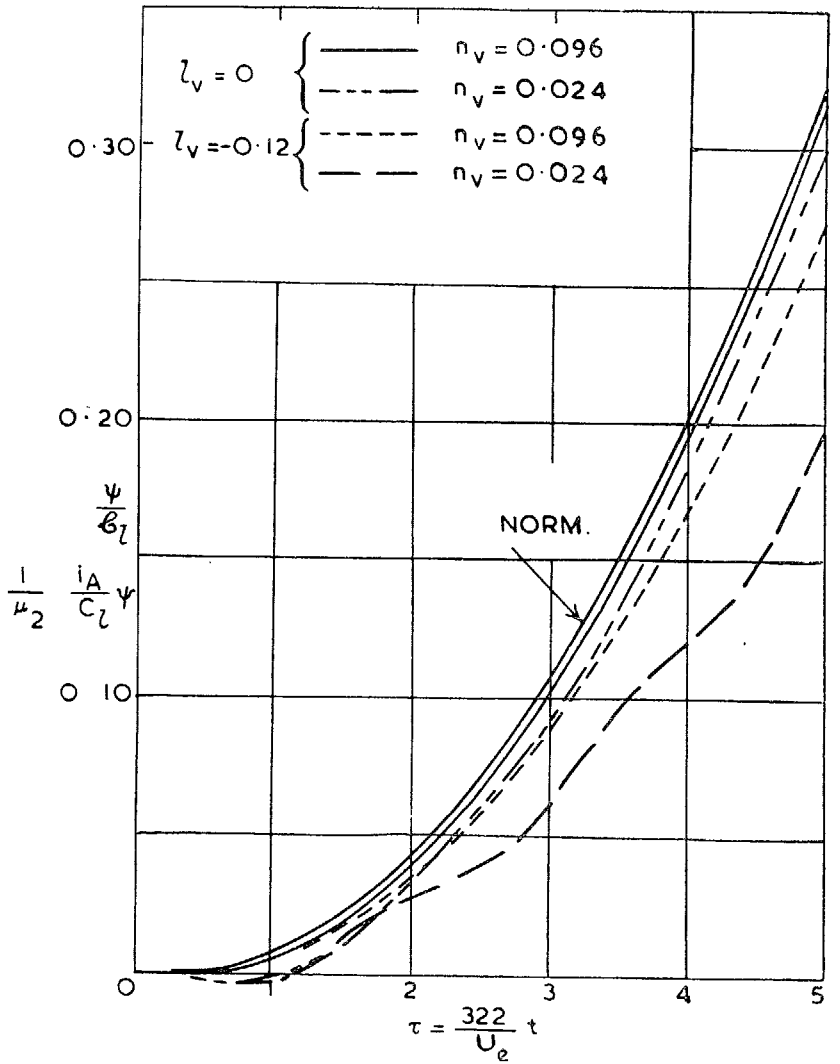

FIG. 58. Response to applied rolling moment. Angle of yaw for $\mu_2 = 80$, $i_A = 0\cdot12$, $i_0 = 0\cdot18$ and varying l_v, n_v.

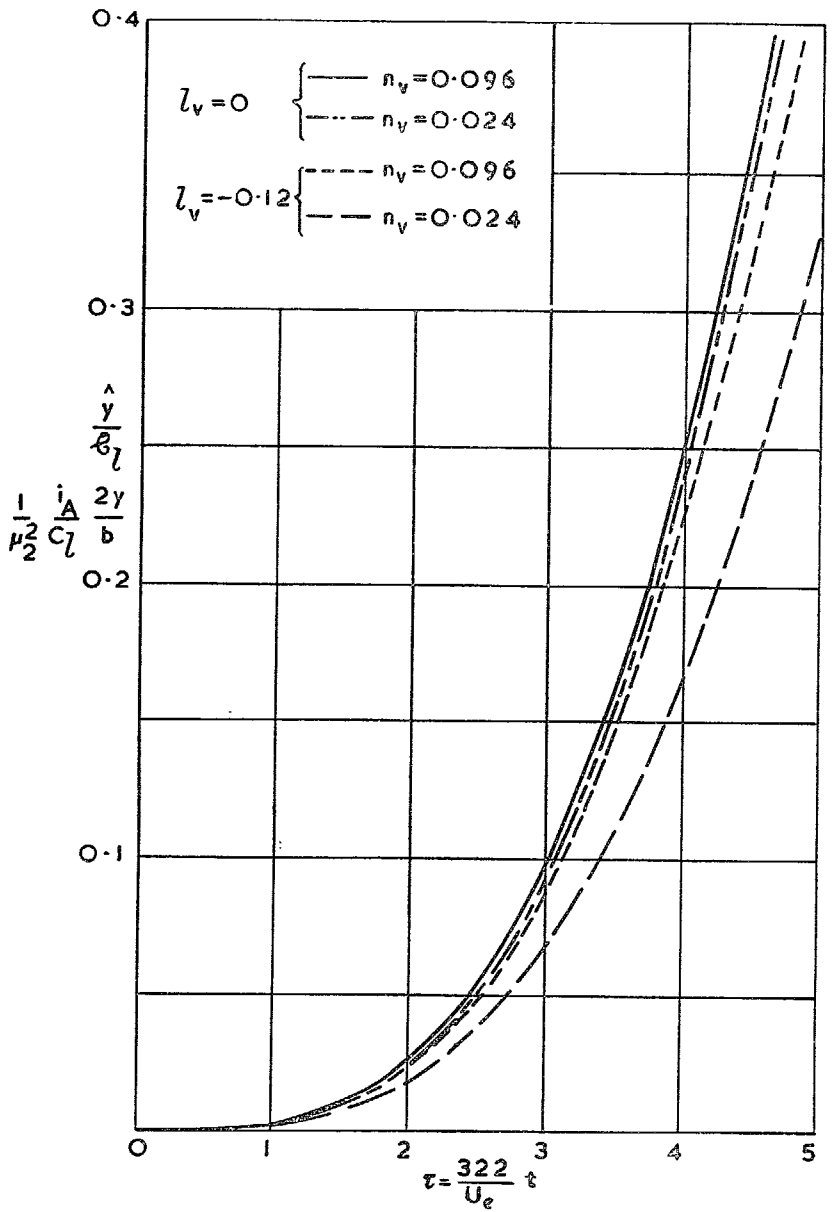

FIG. 59. Response to applied rolling moment. Sideways displacement for $\mu_2 = 80$, $i_A = 0{\cdot}12$, $i_C = 0{\cdot}18$, and varying l_v, n_v. Norm coincides with $l_v = 0$, $n_v = 0{\cdot}096$.

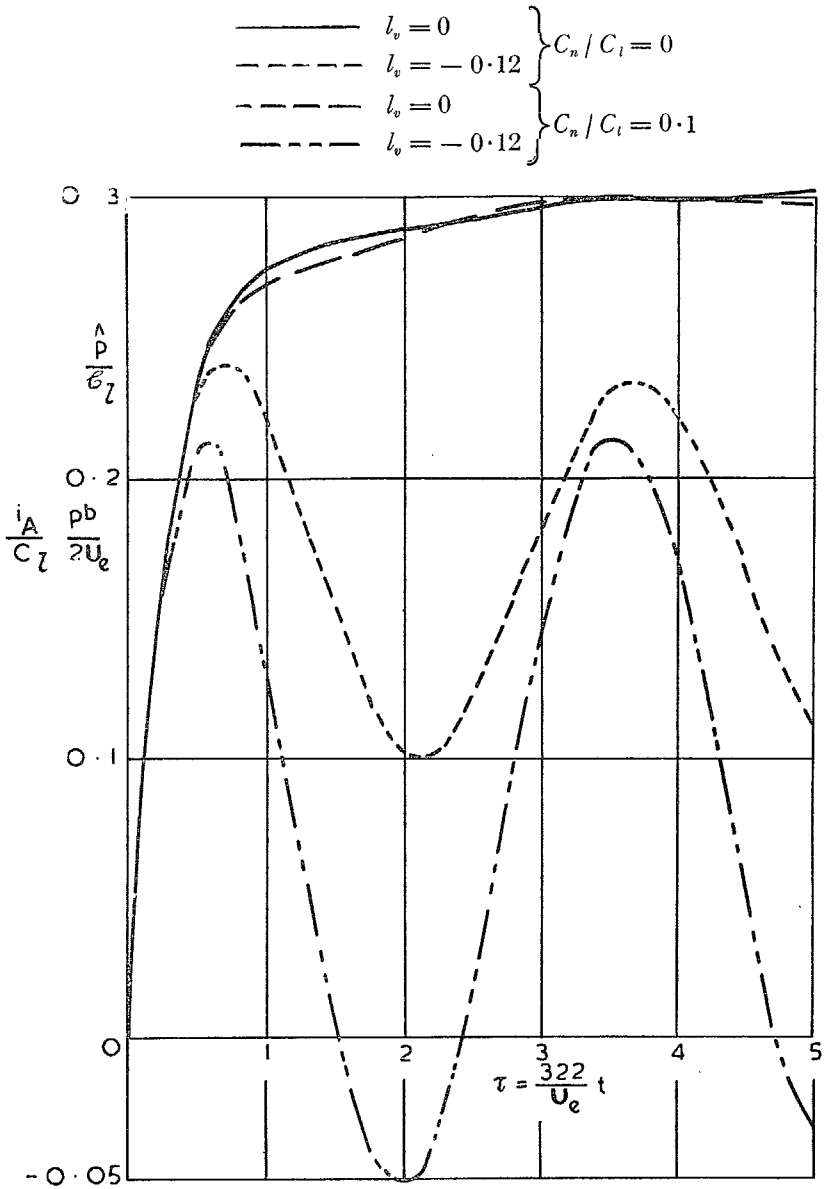

FIG. 60. Response to applied rolling moment with adverse yawing moment. Rate of roll for $\mu_2 = 20$, $n_v = 0{\cdot}024$, $i_A = 0{\cdot}12$, $i_C = 0{\cdot}18$ and varying l_v and C_n/C_l.

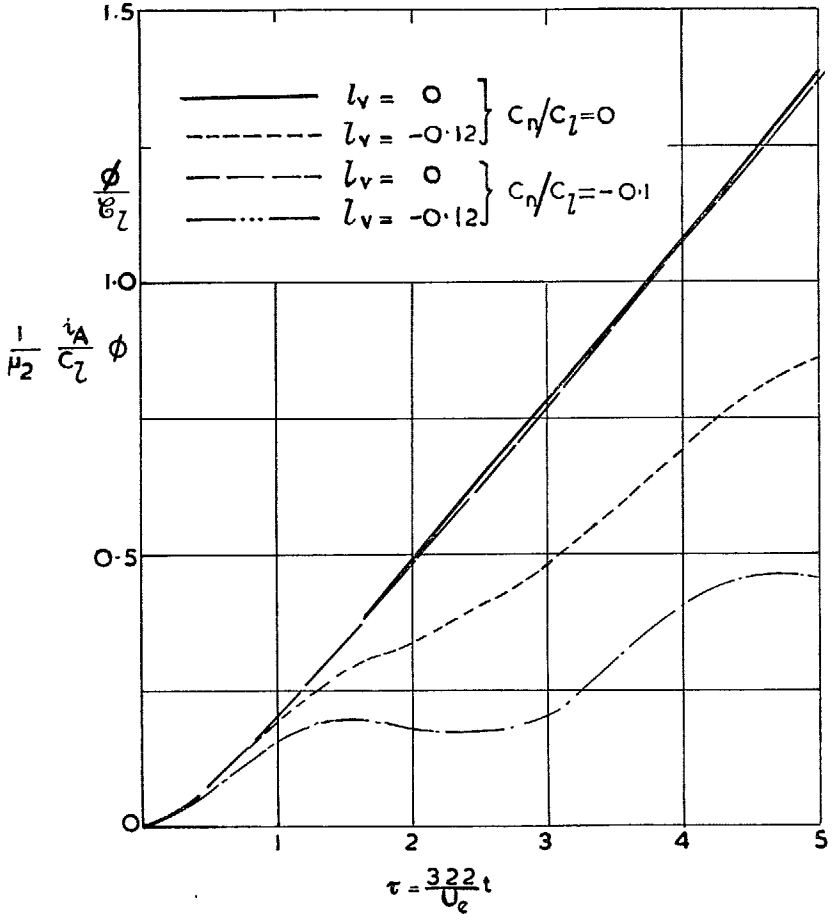

FIG. 61. Response to applied rolling moment with adverse yawing moment. Angle of bank for $\mu_2 = 20$, $n_v = 0·024$, $i_A = 0·12$, $i_0 = 0·18$ and varying l_v and C_n/C_l.

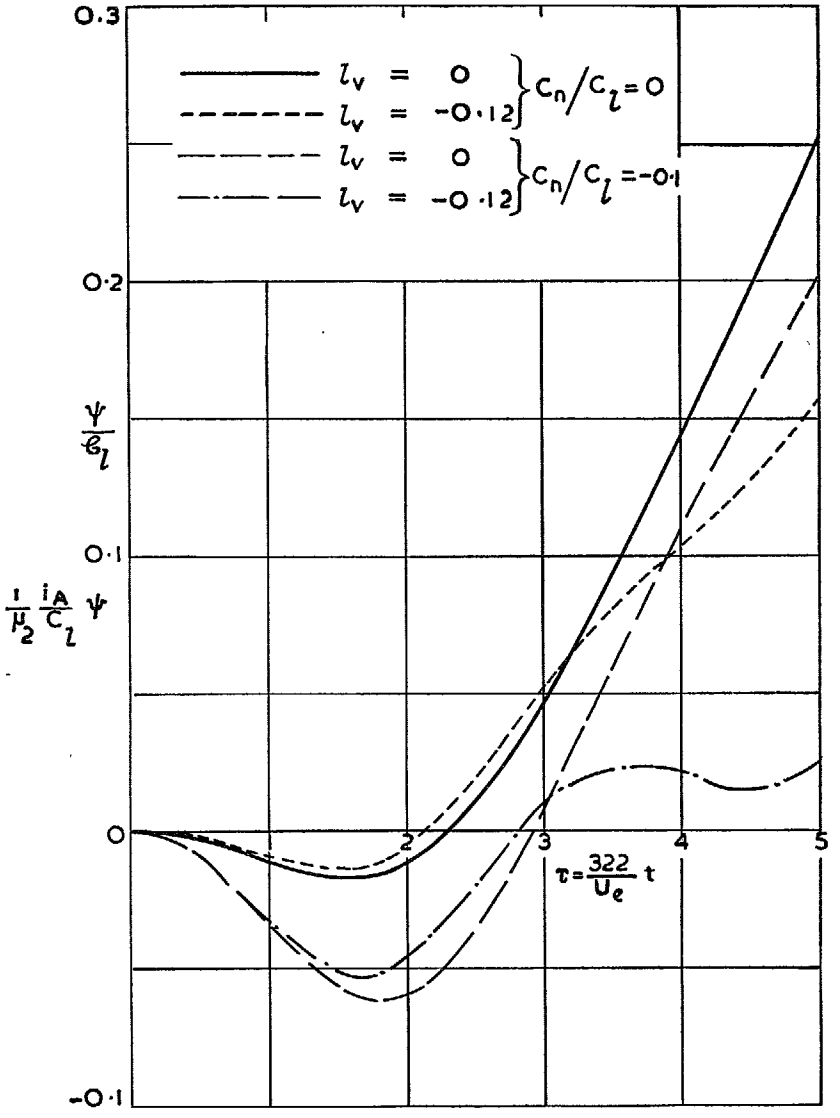

FIG. 62. Response to applied rolling moment with adverse yawing moment. Angle of yaw for $\mu_2 = 20$, $n_v = 0·024$, $i_A = 0·12$, $i_0 = 0·18$ and varying l_v and C_n/C_l.

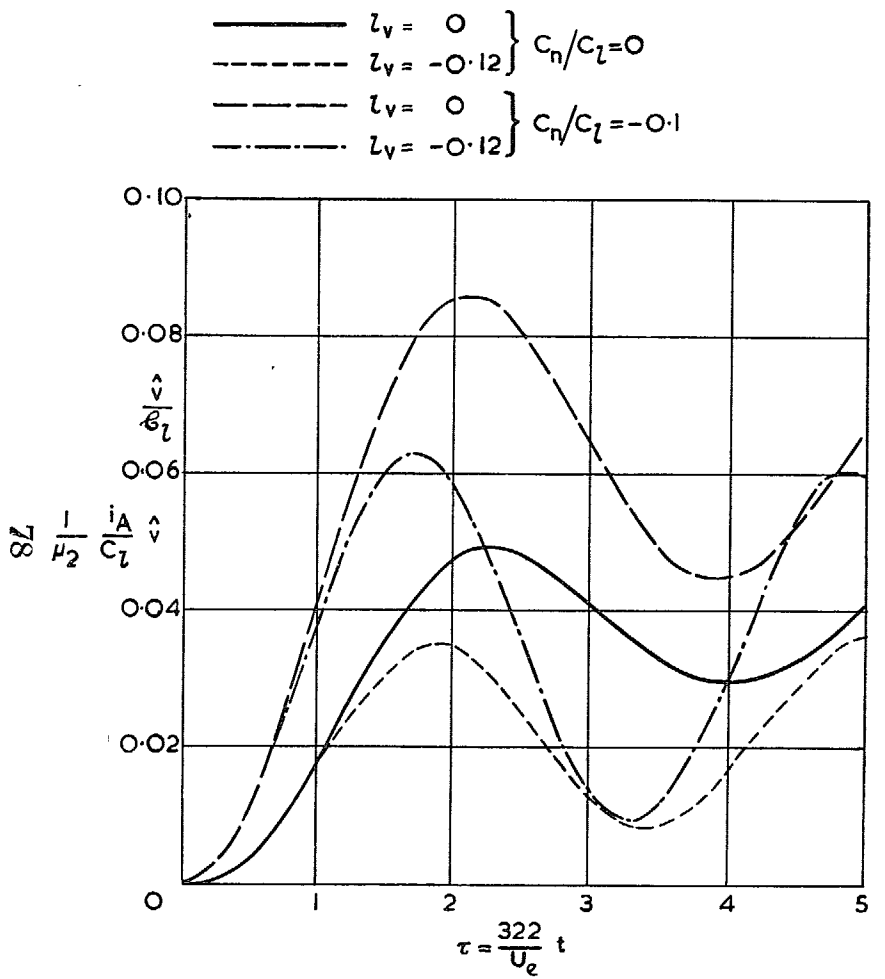

FIG. 63. Response to applied rolling moment with adverse yawing moment. Angle of sideslip for $\mu_2 = 20$, $n_v = 0{\cdot}024$, $i_A = 0{\cdot}12$, $i_\sigma = 0{\cdot}18$ and varying l_v, C_n/C_l.

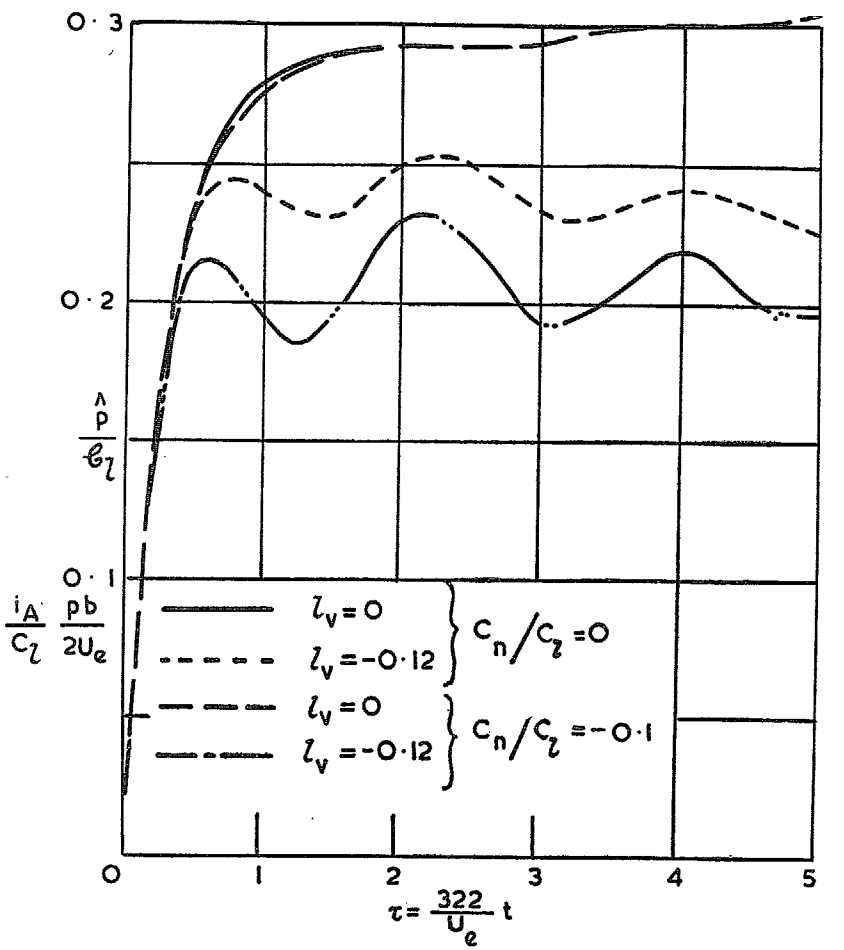

FIG. 64. Response to applied rolling moment with adverse yawing moment. Rate of roll for $i_A = 0{\cdot}12$, $i_\sigma = 0{\cdot}18$, $\mu_2 = 20$, $n_v = 0{\cdot}096$ and varying l_v, C_n/C_l.

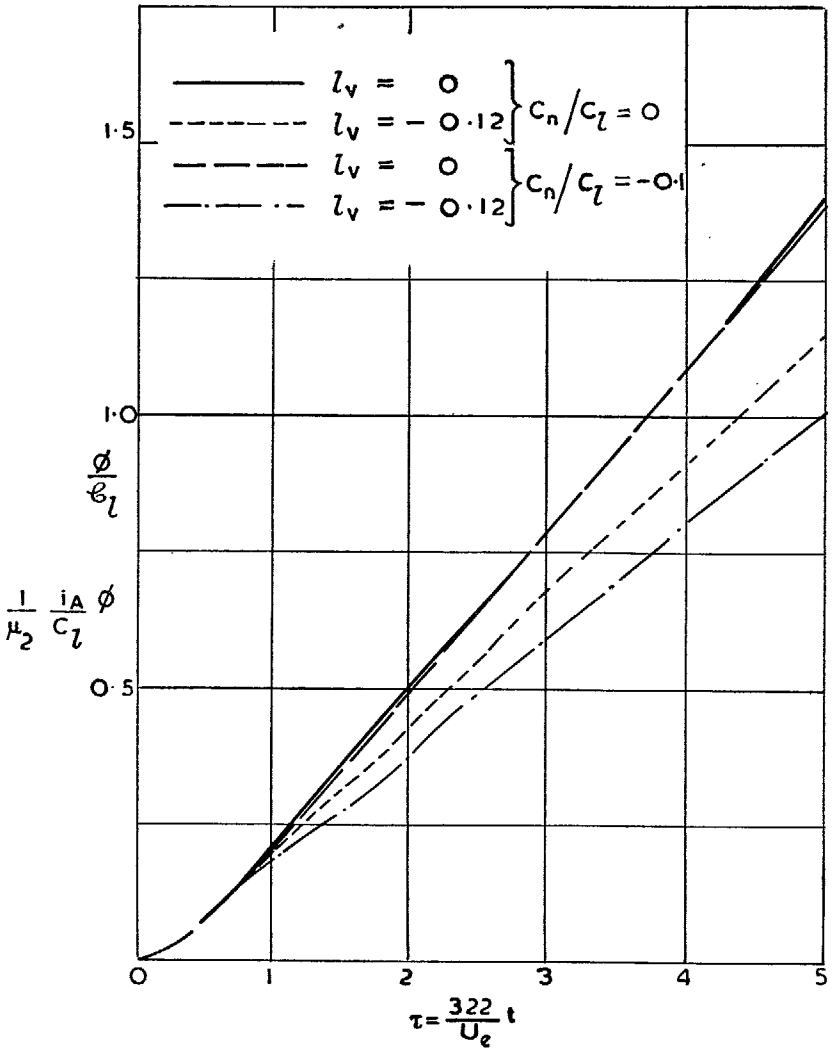

FIG. 65. Response to applied rolling moment with adverse yawing moment. Angle of bank for $\mu_2 = 20$, $n_v = 0{\cdot}096$, $i_A = 0{\cdot}12$, $i_\sigma = 0{\cdot}18$ and varying l_v, C_n/C_l.

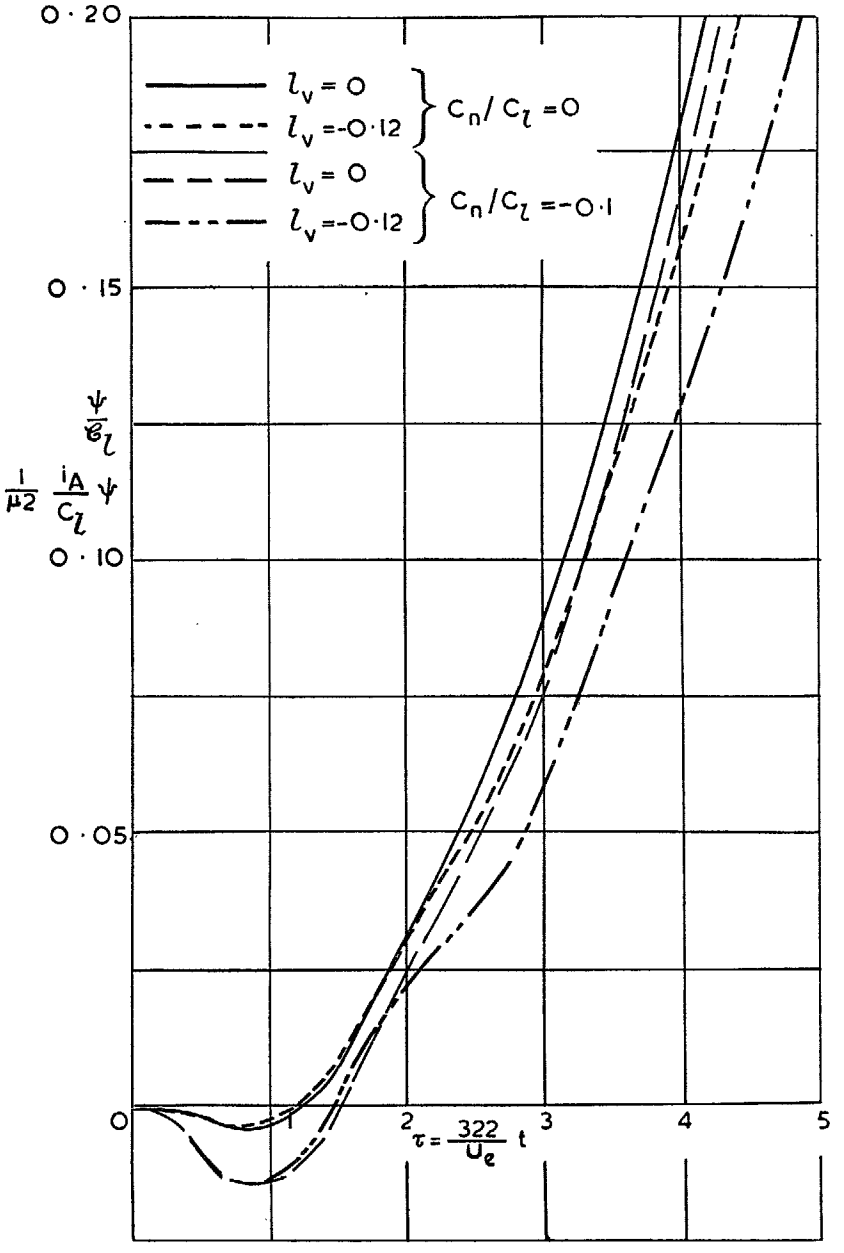

FIG. 66. Response to applied rolling moment with adverse yawing moment. Angle of yaw for $\mu_2 = 20$, $i_A = 0{\cdot}12$, $i_\sigma = 0{\cdot}18$, $n_v = 0{\cdot}096$ and varying l_v, C_n/C_l.

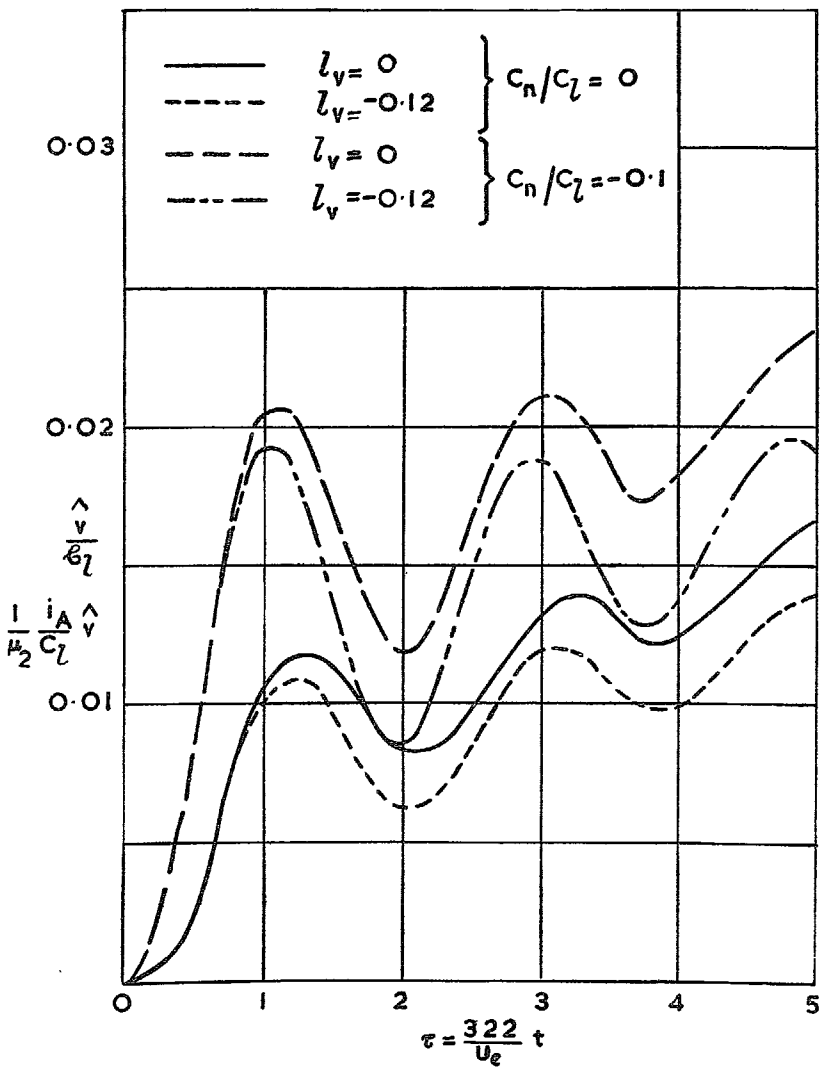

FIG. 67. Response to applied rolling moment with adverse yawing moment. Angle of sideslip for $\mu_2 = 20$, $i_A = 0{\cdot}12$, $i_C = 0{\cdot}18$, $n_v = 0{\cdot}096$ and varying l_v, C_n/C_l.

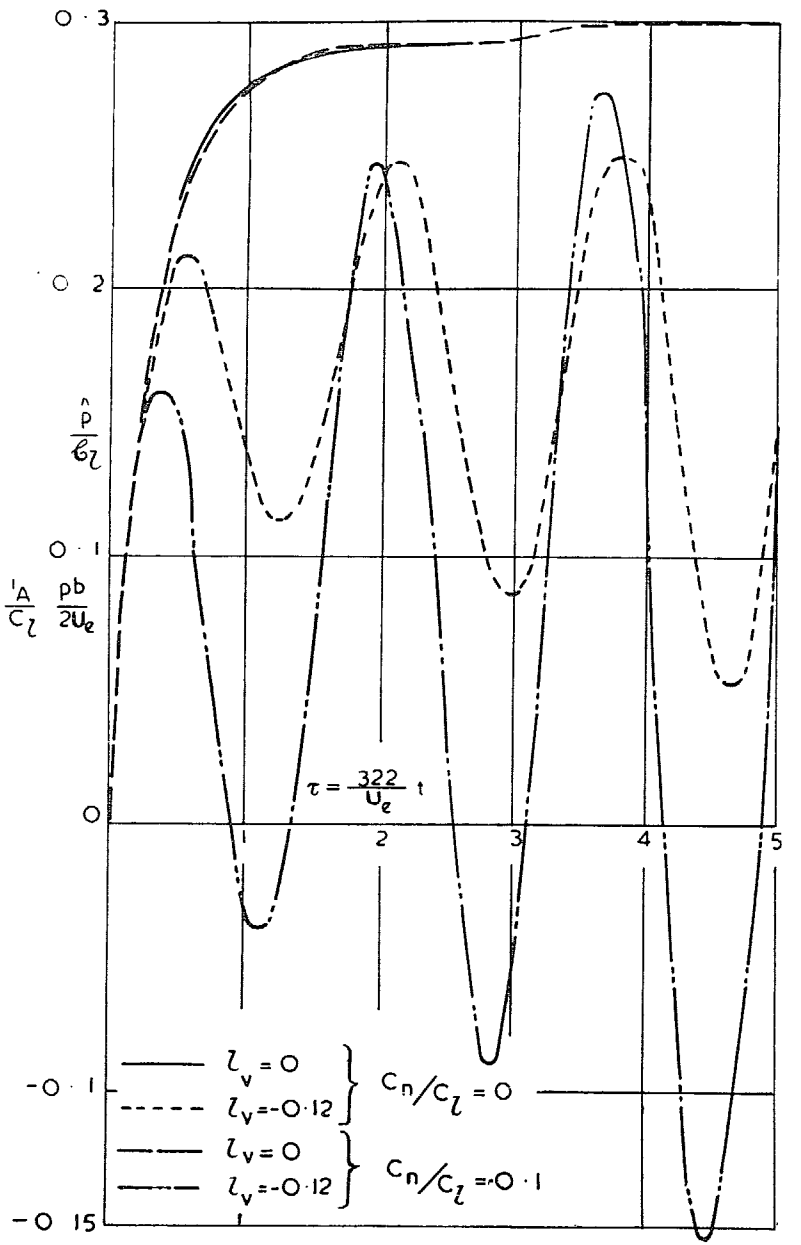

FIG. 68. Response to applied rolling moment with adverse yawing moment. Rate of roll for $\mu_2 = 80$, $n_v = 0{\cdot}024$ and varying l_v and C_n/C_l.

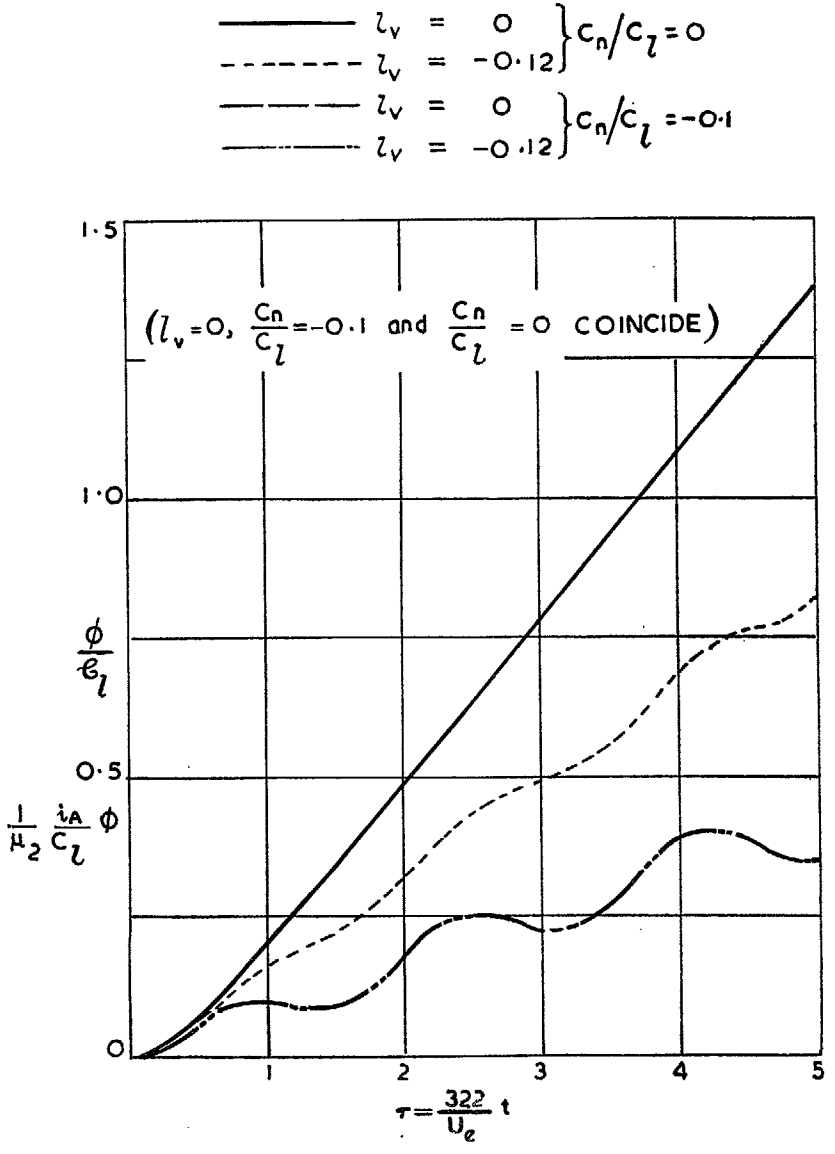

FIG. 69. Response to applied rolling moment with adverse yawing moment. Angle of bank for $\mu_2 = 80$, $n_v = 0{\cdot}024$ and varying l_v and C_n/C_l.

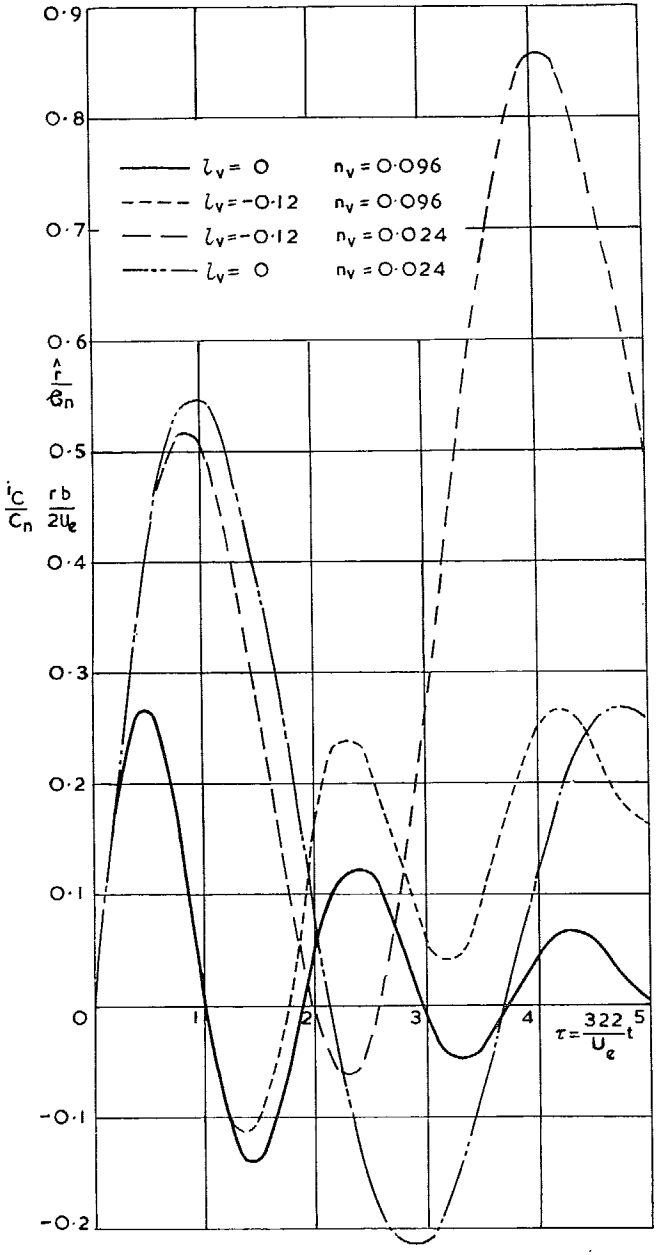

FIG. 70. Response to applied yawing moment. Rate of yaw for $\mu_2 = 20$, $i_A = 0{\cdot}12$, $i_C = 0{\cdot}18$ and varying l_v, n_v

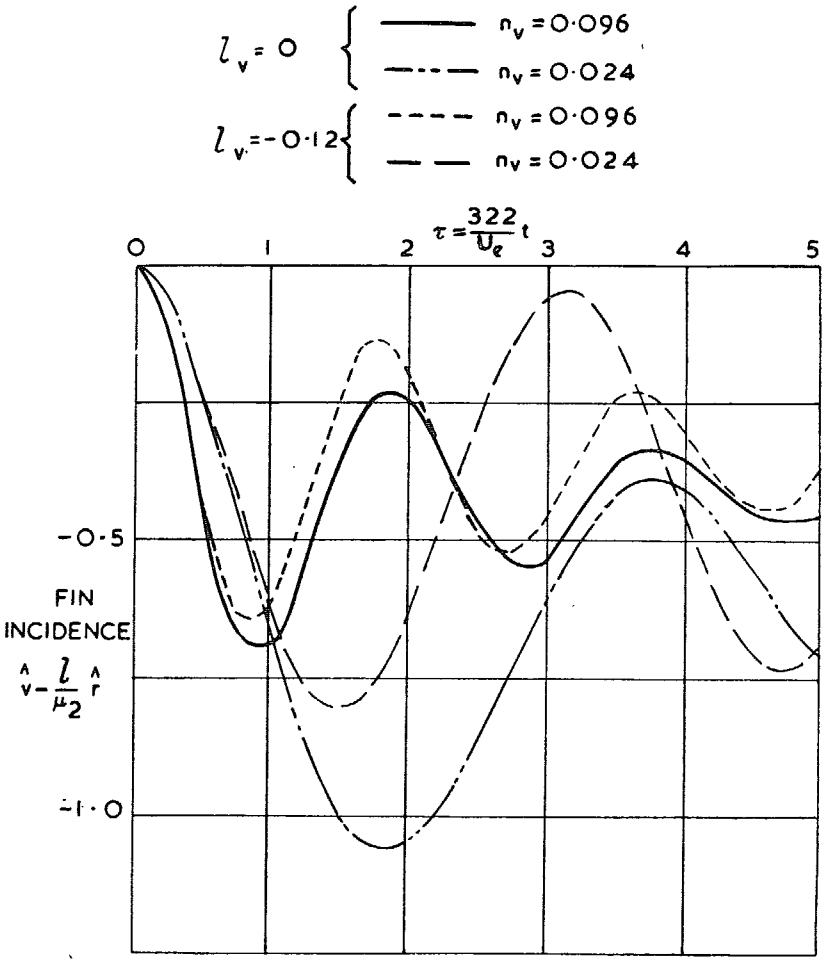

FIG. 71. Fin incidence due to rudder application $\left(\mathscr{C}_n = \frac{1}{3}\frac{\mu_2}{i_0} n_{vf}\right)$ for $\mu_2 = 20$, $i_A = 0{\cdot}12$, $i_0 = 0{\cdot}18$.

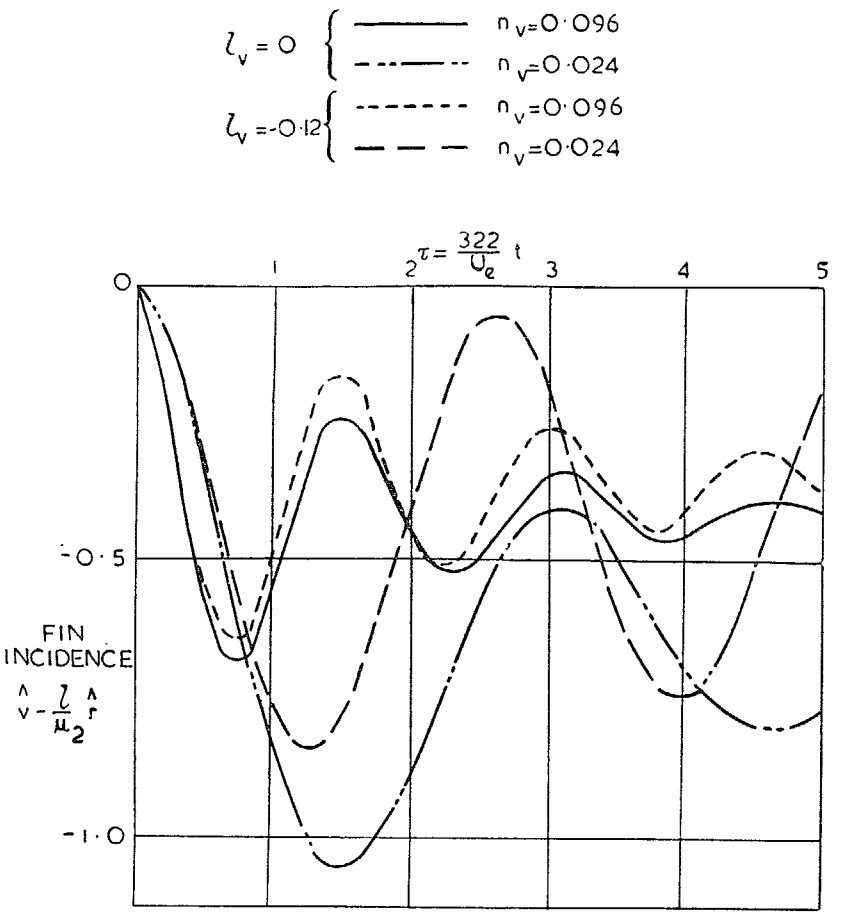

FIG. 72. Fin incidence due to rudder application $\left(\mathscr{C}_n = \frac{1}{3}\frac{\mu_2}{i_0} n_{vf}\right)$ for $\mu_2 = 20$, $i_A = 0{\cdot}06$, $i_0 = 0{\cdot}18$.

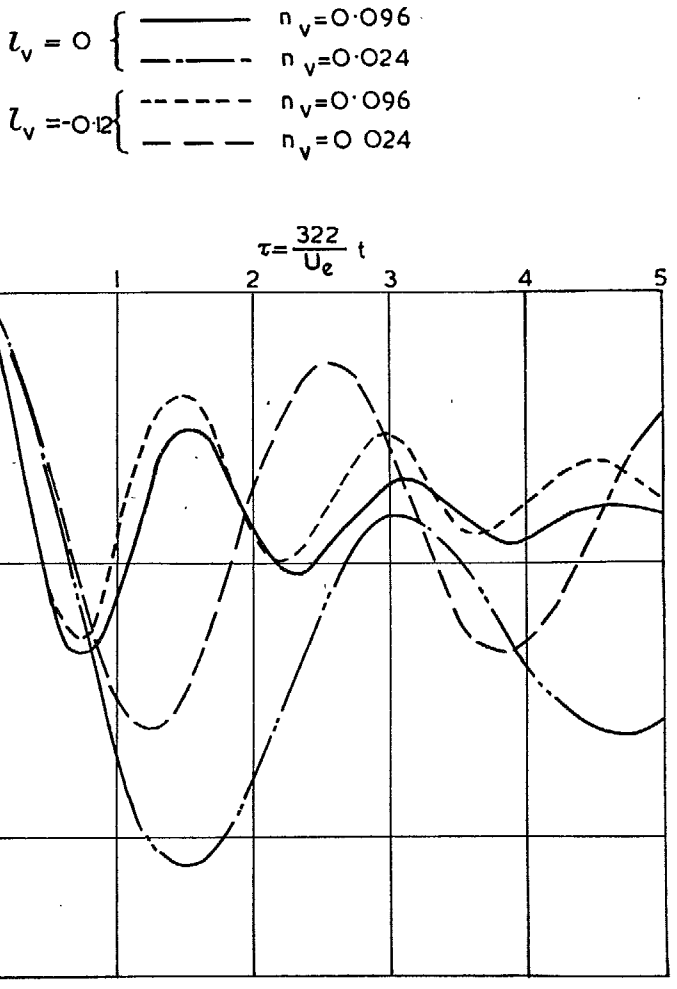

FIG. 73. Fin incidence due to rudder application $\left(\mathscr{C}_n = \frac{1}{3}\frac{\mu_2}{i_C} n_{v_f}\right)$ for $\mu_2 = 20$, $i_A = 0{\cdot}06$, $i_C = 0{\cdot}12$.

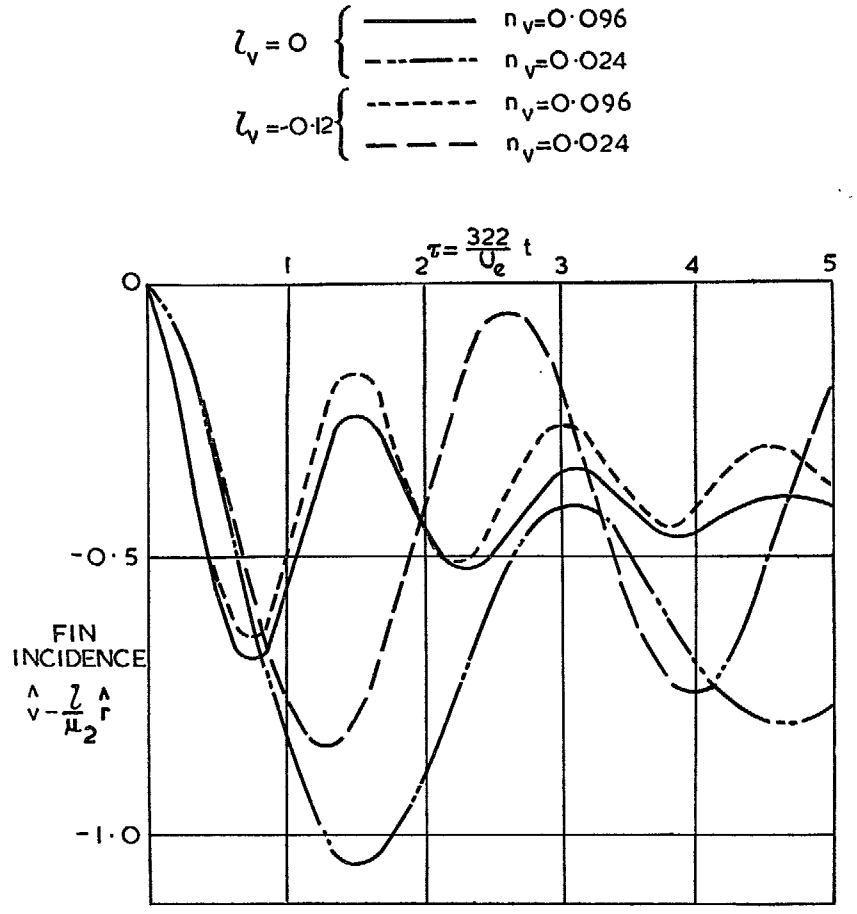

FIG. 74. Fin incidence due to rudder application $\left(\mathscr{C}_n = \frac{1}{3}\frac{\mu_2}{i_C} n_{v_f}\right)$ for $\mu_2 = 20$, $i_A = 0{\cdot}12$, $i_C = 0{\cdot}12$.

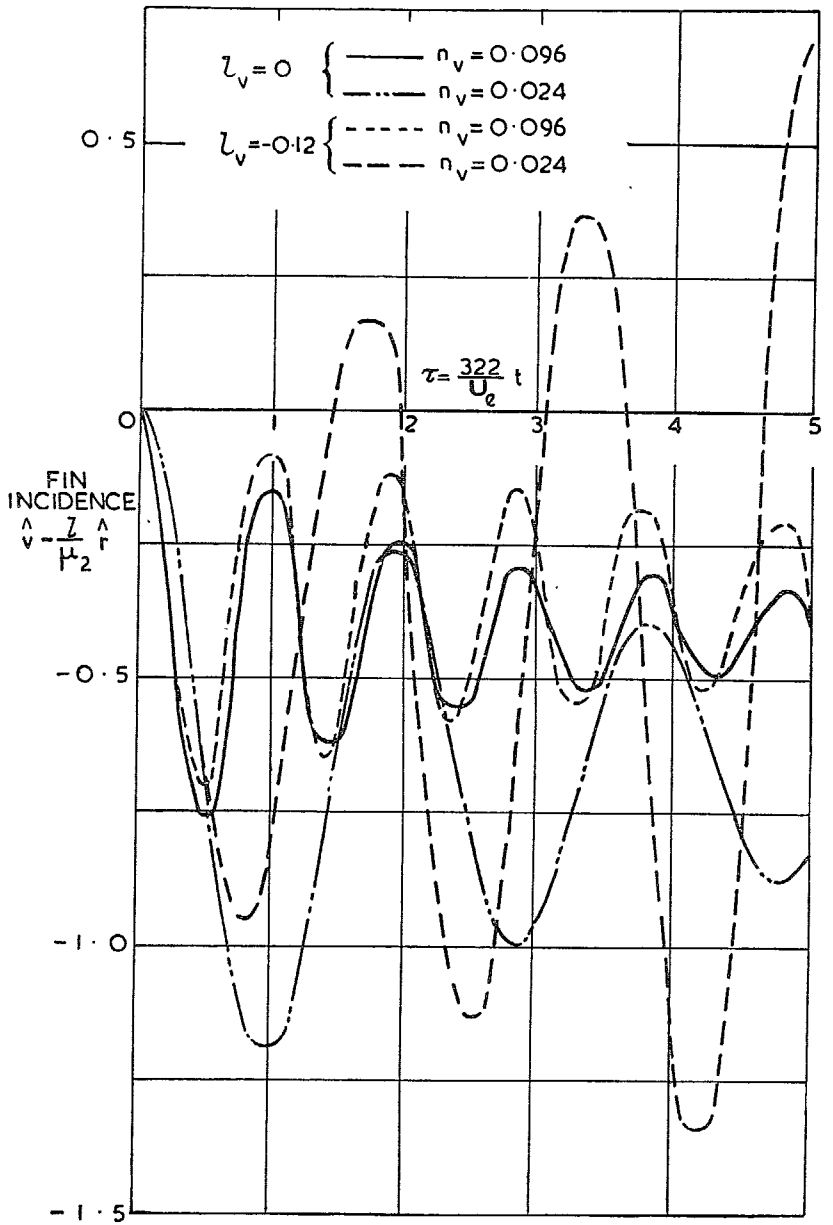

FIG. 75. Fin incidence due to rudder application $\left(\mathscr{C}_n = \frac{1}{3}\frac{\mu_2}{i_c} n_{vf}\right)$ for $\mu_2 = 80$, $i_A = 0{\cdot}12$, $i_c = 0{\cdot}18$.

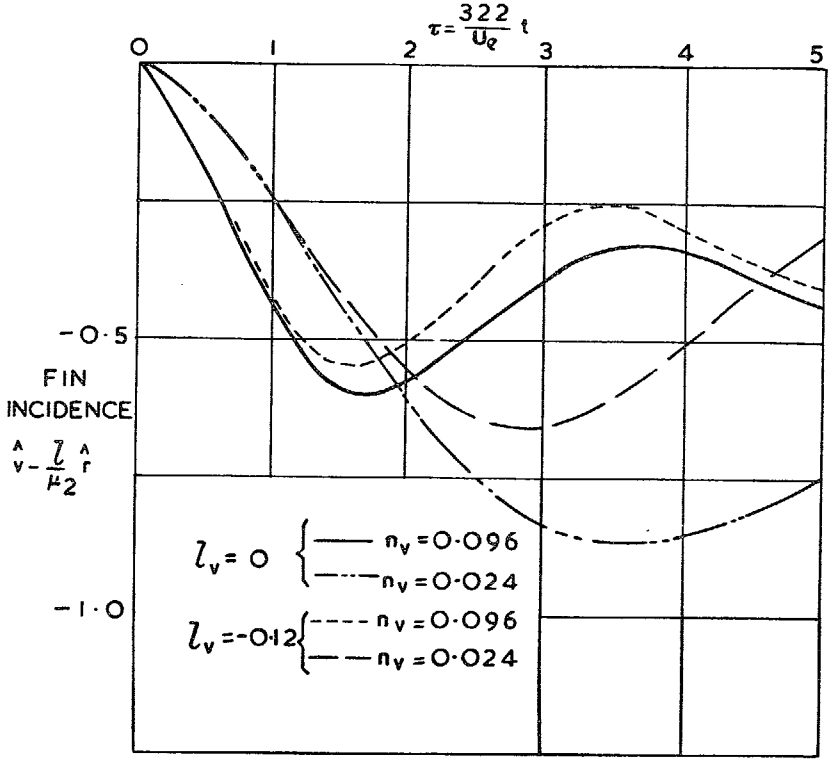

FIG. 76. Fin incidence due to rudder application $\left(\mathscr{C}_n = \frac{1}{3}\frac{\mu_2}{i_c} n_{vf}\right)$ for $\mu_2 = 5$, $i_A = 0{\cdot}12$, $i_c = 0{\cdot}18$.

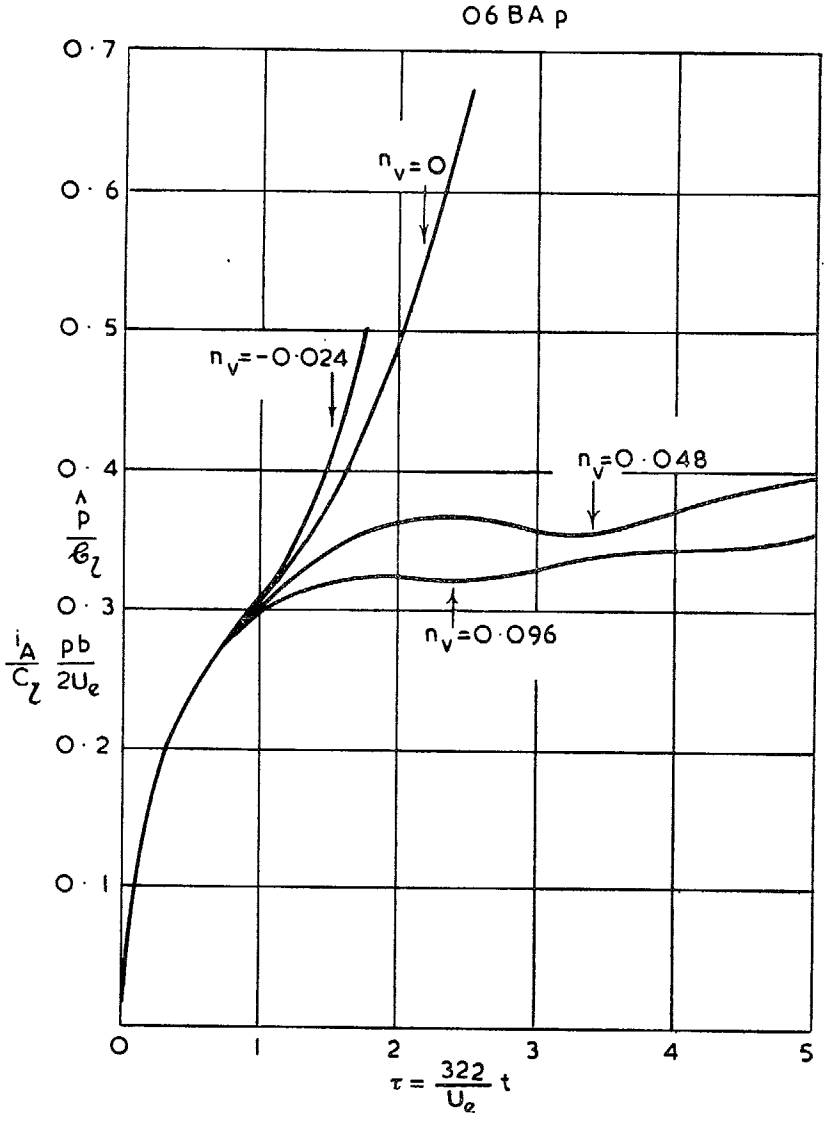

FIG. 77 (S.121). Response to applied rolling moment. Rate of roll for $l_v = 0·06$ and $\mu_2 = 20$. Effect of varying n_v.

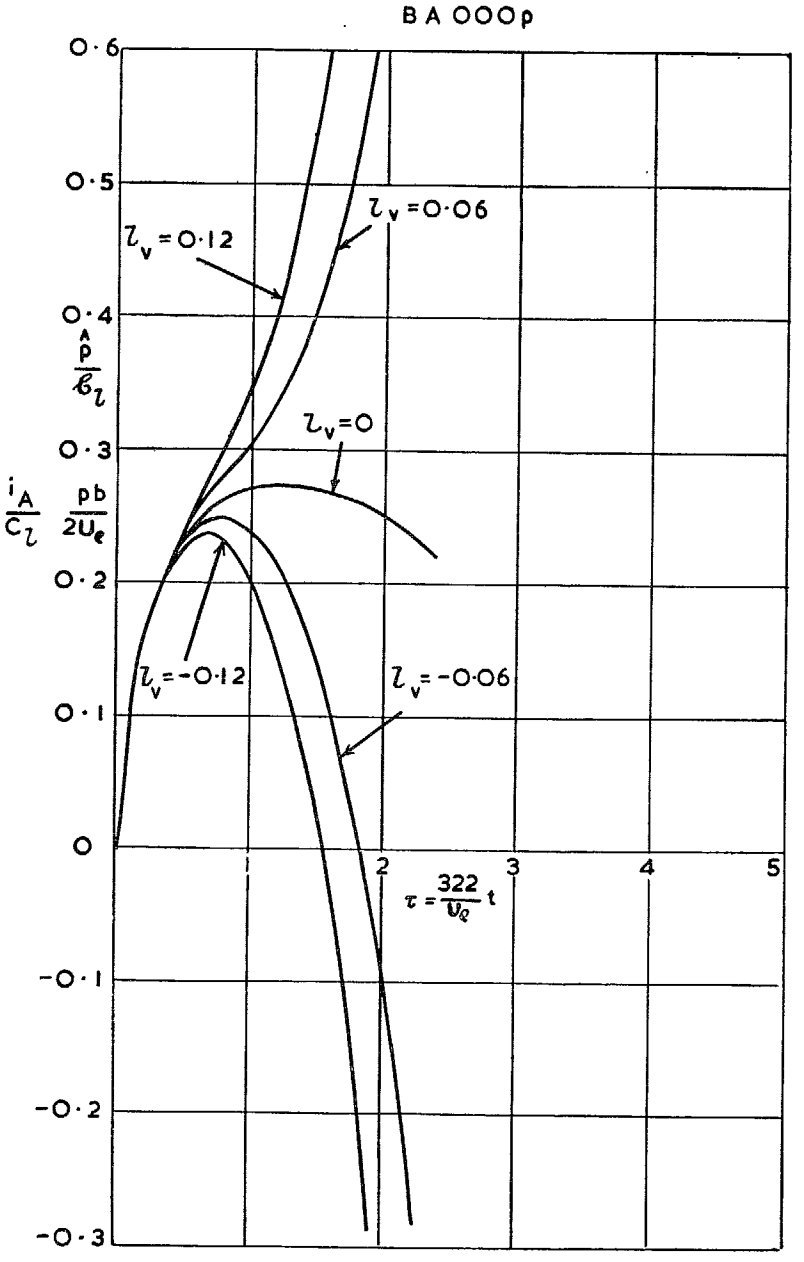

FIG. 78 (S.145). Response to applied rolling moment. Rate of roll for $n_v = 0·024$, $\mu_2 = 20$. Effect of varying l_v.

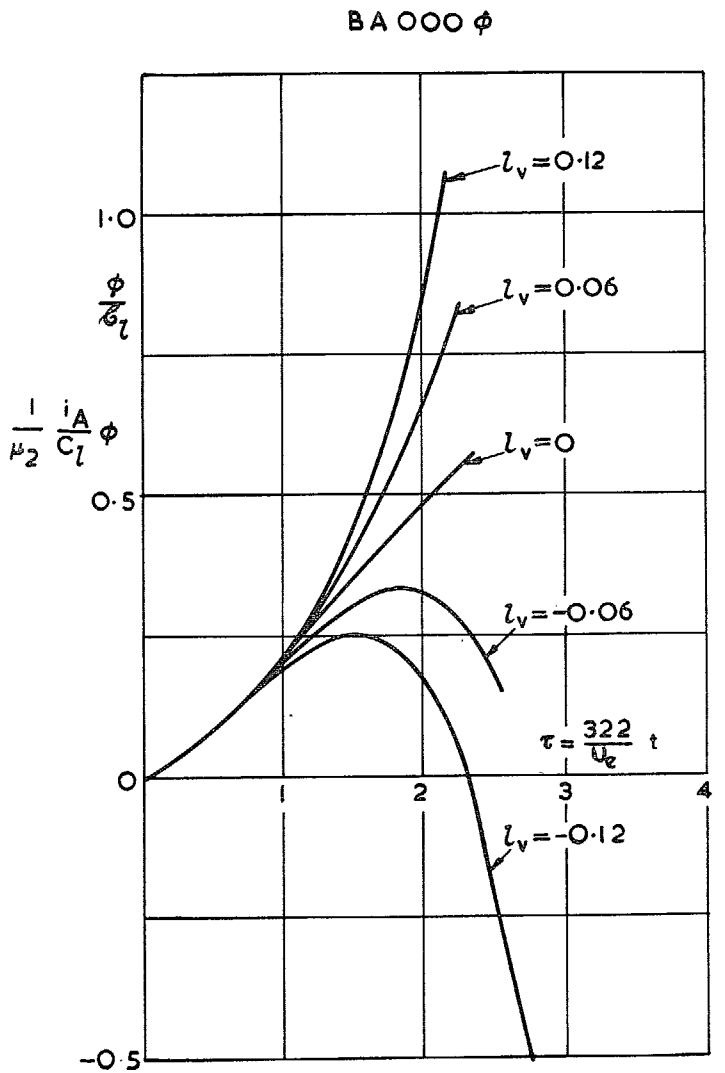

FIG. 79 (S.148). Response to applied rolling moment. Angle of bank for $n_v = -0{\cdot}024$ and $\mu_2 = 20$. Effect of varying l_v.

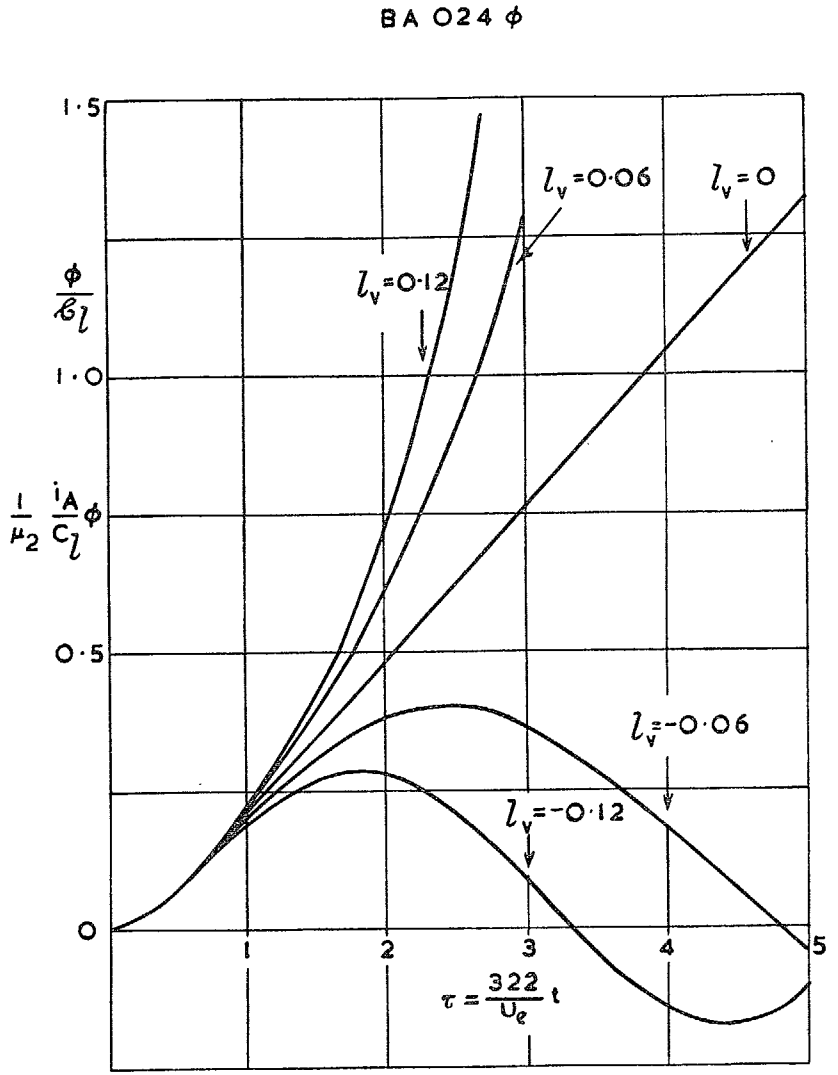

FIG. 80 (S.154). Response to applied rolling moment. Angle of bank for $n^v = 0$ and $\mu_2 = 20$. Effect of varying l_v.

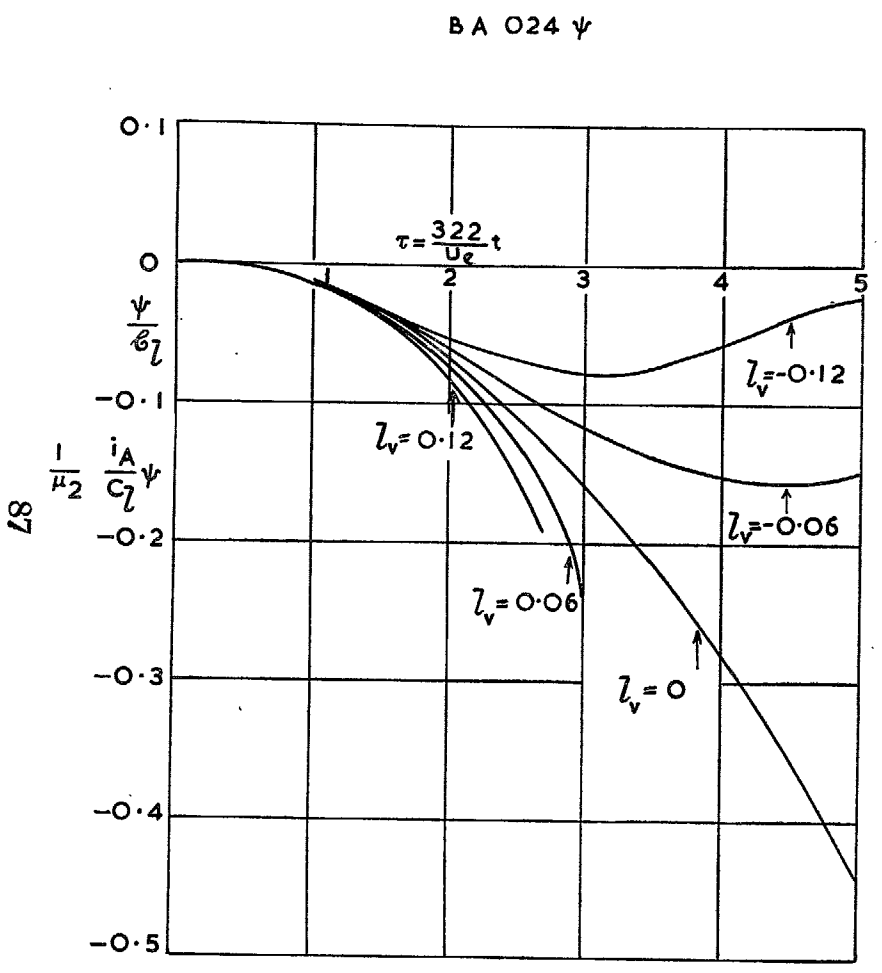

FIG. 81 (S.155). Response to applied rolling moment. Angle of yaw for $n_v = 0$ and $\mu_2 = 20$. Effect of varying l_v.

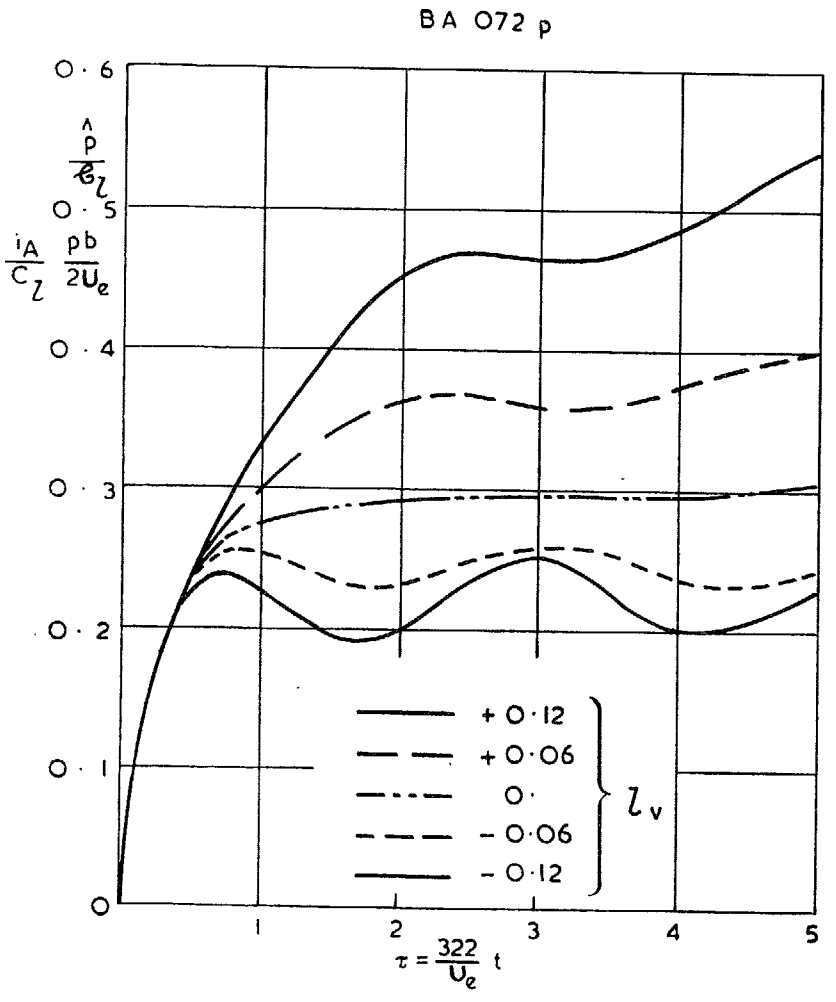

FIG. 82 (S.157). Response to applied rolling moment. Rate of roll for $n_v = 0{\cdot}048$ and $\mu_2 = 20$. Effect of varying l_v.

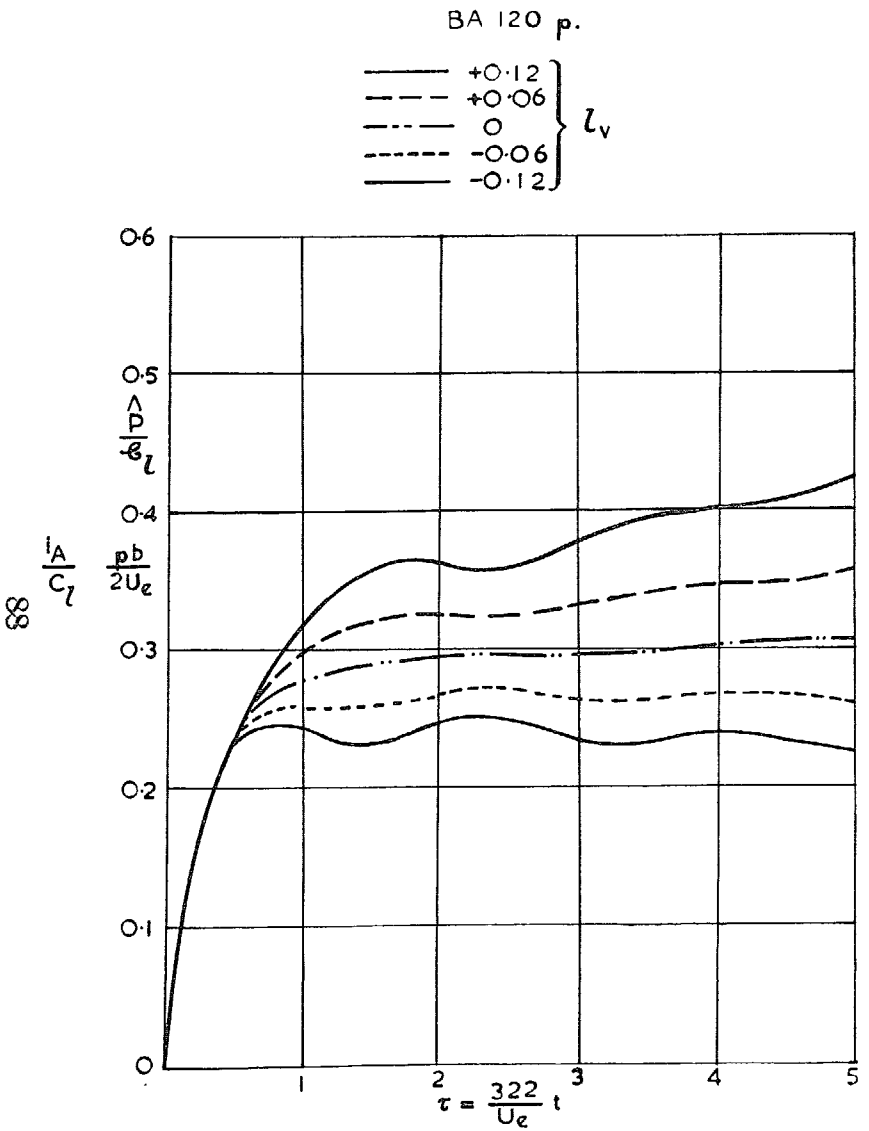

FIG. 83 (S.163). Response to applied rolling moment. Rate of roll for $n_v = 0{\cdot}096$, $\mu_2 = 20$. Effect of varying l_v.

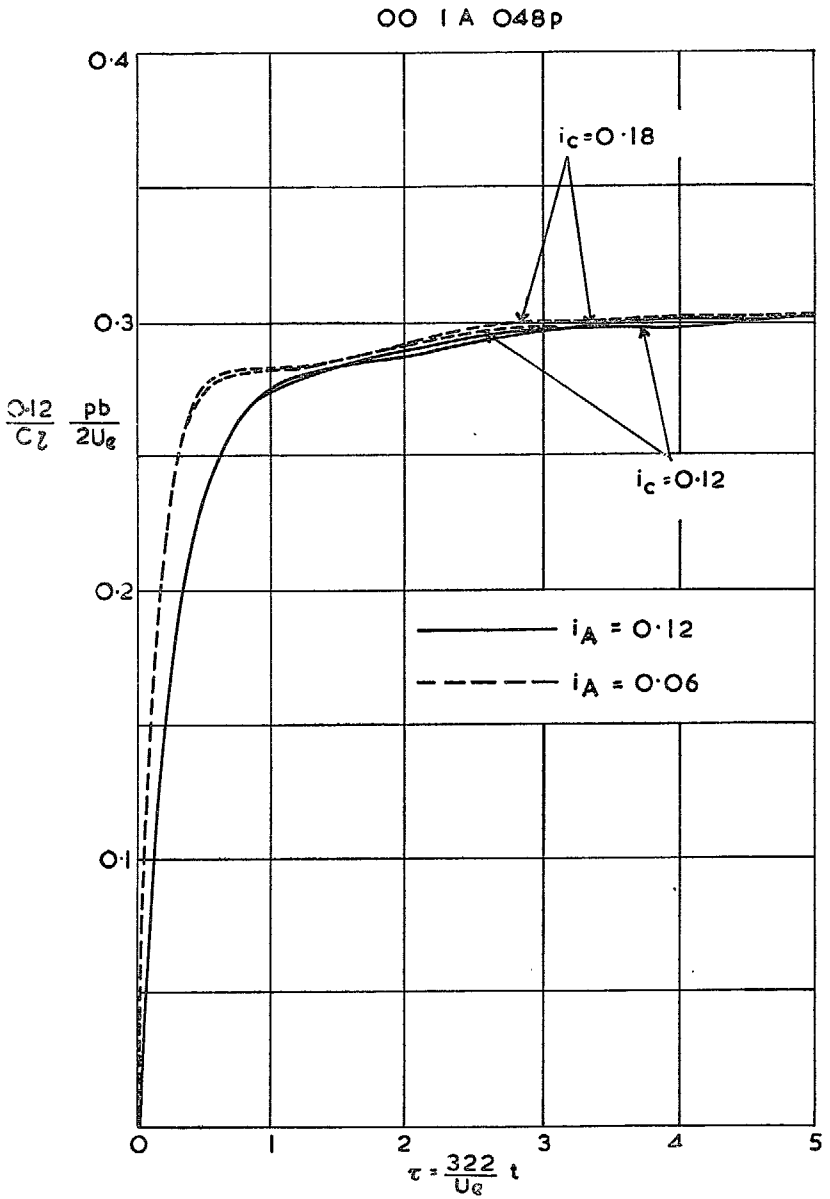

FIG. 84 (S.169). Response to applied rolling moment. Rate of roll for $\mu_2 = 20$, $l_v = 0$, $n_v = 0{\cdot}024$. Effect of varying i_A and i_C.

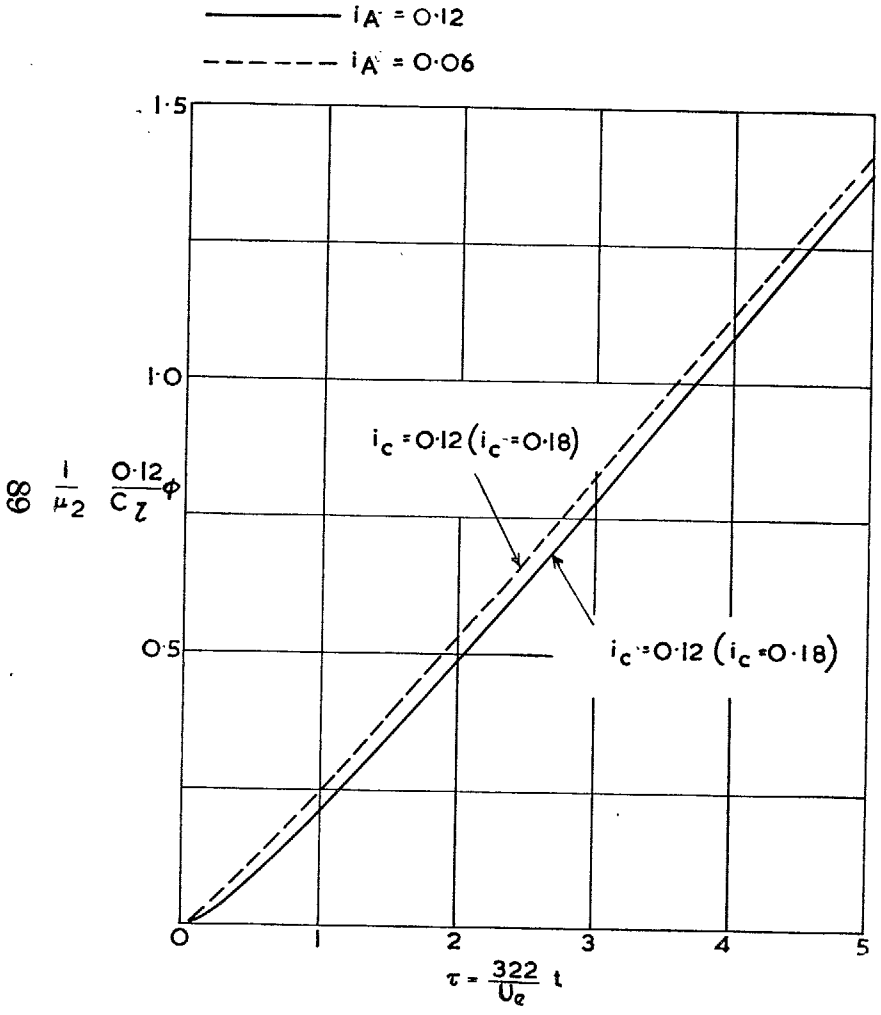

FIG. 85 (S.172). Response to applied rolling moment. Angle of bank for $\mu_2 = 20$, $l_v = 0$, $n_v = 0·024$. Effect of varying i_A and i_c.

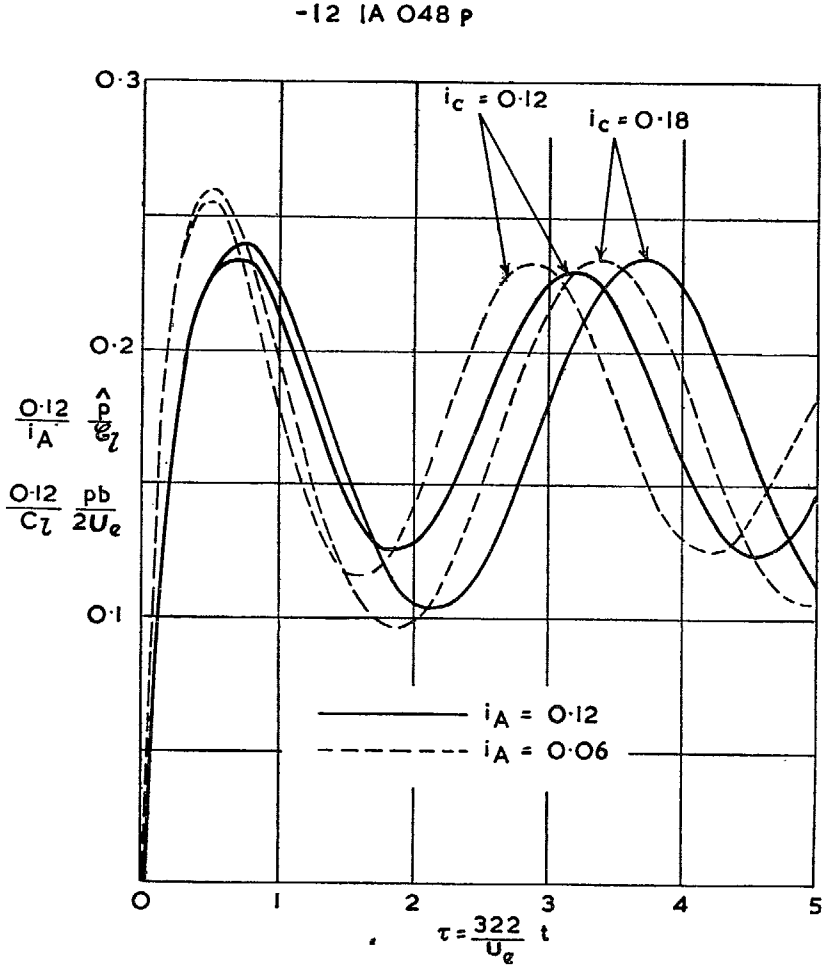

FIG. 86 (S.175). Response to applied rolling moment. Rate of roll for $\mu_2 = 20$, $l_v = -0·12$, $n_v = 0·024$. Effect of varying i_A and i_c.

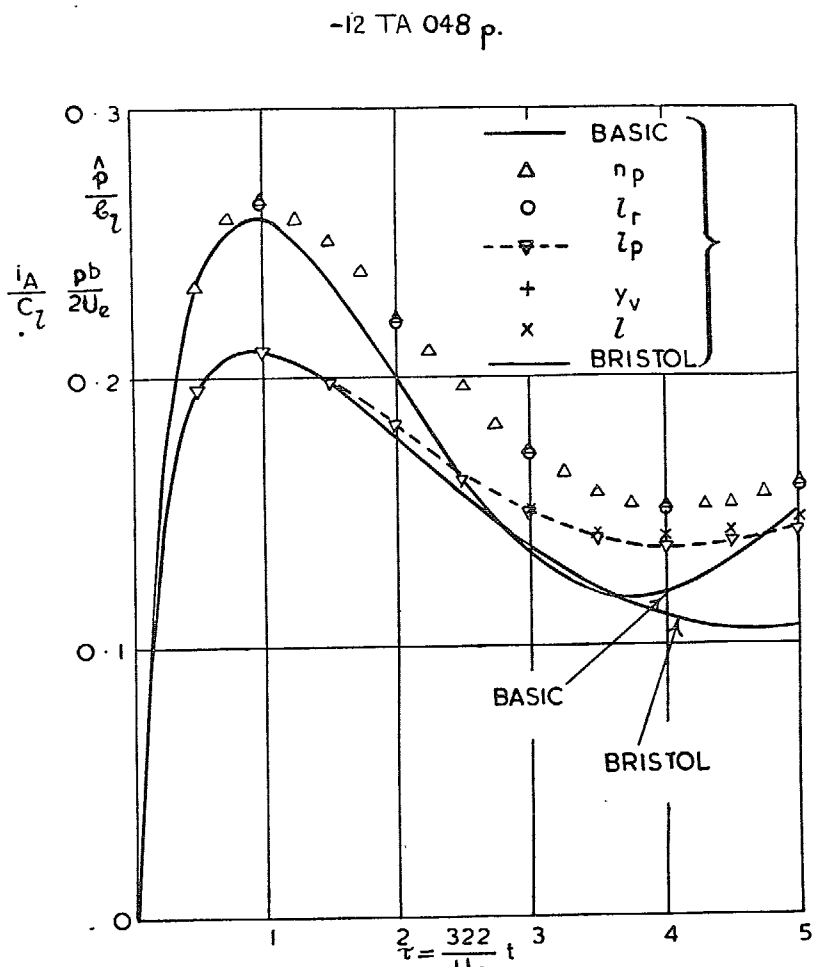

FIG. 87 (S.223). Response to applied rolling moment. Rate of roll for $\mu_2 = 5$, $l_v = -0{\cdot}12$, $n_v = 0{\cdot}024$. Effect of varying rotary derivatives.

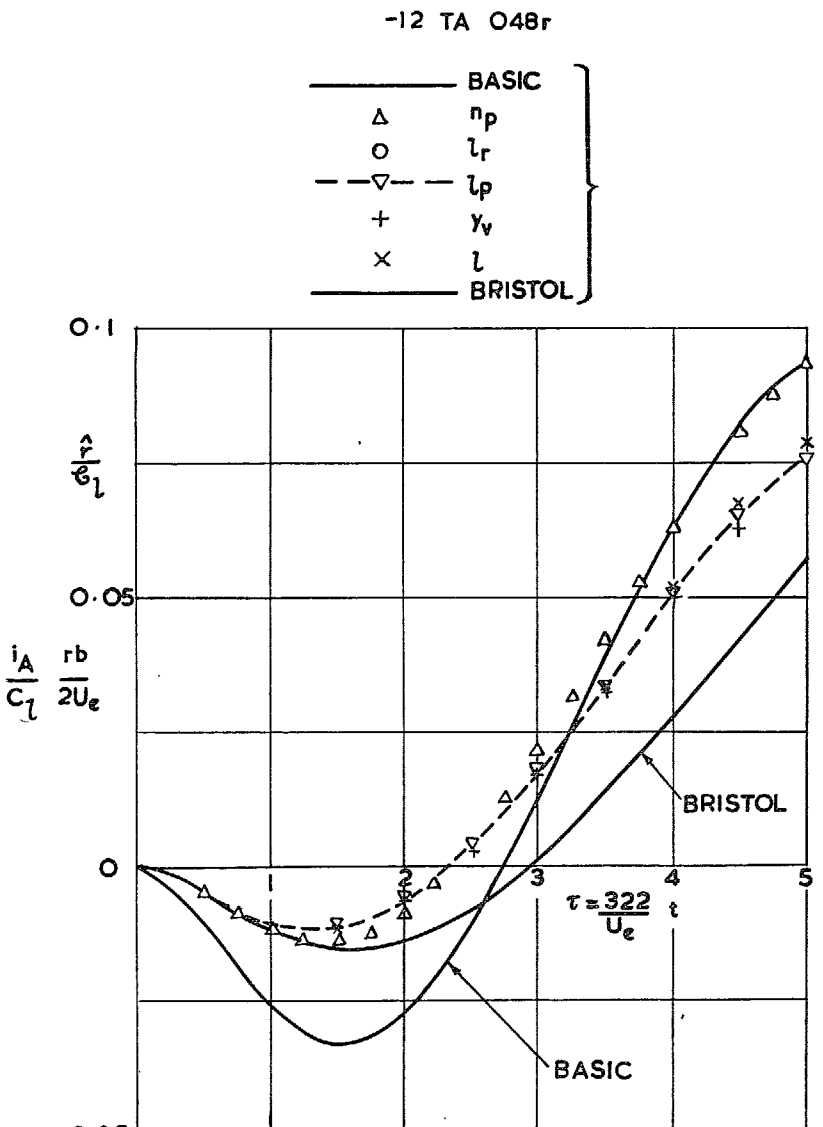

FIG. 88 (S.225). Response to applied rolling moment. Rate of yaw for $\mu_2 = 5$, $l_v = -0{\cdot}12$ and $n_v = 0{\cdot}024$. Effect of varying rotary derivatives.

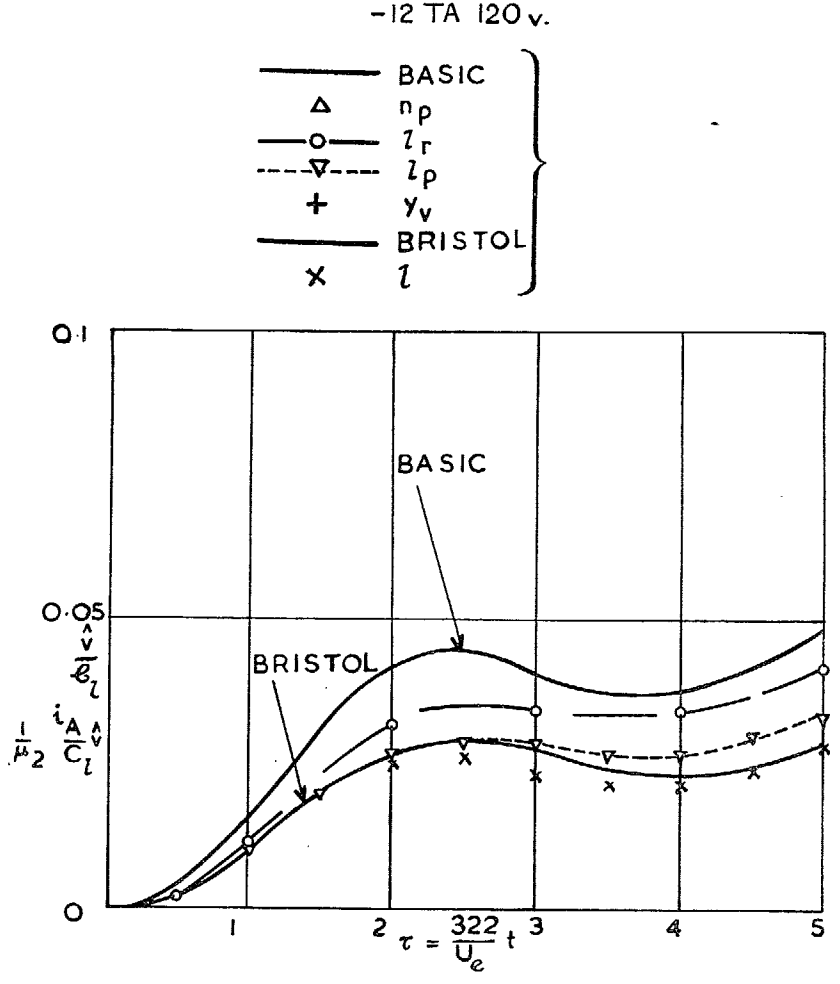

FIG. 89 (S.236). Response to applied rolling moment. Angle of sideslip for $\mu_2 = 5$, $l_v = -0{\cdot}12$, $n_v = 0{\cdot}096$. Effect of varying rotary derivatives.

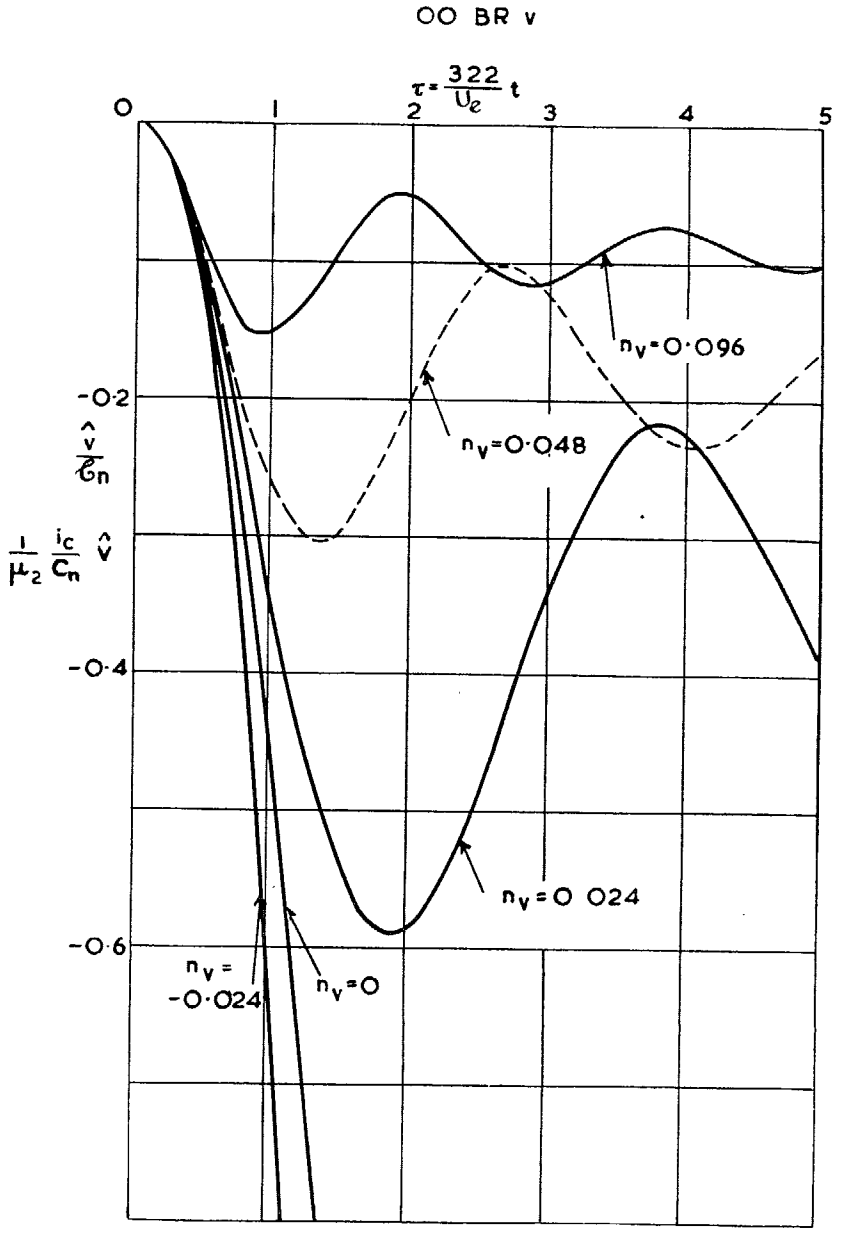

FIG. 90 (S.248). Response to applied yawing moment. Angle of sideslip for $\mu_2 = 20$, $l_v = 0$. Effect of varying n_v.

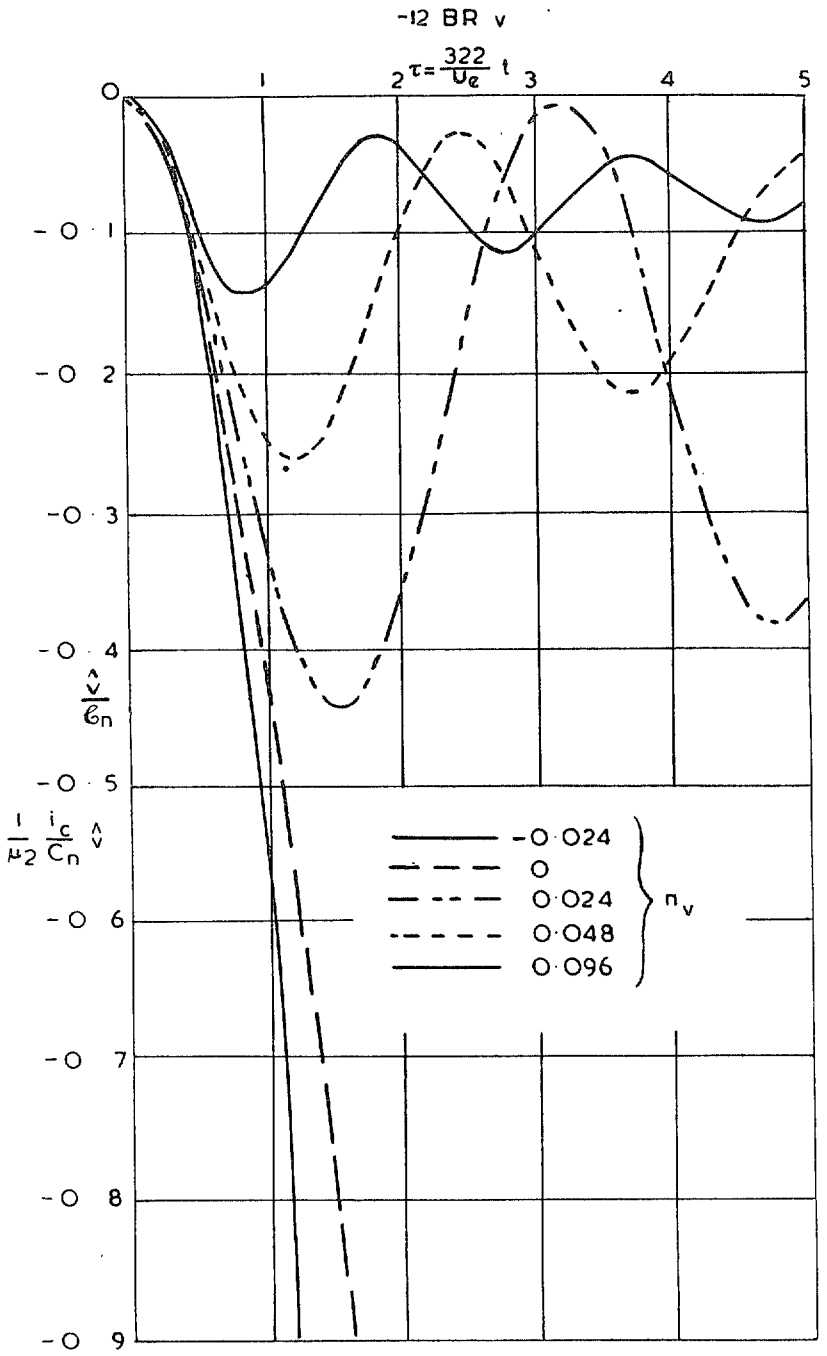

FIG. 91 (S.260). Response to applied yawing moment. Angle of sideslip for $\mu_2 = 20$, $l_v = -0{\cdot}12$. Effect of varying n_v.

(89424) Wt 13/806 K5 12/51 Hw.

PRINTED IN GREAT BRITAIN

Publications of the Aeronautical Research Council

ANNUAL TECHNICAL REPORTS OF THE AERONAUTICAL RESEARCH COUNCIL (BOUND VOLUMES)—

1934–35 Vol. I. Aerodynamics. *Out of print.*
Vol. II. Seaplanes, Structures, Engines, Materials, etc. 40*s.* (40*s.* 8*d*)

1935–36 Vol. I. Aerodynamics. 30*s.* (30*s.* 7*d.*)
Vol. II. Structures, Flutter, Engines, Seaplanes, etc. 30*s.* (30*s.* 7*d.*)

1936 Vol. I. Aerodynamics General, Performance, Airscrews, Flutter and Spinning. 40*s.* (40*s.* 9*d.*)
Vol. II. Stability and Control, Structures, Seaplanes, Engines, etc. 50*s.* (50*s.* 10*d.*)

1937 Vol. I. Aerodynamics General, Performance, Airscrews, Flutter and Spinning. 40*s.* (40*s.* 10*d.*)
Vol. II. Stability and Control, Structures, Seaplanes, Engines, etc. 60*s.* (61*s.*)

1938 Vol. I. Aerodynamics General, Performance, Airscrews 50*s.* (51*s.*)
Vol. II. Stability and Control, Flutter, Structures, Seaplanes, Wind Tunnels, Materials. 30*s.* (30*s.* 9*d.*)

1939 Vol. I. Aerodynamics General, Performance, Airscrews, Engines. 50*s.* (50*s.* 11*d.*)
Vol. II. Stability and Control, Flutter and Vibration, Instruments, Structures, Seaplanes, etc. 63*s.* (64*s.* 2*d.*)

1940 Aero and Hydrodynamics, Aerofoils, Airscrews, Engines, Flutter, Icing, Stability and Control, Structures, and a miscellaneous section. 50*s.* (51*s.*)

Certain other reports proper to the 1940 *volume will subsequently be included in a separate volume.*

ANNUAL REPORTS OF THE AERONAUTICAL RESEARCH COUNCIL—

1933–34	1*s.* 6*d.* (1*s.* 8*d.*)
1934–35	1*s.* 6*d.* (1*s.* 8*d.*)
April 1, 1935 to December 31, 1936.	4*s.* (4*s.* 4*d.*)
1937	2*s.* (2*s.* 2*d.*)
1938	1*s.* 6*d* (1*s.* 8*d.*)
1939–48	3*s.* (3*s.* 2*d.*)

INDEX TO ALL REPORTS AND MEMORANDA PUBLISHED IN THE ANNUAL TECHNICAL REPORTS, AND SEPARATELY—

April, 1950	R. & M. No. 2600.	2*s.* 6*d.* (2*s.* 7½*d.*)

INDEXES TO THE TECHNICAL REPORTS OF THE AERONAUTICAL RESEARCH COUNCIL—

December 1, 1936 — June 30, 1939.	R. & M. No. 1850.	1*s.* 3*d.* (1*s.* 4½*d.*)
July 1, 1939 — June 30, 1945.	R. & M. No. 1950.	1*s.* (1*s.* 1½*d.*)
July 1, 1945 — June 30, 1946.	R. & M. No. 2050.	1*s.* (1*s.* 1½*d.*)
July 1, 1946 — December 31, 1946.	R. & M. No. 2150.	1*s.* 3*d.* (1*s.* 4½*d.*)
January 1, 1947 — June 30, 1947.	R. & M. No. 2250.	1*s.* 3*d.* (1*s.* 4½*d.*)

Prices in brackets include postage.

Obtainable from

HIS MAJESTY'S STATIONERY OFFICE

York House, Kingsway, LONDON, W.C.2 429 Oxford Street, LONDON, W.1
P.O. Box 569, LONDON, S.E.1
13a Castle Street, EDINBURGH, 2 1 St. Andrew's Crescent, CARDIFF
39 King Street, MANCHESTER, 2 Tower Lane, BRISTOL, 1
2 Edmund Street, BIRMINGHAM, 3 80 Chichester Street, BELFAST

or through any bookseller.